

**KINETIC MODELS FOR REVERSIBLE AND
IRREVERSIBLE INHIBITIONS OF BIOLOGICAL
NITRITE OXIDATION**

BY

BING LIU

DOCTORAL DISSERTATION

AT

THE UNIVERSITY OF KITAKYUSHU

SEPTEMBER 2014

CONTENT

| | |
|---|----|
| ABSTRACT | 1 |
| 1. Introduction | 3 |
| 1.1 Background | 3 |
| 1.1.1 N-cycle in wastewater | 3 |
| 1.1.2 Necessity of N ⁻ removal from wastewater | 4 |
| 1.1.3 Biological N-removal | 5 |
| 1.2 N-removal in activated sludge processes | 6 |
| 1.3 Development of Activated Sludge Model (ASM) | 11 |
| 1.4 Research Objective | 14 |
| 2. Previous Researches | 17 |
| 2.1 Nitrification process | 17 |
| 2.2 Kinetics in nitrification | 19 |
| 2.3 Inhibition model | 25 |
| 2.3.1 Reversible inhibition | 25 |
| 2.3.2 Irreversible inhibition | 33 |
| 2.4 Nitrification inhibition by FNA and FA | 35 |
| 2.4.1 FA and FNA inhibition | 35 |
| 2.4.2 Physiological reason for FA and FNA toxicity | 36 |
| 2.5 Other effect factors on nitrifiers activity | 38 |
| 2.6 Nitrifiers species and kinetics values change with SRT | 42 |
| 3. Nitrite oxidising organism exogenous decay verification using live/dead staining under high nitrite concentration | 46 |
| 3.1 Objective | 46 |

| | |
|---|----|
| 3.2 Material and Method | 48 |
| 3.2.1 Enrichment of NOO sludge..... | 48 |
| 3.2.2 Inhibition test | 49 |
| 3.2.3 Bacteria staining | 51 |
| 3.3 Results | 56 |
| 3.3.1 Exogenous decay by FNA poisoning..... | 56 |
| 3.3.2 Cellular disintegration..... | 58 |
| 3.4 Discussion | 61 |
| 3.4.1 Modelling growth/death of NOO in open culture | 61 |
| 3.4.2 Simulation of OUR and VSS..... | 63 |
| 3.5 Conclusions | 66 |
| 4. Nitrite oxidising organism (NOO) reversible and irreversible inhibition by FNA and FA | 67 |
| 4.1 Background | 67 |
| 4.2 Theoretical development | 72 |
| 4.2.1 Structure of global switching function..... | 72 |
| 4.2.2 Model for reversible inhibition with recovery | 73 |
| 4.2.3 Model for irreversible inhibition..... | 74 |
| 4.3 Material and Method | 75 |
| 4.3.1 Short-term OUR measuring procedure..... | 75 |
| 4.3.2 Long-term OUR measuring procedure..... | 75 |
| 4.3.3 Calculation of FA and FNA | 77 |
| 4.4 Results | 78 |
| 4.4.1 Reversible inhibition verification | 78 |

| | |
|--|-----|
| 4.4.2 Irreversible inhibition verification | 87 |
| 4.4.4 Model structure and kinetics values | 89 |
| 4.5 Discussion | 92 |
| 4.5.1 Marginal inhibition condition | 92 |
| 4.6 Conclusions | 96 |
| 5. Benchmark simulation to verify an inhibition model on decay stage for nitrification | 97 |
| 5.1 Background | 97 |
| 5.2 Material and Method | 101 |
| 5.2.1 Data extraction from WERF benchmark datasets | 101 |
| 5.2.2 Dynamic simulation | 102 |
| 5.3 Results | 105 |
| 5.3.1 Individual evaluation by benchmark datasets using synthetic wastewater | 105 |
| 5.3.2 Individual evaluation by benchmark datasets using dewater solid wastewater | 111 |
| 5.4 Discussion | 114 |
| 5.4.1 Model verification in the nitrification process | 114 |
| 5.5 Conclusion | 120 |
| 6 Bioaugmentation with nitrifiers developed from different substrates | 122 |
| 6.1 Background | 122 |
| 6.2 Material and Methods | 123 |
| 6.2.1 Seed nitrifiers training | 123 |
| 6.2.2 Bioaugmentation analyses | 124 |
| 6.2.3 Model structure | 125 |

| | |
|---|-----|
| 6.3 Results | 126 |
| 6.3.1 Bioaugmentation with nitrifiers developed from high-strength ammonia synthetic waste at 20-day SRT | 126 |
| 6.3.2 Bioaugmentation with nitrifiers developed from dewatered biosolids supernatant at 20-day SRT..... | 131 |
| 6.3.3. Bioaugmentation with nitrifiers from nitrifying tricking filter biomass. ... | 138 |
| 6.4 Conclusion | 144 |
| 7. Conclusion | 145 |
| 8. Reference | 149 |
| List of Figures | 168 |
| List of Tables | 174 |
| Acknowledgement | 176 |
| Publications List | 178 |

ABSTRACT

Biological reactions often experience inhibition from high concentration of substrates, reaction products and other external inhibitory compounds. The inhibitory compounds may affect the enzymatic system leading to different forms of competitive, non-competitive or uncompetitive reversible inhibition. In other situations, the concentration of inhibitory compound could result in poisoning leading to irreversible inhibition. There are several mathematical models to express reversible inhibition, however recovery and adaptation phenomenon are not well described by these models. Furthermore, the modelling approaches for irreversible inhibitions are not well developed.

In this study, an irreversible inhibition function was developed and evaluated using nitrite oxidising organisms (NOO) as a research subject under different nitrite concentrations and pH. A set of batch tests was carried out at pH 7.0 where the nitrite concentration was automatically kept almost constant over the experimental periods for 7 days. During the experiments oxygen uptake rate (OUR) and microscopic cell-counting using bacterial staining (live/dead method) were performed at 24-hr interval. The OUR at 50 mg-N-NaNO₂/L linearly increased with an increase of 'living cells' whilst the OUR and the living cells without nitrite decreased logarithmically showing that decay took place. On the other hand, when the nitrite concentration was set at over 500 mg-N/L, both OUR and living cells decreased at higher specific decay rates than that without nitrite. In the conditions the number of cells stained as 'dead' (cells with damaged cell membrane) increased along with time but did not correspond to the loss of

living cells, suggesting a deformation of cell particulates after death. Based on the response the behaviours for NOO and other cryptic growing microorganisms were expressed on Gujer-matrix and these kinetics were estimated.

Nitrite and ammonia may exist in the nitrification process in N-removal of wastewater treatment, and free nitrous acid (FNA) and free ammonia (FA) was identified as reversible inhibitors for NOO and ammonia oxidising organisms (AOO) in previous researches. To evaluate and model for reversible and irreversible inhibition by FNA and FA, Batch experiments were conducted using nitrite-N concentration in the range of 125 - 2000 mg-N/L (the N concentration ratio of nitrite and ammonia was kept at 1 in parallel experiments), and the OURs were measured as dynamic reaction responses.

OUR responses revealed that the inhibition effect of FNA and FA disappeared after several hours due to microbial adaptation from the shock loading. The OUR tests also indicated irreversible inhibition (poisoning) leading to a perpetual reduction in activity at higher doses of inhibitory compounds. For the reversible inhibition a time-dependent switching function was developed to express the degree of adaptation. The irreversible poisoning phenomenon was defined as an additional first-order type decay/death process that was initiated when the inhibitory concentration exceeded the threshold level. The modified model developed from the batch experimental data was able to reasonably reproduce the effluent nitrogenous concentration in the WERF benchmark datasets of over 250 days.

1. Introduction

1.1 Background

1.1.1 N-cycle in wastewater

Nitrogen makes up approximate 80% of atmosphere and is an important component of organics, for instance proteins, lipids, nucleic that are integral materials for life. As there are 5 outermost electron in nitrogen atom, so it is possible to form many oxidation states from -3 to +5 shown in Fig.1.1. In wastewater, Ammonia (NH_4^+), nitrite (NO_2^-), nitrate (NO_3^-) are the three common stable soluble N forms in the many possible compounds of nitrogen.

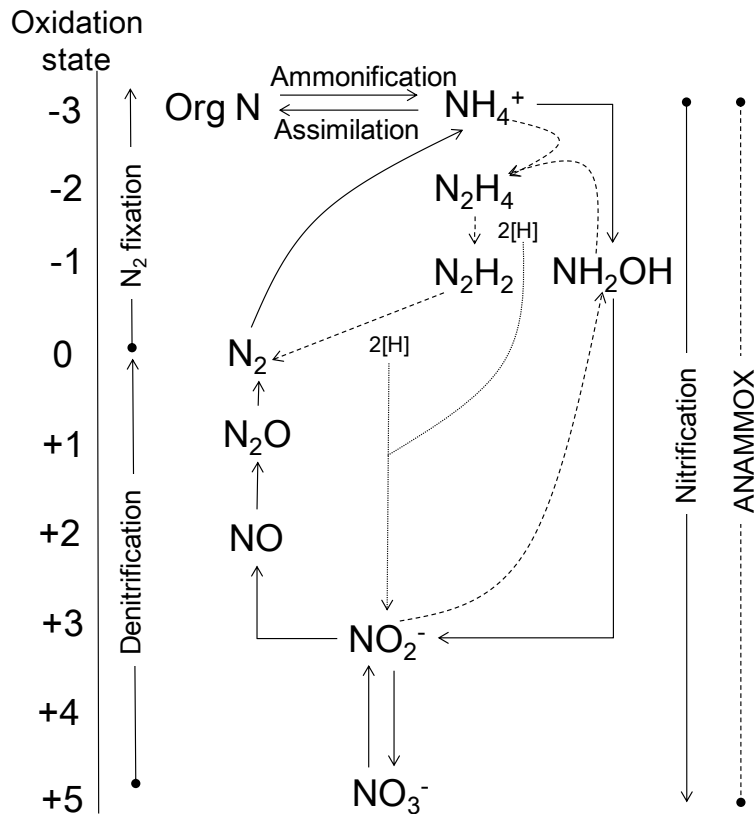


Figure 1. 1 Simplified nitrogen cycle in nature (WEF, 2010)

Nitrogen is being changed from one form to another constantly by biological reactions. These changes are selected and mapped in Fig1.1. In the biological wastewater treatment process, organic nitrogen (Org N) and ammonia were considered as influent nitrogen source and enter N-removal cycle, and the ammonia was considered as the main dissolved inorganic nitrogen in influent. In some instances, other nitrogen forms (e.g. NO_2^- and NO_3^-) also may exist.

1.1.2 Necessity of N- removal from wastewater

Inorganic nitrogen and phosphorus provide nutrient sources for algae bloom and eutrophication in receiving waters. Algae can cause taste and odor problems in a water body. If the water was supplied for drinking water, this problem can be significant and harmful to health. Because algae covers the surface of the water body and hinders oxygen transfer into water from air, dissolved oxygen (DO) concentration becomes low resulting in death of fish and other aquatic organisms.

Additionally a high concentration ammonia is toxic to many aquatic species, even killing fish and aquatic organisms in the receiving stream. Nitrate, one of nitrogen forms in N-cycle, can act as a nutrient material in receiving streams and poses a health risk to contaminate drinking water supplies when beyond a certain level. Research has shown that when water contains elevated levels of nitrate ($> 20 \text{ mg/L}$), an illnesses known as methemoglobinemia, hypertension and stomach cancer can occur. Typically

methemoglobinemia can affect from infants to the elderly, and causes its victims to turn a pale blue/gray and become lethargic and ultimately comatose. Finally death follows soon if no treatment is administered. For all the above reasons and factors, it is necessary to control nitrogenous compounds and remove nitrogen in water bodies. (Fuh, 1974; Shindala, 1972; Stensel, 1971; Stensel, 1973; WEF 2005; WEF 2010.)

1.1.3 Biological N-removal

In the natural world, changes to nitrogen compounds are mostly accomplished biologically, by living organisms. These organisms live in environments that are aerobic, anaerobic and even anoxic (WEF, 2010). In modern wastewater treatment plants nitrogen compounds can be changed among different N-forms. Typically, nitrogen is input into a wastewater treatment plant in the form of ammonia and organic nitrogen as influent nitrogen. The general N-removal process in biological wastewater treatment is that nitrogen compounds enter the influent (mainly ammonia) and are converted to nitrite, or nitrate and then converted into nitrogen gas (N_2). N_2 is released back into the atmosphere, completing the N-cycle. The above processes are known as nitrification by nitrifying bacteria and denitrification by denitrifying bacteria that will be introduced in the following section.

1.2 N-removal in activated sludge processes

The nitrogen cycle in the activated sludge process is shown in Fig. 1.1 from ammonia to nitrogen gas. Traditional biological nitrogen removal (BNR) is from ammonia to hydroxylamine, nitrite and nitrate, then nitrate is changed to dinitrogen gas linked by the solid line in Fig.1.1. The whole process can be separated by two steps, nitrification and denitrification.

1.2.1 Nitrification

The nitrification process is the biological oxidation of ammonia to nitrite and then nitrate. The two-step nitrification process is carried out by two types of bacteria: AOO and NOO. In previous description, ammonia oxidizing bacteria (AOB) and nitrite oxidizing bacteria (NOB) were utilized to express the bacterial types acting on two-step nitrification. However, according to recent research, the biological species on nitrification are not only *eukaryotes* but also *prokaryotes*. To describe the facts, ammonia oxidizing organism (AOO) and nitrite oxidizing organism (NOO) were suggested to be utilized (Corominas et al., 2010). In this study, the names of AOO and NOO will be utilized.

AOO is responsible for ammonia oxidation changing NH_4^+ into NO_2^- according to following Eq.1.1-1.3 (Kowalchuk and Stephen 2001). AOO first use the membrane-bound enzyme AMO to catalyze the oxidation of ammonia to hydroxylamine (NH_2OH) shown in Eq.1.1, this process requires one

oxygen (O₂), two protons, and two electrons. One O is inserted into NH₃ to form NH₂OH, and the other O is combined with the two protons and electrons to form H₂O (Wood, 1986; Hooper et al., 1997; Poughon et al., 2001). After the oxidation of NH₃ to NH₂OH, in the periplasmic space, HAO is used to catalyze the oxidation of NH₂OH to NO₂⁻ shown in Eq.1.2. In this process, four electrons are released and channeled through the tetraheme cytochrome C₅₅₄, C₅₅₂ to ubiquinone pool where electrons are partitioned, two electrons go to support further ammonia oxidation by AMO. And two electrons pass through the electron transport chain to generate a proton gradient for ATP generation and to provide a reductant for other cellular processes shown in Fig.1.2. The final oxidation reduction reaction that the two electrons attended by Cytaa3 oxidase can be expressed by Eq.1.3. It needs to be mentioned that electrons released from NH₂OH oxidation are not expected to have a forward flow through NADH oxidoreductase as shown in Fig.1.2.



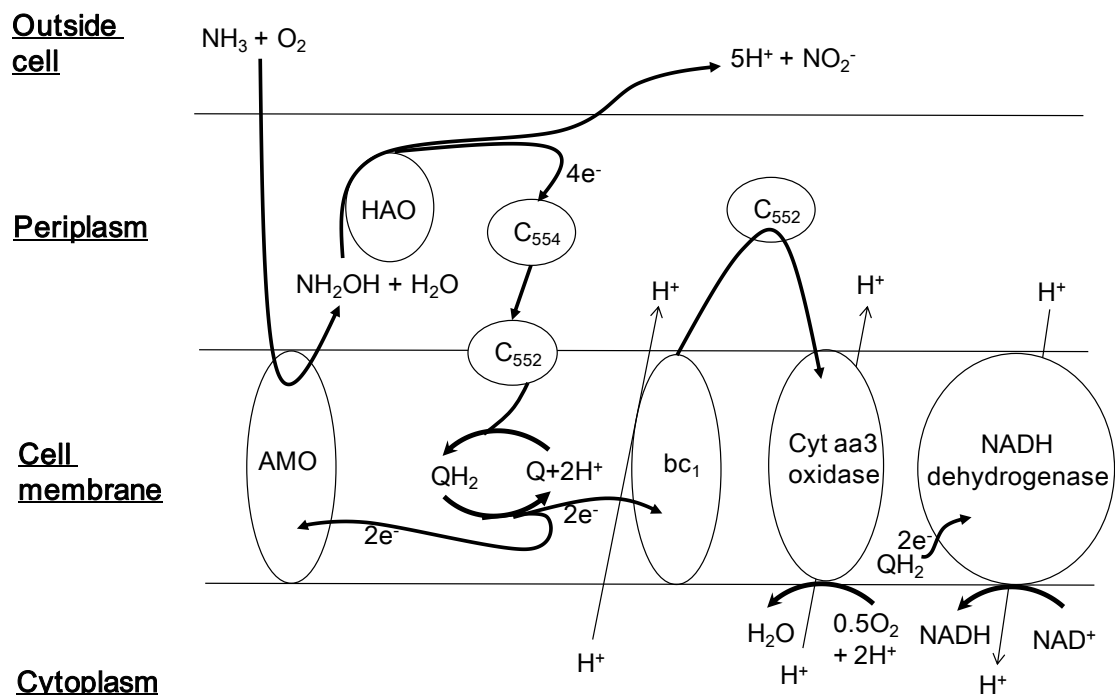


Figure 1. 2 Biochemical pathway for ammonia oxidation (Hopper *et al.*, 1997; Arp & Stein, 2003)

- | | |
|------------------------------------|--|
| AMO – ammonia monooxygenase; | C552 –cytochrome c552; |
| HAO– hydroxylamine oxidoreductase; | C554–cytochrome c554 |
| P460 – cytochrome P460; | bc_1 –cytochrome $\text{bc}1$ |
| Q –Ubiquinone-8; | Nick – nitrite reductase; |
| QH_2 –Quinol; | Cytaa3 oxidase– cytochrome oxidase; |

The NOO is responsible for nitrite oxidation changing NO_2^- into NO_3^- . The empirical mechanism was described by Eq.1.4 and Eq.1.5. The oxidation of one molecule of nitrite produces 2H^+ and 2 molecules electrons shown in Eq.1.4, then 0.5 molecule O_2 is combined with the two protons and electrons to form H_2O shown in Eq.1.5. As the details of energy generation from NO_2^- oxidation are still uncertain and primarily due to limited research and few publications, the sample transport process was shown in Fig.1.3.

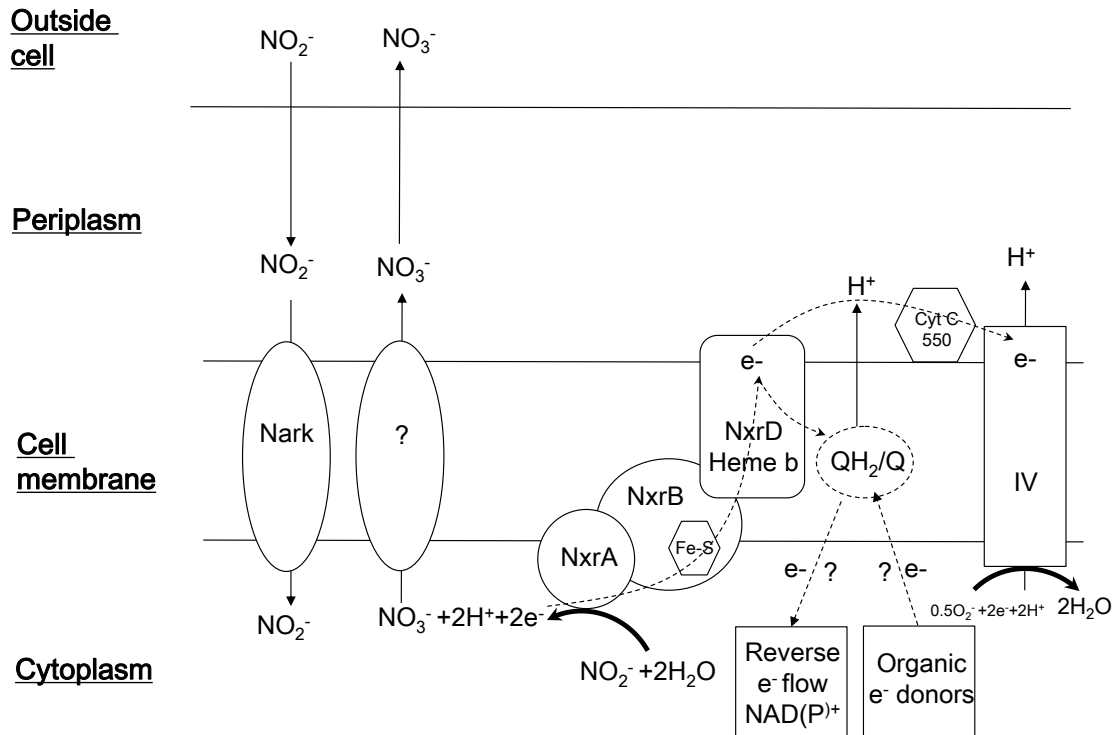


Figure 1. 3 Biochemical pathway for nitrite oxidation in *Nitrobacter*. (Bess *et al.*, 2011)

Nark – Membrane protein Nark;

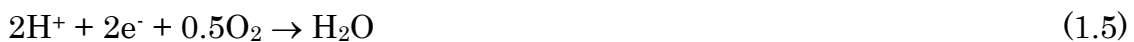
NxrD– Nitrite oxidizing enzyme D;;

NxrA– Nitrite oxidizing enzyme A;

QH₂ –Quinol;

NxrB– Nitrite oxidizing enzyme B;

CytC550 –cytochrome c550;



1.2.2 Denitrification

Denitrification is the biological oxidation of nitrate to nitrite and then nitrogen gas, in this process nitrogen gas can be in the form of NO, N₂O and N₂ according to different oxidation station of nitrogen shown in Figure. 1.1.

The complete denitrification process can be expressed as in Eq. 1.6.



Except traditional N-removal process, a new BNR process – anaerobic ammonia oxidation (ANAMMOX) process that can produce nitrogen gas by ammonia and nitrite exists shown in Fig. 1.1 that process was linked and marked by dotted lines. The ANAMMOX process has the advantages of less energy consumption and no need for COD input.

With the development of biological wastewater treatment technology especially ANAMMOX, partial nitrification (from ammonia to nitrite) became a key step to achieve ANAMMOX process. To achieve partial nitrification, the inhibition of NOO's activity while maintains AOO's activity became a focal research point.

1.3 Development of Activated Sludge Model (ASM)

Modelling of activated sludge processes has become a common part of the design and operation of wastewater treatment plants. Today models are being used in design, control, teaching and research (Henze *et al.*, 2000).

A task group on mathematical modeling for design and operation of activated sludge processes was established by the International Association on Water Pollution Research and Control (IAWPRC) in 1982. The aim of the task group was to create a common platform that could be utilized for future model development for nitrogen-removal processes using activated sludge. It required the developed model to be easy to use with minimum complexity. In 1986 the first IAWQ model named ASM1 was constructed and incorporated into a basic model for COD removal, oxygen demand, bacterial growth and biomass degradation. An example process kinetics and stoichiometry using heterotrophic bacteria for growth and decay in an aerobic environment was shown in Table 1.1

In ASM1, nitrification was expressed as a one-step process from ammonia to nitrate. The process kinetics and stoichiometry for nitrification was shown in Table 2. Inhibition in ASM1 was described using substrates (S_s , O_2) Monod-type function. In extended models based on ASM1, ASM2, ASM2d, and ASM3 were developed using Monod-type expressions on the growth

stage.

Table 1. 1 Process kinetics and stoichiometry for heterotrophic bacterial growth in an aerobic environment

| component→ | i | 1 | 2 | 3 | Process Rate, ρ_j |
|--|---|-----------------------------|-------------------------------|---|--|
| j process ↓ | | X_B | S_S | S_O | $[ML^{-3}T^{-1}]$ |
| 1 Growth | | 1 | $-1/Y$ | $-(1-Y)/Y$ | $\frac{\mu_{max} S_S}{K_S + S_S} X_B$ |
| 2 Decay | | -1 | | -1 | bX_B |
| Stoichiometric parameters: Y: True growth yield | | Biomass $[M(COD)L^{-3}]$ | Substrate $[M(COD)L^{-3}]$ | Oxygen (negative COD) $[M(-COD)L^{-3}]$ | Kinetic parameter: μ_{max} : Maximum specific growth rate K_S : Half-saturation coefficient. b: Decay rate (d^{-1}) |

Table 1. 2 Process kinetics and stoichiometry for nitrification

| component → | i | S_{NH4} | S_{NO3} | S_{O2} | $X_{B,A}$ | X_{CB} | X_U | Process Rate, ρ_j [$ML^{-3}T^{-1}$] |
|--|--------|-------------------------------|---------------------------------|--|--|--|---|--|
| j process ↓ | | | | | | | | |
| 1 | Growth | $i_{XB} - \frac{1}{Y_A}$ | $1/Y_A$ | $-\frac{4.57 - Y_A}{Y_A}$ | 1 | | | $\frac{\mu_{max,A} S_S}{K_S + S_S} \frac{S_O}{K_{O,A} + S_O} X_B$ |
| 2 | Decay | | | | -1 | $1 \cdot f_U$ | f_U | $b_A X_{B,A}$ |
| Stoichiometric parameters: Y_A : Autotrophic yield. f_U : Fraction of biomass yielding particulate products. i_{XB} : Mass N/Mass COD in biomass. | | Biomass [$M(COD)L^{-3}$] | Substrate [$M(COD)L^{-3}$] | Oxygen (negative COD) [$M(-COD)L^{-3}$] | Active autotrophic [$M(COD)L^{-3}$] | Slowly biodegradable substrate [$M(COD)L^{-3}$] | Particulate products arising from biomass decay [$M(COD)L^{-3}$] | Kinetic parameter: $\mu_{max,A}$: Autotrophic maximum specific growth rate. K_S : Half-saturation coefficient. b_A : Autotrophic decay rate. |

1.4 Research Objective

In the BNR process, inhibition was focused on with in-depth study on the development of new technology, for instance single reactor systems for high ammonia removal over nitrite (Sharon), and ANaerobic AMmonia Oxidation (ANAMMOX) (van Dongen et al., 2001).

Biological reactions often experience inhibition conditions from high concentration of substrates, reaction products or other external inhibitory compounds. The inhibitory compounds may affect the enzymatic system leading to different forms of competitive, non-competitive or uncompetitive reversible enzyme inhibition. In other situations, the concentration of inhibitory compounds could result in poisoning leading to irreversible inhibition. There are several mathematical models to express reversible inhibition, however the recovery/adaptation phenomenon is not well described by these models. Furthermore, the modelling approaches for irreversible inhibitions are not well developed.

In previous researches, AOO and NOO were selected as study object for substrate inhibition, due to the fact that they can be inhibited by their own substrates, ammonia and nitrite are the intermediates and products of the nitrification process. In AOO reaction, pH changes significantly by ammonia oxidizing to nitrite, and pH in NOO reaction changes very slight by nitrite oxidizing to nitrate. In this study NOO was selected to explore and model the

inhibition phenomenon.

The objectives of this study are as follows:

1. To verify and evaluate irreversible inhibition acting on decay stage.
2. To construct a new function to describe the irreversible inhibition.
3. To combine the reversible and the irreversible inhibition into one model, simulating OUR using different inhibitory concentrations.
4. Model simulation to verify the benchmark datasets.

The thesis content was composed by 7 chapters.

In chapter 1, the research background is introduced identifying the research objectives. Previous research about nitrification, inhibition, models are discussed in chapter 2. Reversible inhibitions acting on growth stage were studied in many previous research, while there is limited documentation about irreversible inhibition acting on decay stage. To contribute to research filed, NOO batch tests were operated under different nitrite concentrations with live/dead staining to verify irreversible inhibition in chapter 3, and a model with irreversible function acting on decay stage was suggested. In chapter 4, a model combining reversible inhibition with irreversible inhibition of FNA and FA was constructed, and six datasets from batch tests using different concentrations of nitrite and ammonia as substrates were simulated successfully using the model. Four benchmark datasets published by IWA and a continuous operation to achieve partial nitrification in the lab were simulated successfully using irreversible inhibition model in chapter 5. In

chapter 6, three sets of bioaugmentation datasets with nitrifiers development from different substrates were simulated to verify the bioaugmentation ability according to obtained kinetics from simulation. The research is then summarized in chapter 7.

2. Previous Researches

2.1 Nitrification process

Nitrification and denitrification as the key processes in biological N-removal from wastewater are carried out by nitrifying bacteria and denitrifying bacteria separately.

In the nitrification process, the two steps are carried out by distinct group of bacteria: ammonium is firstly oxidized to nitrite by autotrophic ammonia oxidizing organism (AOO), then nitrite is oxidized to nitrate by autotrophic nitrite oxidizing organism (NOO) as mentioned in Chapter 1.

In wastewater treatment plants, the most common AOO belong to the genus *Nitrosomonas*. Other genera with similar capability include *Nitrosococcus*, *Nitrospira*, *Nitrosolobus*, and *Nitrosorobrio* (Painter, 1970). And in activated sludge system, *Nitrobacter spp.* has been believed to be most common nitrite oxidizer. However some recent researches suggest that *Nitrospira*-like bacteria are the dominant NOO in wastewater treatment systems (Schramm *et al.*, 1998). Additionally, there are other genera capable of oxidizing nitrite to nitrate for energy including *Nitrococcus*, *Nitrospina* and *Nitrocystis* (Metcalf and Eddy, 2003). AOO and NOO are referred collectively to as nitrifiers in one-step nitrification process. Although AOO and NOO can exist in similar conditions and were classified together, they

are not related phylogenetically. The microbial ecology of ammonia oxidizing bacteria (AOB) and nitrite oxidizing bacteria (NOB) relevant to activated sludge is given in Figure.2.1

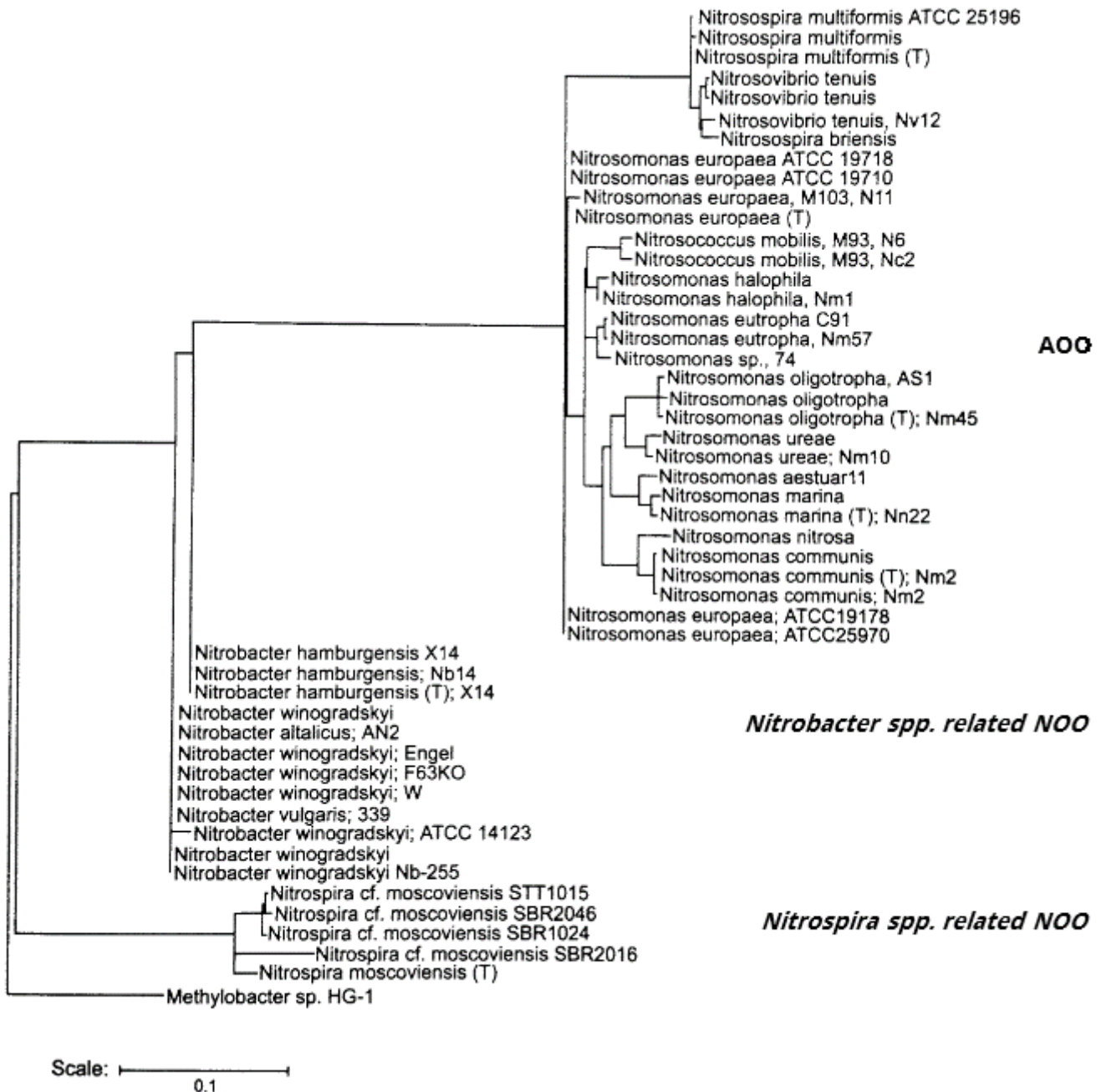
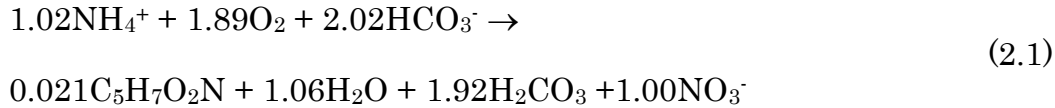


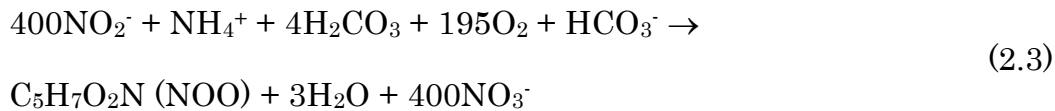
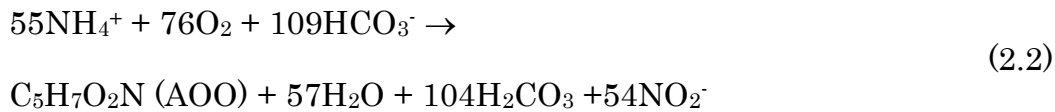
Figure 2. 1 Microbial ecology and phylogenetic diversity of ammonia oxidizing bacteria and nitrite oxidizing bacteria relevant to activated sludge (WEF, 2010).

2.2 Kinetics in nitrification

According to Gujer and Jenkins's researches (1974), the overall nitrification reaction can be summarized as in Eq. (2.1):



To explore oxidation by AOO and NOO separately, one research was reported by Haug and McCarty (1972) noted that the oxidation of 100 mg of ammonia to nitrate resulted in the production of 14.6 mg of AOO biomass and 2.0 mg of NOO biomass, as follows Eq. (2.2) and (2.3):



Nitrification typically limits overall traditional biological nitrogen removal process due to lower specific growth rates and higher sensitivity to environmental factors such as temperature, pH and the presence of organic chemicals and heavy metals in nitrifying microorganism (Grady *et al.*, 1999). Further, the nitrifying bacteria including AOO and NOO can also be inhibited by their own substrates, the intermediates and products of the nitrification process, ammonia and nitrite. Therefore, to ensure proper

design and operation of bioreactors for nitrogen removal, it is essential to obtain estimates of the kinetics of nitrification.

The Monod equation is utilized to describe the effect of substrates on bacterial growth that was found by Monod in 1949 (Monod, 1949). If assuming no alkalinity limitation, the bacterial growth rate can be expressed using Eq. (2.4) taking AOO as an example:

$$\mu_{AOO} = \mu_{\max,AOO} \left(\frac{S_{NH_4}}{S_{NH_4} + K_{S,NH_4,AOO}} \right) \left(\frac{S_{O_2}}{S_{O_2} + K_{S,O_2,AOO}} \right) \quad (2.4)$$

Where,

μ_{AOO} : Specific growth rate of AOO biomass, d⁻¹;

$\mu_{\max,AOO}$: Maximum specific growth rate of AOO, d⁻¹;

S_{NH_4} : Ammonia concentration, mg-N/L;

$K_{S,NH_4,AOO}$: Half-saturation coefficient for AOO, mg-N/L

S_{O_2} : Dissolved oxygen concentration of bulk mixed liquor or wastewater, mg-O/L;

$K_{S,O_2,AOO}$: Oxygen half-saturation coefficient for AOO, mg-O/L

Since NOO can use both ammonia and nitrite as nitrogen sources as shown in Eq.2.3. As the ammonia is much less than nitrite as NOO substrate, if considering NH₄⁺-N as the nitrogen source, the specific NOO growth rate equation can be expressed as follows Eq. (2.5):

$$\mu_{NOO} = \mu_{\max,NOO} \left(\frac{S_{NH4}}{S_{NH4} + K_{S,NH4,NOO}} \right) \left(\frac{S_{O2}}{S_{O2} + K_{O2,NOO}} \right) \left(\frac{S_{NO2}}{S_{NO2} + K_{S,NO2,NOO}} \right) \quad (2.5)$$

Where,

μ_{NOO} : Specific growth rate of NOO biomass, d⁻¹;

$\mu_{\max,NOO}$: Maximum specific growth rate of NOO, d⁻¹;

S_{NH4} : Ammonia concentration, mg-N/L;

$K_{S,NH4,NOO}$: Half-saturation coefficient for NOO, mg-N/L

S_{O2} : Dissolved oxygen concentration of bulk mixed liquor or wastewater, mg-O/L;

$K_{S,O2,NOO}$: Oxygen half-saturation coefficient for NOO, mg-O/L

S_{NO2} : Nitrite concentration, mg-N/L;

$K_{S,NO2,NOO}$: Nitrite half-saturation coefficient for NOO, mg-N/L

In the above example growth functions, there is a important parameter “K” that represents a half-saturation coefficient for different bacterial organism. “K” determines how rapidly μ approaches μ_{\max} in Monod equations in terms of the substrates concentrations. The value of "K" is defined as the substrate concentration at which μ is equal to half of μ_{\max} . An example relationship between “ μ_{\max} ” and “K” of AOO was shown in Fig.2.2 when DO is not assumed to be not limiting or inhibitive.

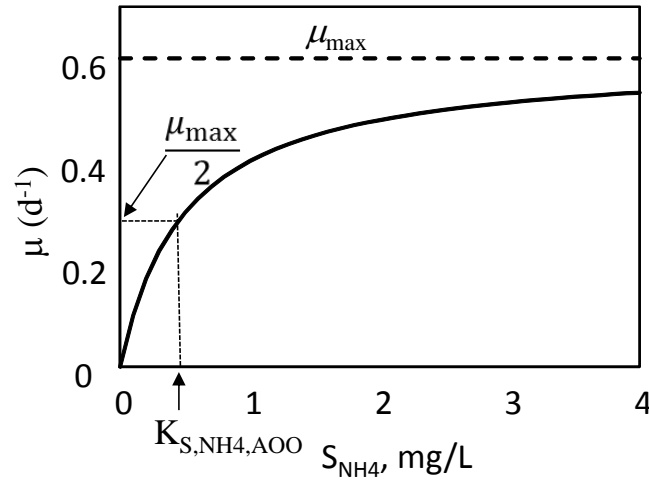


Figure 2. 2 Relationship between specific growth rate of AOO and ammonia-N concentration as predicted by Monod equation (dissolved oxygen is assumed to be no limiting)

In the nitrification process, to describe the specific growth rate, specific oxidation rates of ammonia or nitrite are approximately similar. The oxygen uptake rate (OUR) can be expressed by following equation (2.6):

$$\text{OUR} = \mu_A \cdot (1 - Y_A) / Y_A \quad (2.6)$$

Where,

OUR: specific ammonia or nitrite oxidation rate, g-N/L/d;

Y_A : yield of AOO (or NOO), g-COD/g-N

Specific inherent decay rate (b_D) is the parameter in each species of bacteria by bacterial characteristics. Form literatures the inherent decay rate values for AOO, NOO and OHO were listed in Table 2.1. The main kinetics in AOO and NOO in previous researches was shown in Table 2.2 and Table 2.3

Table 2. 1 Estimated aerobic decay rates at 20°C in conventional activated sludge (CAS) and membrane bioreactor (MBR) system (adapted from Manser, 2006)

| System | Decay for AOO (d ⁻¹) | Decay for NOO (d ⁻¹) | Decay for OHO (d ⁻¹) |
|--------|-------------------------------------|-------------------------------------|-------------------------------------|
| CAS | 0.15±0.02 | 0.15±0.01 | 0.28±0.05 |
| MBR | 0.14±0.01 | 0.14±0.01 | 0.23±0.03 |

Table 2. 2 AOO and NOO yield values

| Reference | AOO yield (gCOD/gNH ₄ -N) | NOO yield (gCOD/gNO ₂ -N) | Y _{AOO} /Y _{NOO} |
|--------------------------------|---|---|------------------------------------|
| Knowles <i>et al.</i> , 1965 | 0.05 | 0.02 | 2.50 |
| Gee <i>et al.</i> , 1990 (a) | 0.43 | 0.132 | 3.25 |
| Gee <i>et al.</i> , 1990 (a) | 0.40 | 0.114 | 3.50 |
| Wiesmann, 1994 | 0.147 | 0.042 | 3.50 |
| Kopp and Murphy, 1995 | - | 0.015 | - |
| Schintuch <i>et al.</i> , 1995 | 0.14 | - | - |
| Hellinga <i>et al.</i> , 1999 | 0.15 | 0.041 | 3.65 |
| Chandran and Smets, 2000 | 0.28 | 0.11 | 2.61 |
| Pynaert, 2003 | 0.04-0.13 | 0.02-0.08 | - |
| Guisasola <i>et al.</i> , 2005 | 0.21 | 0.08 | 2.62 |
| Hiatt and Grady, 2008 | 0.18 | 0.06 | - |
| Sin <i>et al.</i> , 2008 | 0.11-0.21 | 0.03-0.09 | - |

Table 2. 3 Comparison of kinetics parameter for ammonia oxidizing organism (AOO) and nitrite oxidizing organism (NOO)

| Bacteria | AOO | | | | NOO | | | |
|--------------------------------|--------------------------|------------------|---------------------------------|----------------------------------|--------------------------|------------------|---------------------------------|----------------------------------|
| Kinetics | $\mu_{\max, \text{AOO}}$ | b_{AOO} | $K_{S, \text{O}_2, \text{AOO}}$ | $K_{S, \text{NH}_4, \text{AOO}}$ | $\mu_{\max, \text{NOO}}$ | b_{NOO} | $K_{S, \text{O}_2, \text{NOO}}$ | $K_{S, \text{NO}_2, \text{NOO}}$ |
| Unit | d^{-1} | d^{-1} | $\text{mg-O}_2/\text{L}$ | mg-N/L | d^{-1} | d^{-1} | $\text{mg-O}_2/\text{L}$ | mg-N/L |
| Wiesman, 1994 | 2.05 | 0.13 | 0.6 | 2.4 | 1.45 | 0.06 | 2.2 | 5.5 |
| Hellings <i>et al.</i> , 1998 | 2.10 | - | - | 0.5-7.0 | 0.02-0.17 | - | - | 0.26 |
| Hellings <i>et al.</i> , 1999 | 2.10 | - | 1.45 | 0.468 | 1.05 | - | 1.10 | 0.0014 |
| Chandran and Smets, 2000 | 0.2-0.6 | - | - | 0.5 | 0.6 | - | - | 1.5 |
| Wett and Rauch, 2003 | 4.04 | 1.0 | 0.4 | 0.13 | 3.21 | 0.87 | 1.0 | 0.3 |
| Pynaert, 2003 | 0.3-2.2 | - | 0.03-1.3 | 0.06-27.5 | 0.2-2.5 | - | 0.3-2.5 | 0.1-15 |
| Carrera <i>et al.</i> , 2004 | - | - | - | 0.2 | - | - | - | 0.00012 |
| Van Hulle, 2004 | 1.0±0.2 | - | 0.94±0.091 | 0.75±0.052 | - | - | - | - |
| Manser <i>et al.</i> , 2005 | - | 0.15 | 0.8 | 0.14 | - | 0.22 | 0.8 | 0.28 |
| Guisasola <i>et al.</i> , 2005 | - | - | 0.74±0.02 | - | - | - | 1.75±0.01 | - |
| Magri <i>et al.</i> , 2007 | 4.55 | 0.08 | 0.75 | 0.88 | 1.2 | 0.007 | 1.22 | 0.004 |
| Iacopozzi <i>et al.</i> , 2007 | 0.6313 | 0.061 | 0.5 | 2.0 | 1.0476 | 0.061 | 0.5 | 0.5 |
| Sin <i>et al.</i> , 2008 | 0.5-2.1 | 0.15 | 0.5-3.0 | 0.14-5.0 | 0.9-1.8 | 0.15 | 0.3-1.1 | 0.05-3.0 |
| Hiatt and Grady, 2008 | 0.78 | 0.096 | - | - | 0.78 | 0.096 | 1.2 | - |

2.3 Inhibition model

2.3.1 Reversible inhibition

Different kinds of reaction rate expressions including zero-order, first-order and Monod type have been proposed and experimentally determined for the nitrification process (Hassan, 1981, 1987). At present, these kinds of expression types are utilized and applied to describe biological reaction rate. Based on Monod-type expression, some reaction rates were developed to describe inhibition or limitation on growth stage.

The zero-order reaction rate is independent of substrate concentration shown in Eq. 2.7, in batch test condition, (dS/dt) of Eq.2.8 is the rate of consumption of substrate due to oxidation and K_0 is the zero-order rate constant. When initial $S = S_0$ at $T = 0$, the Eq. 2.9 can be obtained from Eq. 2.7 and Eq. 2.8.

$$r = K_0 \quad (2.7)$$

$$-\frac{dS}{dt} = K_0 \quad (2.8)$$

$$S = S_0 - K_0 t \quad (2.9)$$

The first-order reaction rate is a proportion to the first power of reactant concentration shown in Eq. 2.10, Where K_1 is the first-order reaction rate constant. When $S = S_0$ at initial phase of reaction, the solution (S) can be calculated by Eq.2.11.

$$-\frac{dS}{dt} = K_1 S \quad (2.10)$$

$$S = S_0 \exp(-K_1 t) \quad (2.11)$$

The Monod expression is one of the most widely used expression on microbial reaction rate kinetics (Monod, 1949), which relates the bacterial growth rate to the concentration of a single growth controlling substrate represented by the following Eq. 2.12, a relationship example was shown in Fig. 2.2 of last section. In batch test, the relationship of substrate concentration and reaction time (t) can be expressed by Eq. 2.13.

$$\mu = \mu_{\max} \frac{S}{K_S + S} \quad (2.12)$$

$$S = S_0 - \mu \cdot t \quad (2.13)$$

Where μ is specific growth rate of mixed microbial culture(d^{-1}), S is limiting substrate concentration($mg\text{-}S/L$), μ_{\max} is maximum specific growth rate of the culture (d^{-1}), K_S is half saturation constant ($mg\text{-}S/L$).

When $S \gg K_S$, Eq. (2.12) becomes to first-order expression, while $S \ll K_S$, it becomes a zero-order expression.

Inhibition is an important issue in biological reaction, if bacterial activity can be recovered absolutely upon removal of the inhibitor, this kind of inhibition is called reversible inhibition (Hassan, 1987). Though different researches (Kumar *et al.*, 2005; Nuhoglu and Yalcin, 2005; Okpokwasili and Nweke, 2005) several mathematical models were proposed to express the culture growth and substrate utilization. Bacterial growth can be modeled by

simple Monod equation (Kovarand Egli, 1998). However this equation cannot be utilized to describe a phenomenon of growth in presence of some inhibitory substance. The Haldane-type inhibition function can be utilized traditionally to express the growth in both lower and higher concentrations of inhibitory substances. Haldane-type function was shown in Eq. 2.14 (Wang and Loh, 1999):

$$\mu = \mu_{\max} \frac{S}{K_S + S + \frac{S^2}{K_I}} \quad (2.14)$$

Where K_I is the substrate inhibition constant (mg-S/L).

Due to its advantage of broad applicability, Haldane-type function was widely adopted by most of researchers. However there are others types of function to describe inhibition developed by researchers.

Aiba *et al.* (1968) developed a function to express bacterial growth rate as Eq. (2.15):

$$\mu = \mu_{\max} \frac{S \exp\left(-\frac{S}{K_I}\right)}{K_S + S} \quad (2.15)$$

Based on a theoretical study on the dynamic behavior of continuous fermentation in a single container at high concentration of rate limiting substrates, Yano and Koga (1969) proposed a growth function shown in Eq.2.16.

$$\mu = \mu_{\max} \frac{S}{K_S + S + \frac{S^2}{K_{I,1}} + \frac{S^3}{K_{I,2}}} \quad (2.16)$$

Where $K_{I,1}$, $K_{I,2}$ are the positive constants.

Based on Haldane function, Edward (Webb, 1970) proposed the modified form shown in Eq.(2.17):

$$\mu = \mu_{\max} \frac{S \left(1 + \frac{S}{K_I} \right)}{K_S + S + \frac{S^2}{K_I}} \quad (2.17)$$

Where K_I is the substrate inhibition constant.

From the above model developed by Edward, it was found that there are not many significant improvements to Haldane model (Mulchandani and Luong, 1989). So Teisser (1970) proposed and developed another function to predict substrate inhibition at higher substrate concentration shown in Eq.2.18:

$$\mu = \mu_{\max} \left[\exp\left(-\frac{S}{K_I}\right) - \exp\left(-\frac{S}{K_S}\right) \right] \quad (2.18)$$

In the research of Neufeld *et al.* (1980), phenol and FA inhibition was studied on Nitrosomonas activity using Eq. 2.19.

$$\mu = \mu_{\max} \frac{1}{\left[1 + \frac{(S_P)^{0.5}}{K_{I,P}} \right] [K_{I,N} + S_N]} \quad (2.19)$$

Where, μ is the specific growth rate (d^{-1}), μ_{\max} the maximum specific growth rate (d^{-1}), S_P is the phenol concentration (mM), S_N is the FA concentration (mM), $K_{I,P}$ and $K_{I,N}$ are the inhibitors concentrations (mg/L).

Based on Monod function, a model developed by Luong (1987) shown in Eq. 2.20 appeared to be useful for representing the kinetics of substrate inhibition. Though this function is generalized, a significant reproduction can be obtained using this function at both low and high concentrations. In this function, the maximum threshold substrate concentration S_I was included. Above S_I the reaction can be inhibited completely (Luong 1987).

$$\mu = \mu_{\max} \frac{S}{K_S + S} \left(\frac{1 - S}{S_I} \right)^n \quad (2.20)$$

Where n is an empirical constant.

A function was developed by Han and Levenspiel (1988) to express substrate degradation rate (v) shown Eq. 2.21. This function can involve a delay phenomenon, which is an exponential form and incorporates the critical product or substrate concentration corresponding to the inflection point on the growth (Han and Levenspiel, 1988; Okpokwasili and Nweke, 2005).

$$v = v_{\max} \frac{S \left(1 - \frac{S}{S_I} \right)^n}{K_S + S - \left(1 - \frac{S}{S_I} \right)^m} \quad (2.21)$$

Where v is the specific substrate degradation rate (d^{-1}), v_{max} is the maximum specific substrate degradation rate (d^{-1}), S_I is the critical inhibitor concentration (mg-S/L) above which the reactions stops, and m and n are the empirical constants.

An inhibition equation was obtained by Strous (1999) shown in Eq.(2.22) in which a power factor n was included.

$$\mu = \mu_{max} \frac{S \left(1 - \frac{S}{K_I}\right)^n}{K_S + S} \quad (2.22)$$

Where, μ is the specific growth rate (d^{-1}), μ_{max} the maximum specific growth rate (d^{-1}), S is the substrate for reactor (mM), K_I is the inhibitor concentration (mg/L), n is curve shape factor.

In present inhibition function applications, non-competitive Monod-type function that can be conversed from Haldane-type function was usually utilized shown in Eq. 2.23. The kinetics values of non-competitive Monod-type function were listed in Table 2.4 from literatures.

$$\mu = \mu_{max} \frac{S}{K_S + S} \frac{K_I}{K_I + S_I} \quad (2.23)$$

Where, μ is the specific growth rate (d^{-1}), μ_{max} the maximum specific growth rate (d^{-1}), S is the substrate for reactor (mM), K_I is the inhibitor concentration (mg/L), n is curve shape factor.

Table 2. 4 The kinetics values of non-competitive Monod-type function from literatures.

| Reference | Bacterial species | μ_{\max}/v_{\max} | K_s | S_i | K_i |
|------------------------|-------------------|--|------------------------------------|----------------|--------------------------|
| Gastens, 1981 | AOO | $\mu_{\max} = 0.528 \text{ d}^{-1}$ | 10 mg-N/L | ammonia | 30 mg-N/L |
| Gee et al., 1990 | AOO | $\mu_{\max} = 0.552 \text{ d}^{-1}$ | 0.7 mg-N/L | ammonia | 9000 mg-N/L |
| Gee et al., 1990 | NOO | $\mu_{\max} = 0.432 \text{ d}^{-1}$ | 1 mg-N/L | nitrite | 173 mg-N/L |
| Sheintuch et al., 1995 | NOO | $\mu_{\max} = 0.1272 \text{ d}^{-1}$ | 1.7 mg-N/L | nitrite | 197.8 mg-N/L |
| Henze et al., 2000 | NOO | $\mu_{\max} = 0.8 \text{ d}^{-1}$ | 0.5 mg-N/L | ammonia | 5 mg-N/L |
| Jubany et al., 2005 | NOO | $\mu_{\max} = 0.456 \pm 0.0096 \text{ d}^{-1}$ | 12.6±0.5 mg-N/L | FNA | 0.45±0.01 mg/L |
| Jubany et al., 2007 | AOO | $\mu_{\max} = 1.21 \text{ d}^{-1}$ | 0.24 mg-NH ₄ /L | FA | 7 mg/L |
| Jubany et al., 2007 | AOO | $\mu_{\max} = 1.21 \text{ d}^{-1}$ | 0.24 mg-NH ₄ /L | FNA | 0.55 mg/L |
| Jubany et al., 2007 | NOO | $\mu_{\max} = 1.02 \text{ d}^{-1}$ | 0.0004 mg-HNO ₂ /L | FA | 0.95 mg/L |
| Jubany et al., 2007 | NOO | $\mu_{\max} = 1.02 \text{ d}^{-1}$ | 0.0004 mg-HNO ₂ /L | FNA | 0.06 mg/L |
| Jubany et al., 2008 | NOO | $\mu_{\max} = 1.02 \text{ d}^{-1}$ | 0.008 mg-HNO ₂ /L | FA | 0.95 mg/L |
| Jubany et al., 2009 | AOO | $\mu_{\max} = 1.21 \text{ d}^{-1}$ | 0.34±0.06 mg-NH ₃ /L | FA | 93±14 mg/L |
| Jubany et al., 2009 | AOO | $\mu_{\max} = 1.21 \text{ d}^{-1}$ | 0.34±0.06 mg-NH ₃ /L | FNA | 0.55±0.14 mg/L |
| Kaelin et al., 2009 | OHO | $\mu_{\max} = 3 \text{ d}^{-1}$ | 0.8 mg/L | O ₂ | 0.2 mg-O ₂ /L |

Table 2.4 The kinetics values of non-competitive Monod-type function from literatures.
(Continued)

| Reference | Bacterial species | μ_{\max}/v_{\max} | K_s | S_I | K_I |
|------------------------|-------------------|---|----------------------------|---------------|--------------------------|
| Park S. & Bae W., 2009 | AOO (WWTP) | $v_{\max} = 1.1 \pm 0.15$ mg-N/mg-VSS.d | 51.3 ± 11.27 mg-N/L | FA (pH=7) | 5.2 ± 1.48 mg/L |
| Park S. & Bae W., 2009 | AOO (SBR) | $v_{\max} = 0.9 \pm 0.108$ mg-N/mg-VSS.d | 37.2 ± 8.34 mg-N/L | FA (pH=7) | 22.3 ± 36.12 mg/L |
| Park S. & Bae W., 2009 | AOO (SBNR) | $v_{\max} = 0.9 \pm 0.03$ mg-N/mg-VSS.d | 24.5 ± 2.74 mg-N/L | FA (pH=7) | 27.3 ± 2.82 mg/L |
| Park S. & Bae W., 2009 | NOO (WWTP) | $v_{\max} = 0.3 \pm 0.08$ mg-N/mg-VSS.d | 7.8 ± 4.88 mg-N/L | FNA (pH=7) | 0.09 ± 0.04 mg/L |
| Park S. & Bae W., 2009 | NOO (SBR) | $v_{\max} = 1.27 \pm 0.01$ mg-N/mg-VSS.d | 11.9 ± 0.28 mg-N/L | FNA (pH=7) | 0.19 ± 0.01 mg/L |
| Park S. & Bae W., 2009 | NOO (SBNR) | $v_{\max} = 0.07 \pm 0.01$ mg-N/mg-VSS.d | 23.3 ± 8.73 mg-N/L | FNA (pH=7) | 0.32 ± 0.01 mg/L |
| Hellinga et al., 1999 | AOO | - | 3.3 mM | FNA | 15 μ M |
| Hellinga et al., 1999 | NOO | - | 0.15 mM | FNA | 19 μ M |
| Magri et al., 2007 | AOO | - | 4.5 mM | FA | 3300 μ M |
| Magri et al., 2007 | AOO | - | 4.5 mM | FNA | 17 μ M |
| Magri et al., 2007 | NOO | - | 0.48 mM | FA | 1400 μ M |
| Magri et al., 2007 | NOO | - | 0.48 mM | FNA | 165 μ M |
| Van Hulle et al. 2007 | AOO | - | 5.3 mM | FNA | 146 μ M |
| Carvallo et al., 2002 | AOO | - | 0.79 mM | TAN | 4500 μ M |
| Carvallo et al., 2002 | NOO | - | 0.29 mM | TNN | 25 μ M |

Table 2.4 The kinetics values of non-competitive Monod-type function from literatures.

(Continued)

| Reference | Bacterial species | μ_{\max}/v_{\max} | K_S | S_I | K_I |
|------------------------|-------------------|----------------------------------|---------------|---------------------|----------------|
| Carrera et al., 2004 | NOO (SBS) | $v_{\max} = 0.56$ mg-N/L.min | 13 mg-N/L | ammonia | 384 mg-N/L |
| Carrera et al., 2004 | NOO (IBS) | $v_{\max} = 0.19$ mg-N/L.min | 33 mg-N/L | ammonia | 1910 mg-N/L |
| Carrera et al., 2004 | AOO (SBS) | $v_{\max} = 0.16$ mg-N/L.min | 1.6 mg-N/L | nitrite | 235 mg-N/L |
| Carrera et al., 2004 | AOO (IBS) | $v_{\max} = 0.162$ mg-N/L.min | 4.1 mg-N/L | nitrite | 1407 mg-N/L |
| Boon & Laudelout, 1962 | NOO | - | 1.6 mM | FNA | 13.5 μ M |
| Shafkat et al., 1987 | Nitrifier | $v_{\max} = 1.466$ mg/L.min | 2.349 mg/L | Trivalent arsenic | 273 mg/L |
| Shafkat et al., 1987 | Nitrifier | $v_{\max} = 1.466$ mg/L.min | 2.349 mg/L | Hexavalent chromium | 56 mg/L |
| Shafkat et al., 1987 | Nitrifier | $v_{\max} = 1.466$ mg/L.min | 2.349 mg/L | Fluoride | 1185 mg/L |

2.3.2 Irreversible inhibition

At present, most research works about inhibition focus on reversible inhibition on the growth stage. In ASM 1, a first-order type expression was utilized to describe the decay rate that was kept at a certain level under no-inhibition conditions. In ASM 3, inhibition functions were developed to express AOO (and NOO) decay in aerobic conditions as an oxygen dependent Monod-type function as shown as Eq. 2.24, AOO (and NOO) decay expressions in anoxic conditions as a product of an invert oxygen dependent

Monod-type function and NO_x concentration dependent Monod-type function is shown in Eq. 2.25. Based on the Monod-type function, some decay equations were developed. Some equations used to describe the decay process of NOO as an example in recently published papers on two-step nitrification were described in Table 2.5.

$$b_{AOO} = b_{\max,AOO} \frac{S_{O_2}}{K_{S,O_2} + S_{O_2}} \quad (2.24)$$

$$b_{NOO} = b_{\max,NOO} \frac{K_{S,O_2}}{K_{S,O_2} + S_{O_2}} \frac{S_{NOX}}{K_{S,NOX} + S_{NOX}} \quad (2.25)$$

Table 2. 5 Equations used to describe decay process of NOO in recently published papers on two-step nitrification. Symbols are as reported in the cited papers.

| Kinetics | Reference |
|---|-------------------------------|
| $b_{NOO,ANOX} \frac{K_{S,O_2,H}}{S_{O_2} + K_{S,O_2,H}} + b_{NOO} \frac{S_{O_2}}{S_{O_2} + K_{S,O_2,NOO}}$ | Nowak <i>et al</i> , 1995 |
| $b_{NOO} 0.5 \left(1 + \frac{S_{O_2}}{S_{O_2} + K_{S,O_2}} \right)$ | Wett and Rauch, 2003 |
| $b_{NOO,NO_3} \frac{K_{S,O_2,NOO}}{S_{O_2} + K_{S,O_2,NOO}} \frac{S_{NO_3}}{S_{NO_3} + K_{S,NO_3,NOO}} + b_{NOO} \frac{S_{O_2}}{S_{O_2} + K_{S,O_2,NOO}}$ | Iacopozzi <i>et al</i> , 2007 |
| $b_{NOO} \frac{S_{O_2}}{S_{O_2} + K_{S,O_2,NOO}}$ | Jubany <i>et al</i> , 2009 |
| $b_{NOO} \frac{S_{O_2}}{S_{O_2} + K_{S,O_2,H}} + b_{NOO} \cdot \eta_{H,end} \frac{K_{I,O_2,H}}{S_{O_2} + K_{I,O_2,H}} \frac{S_{NO_3}}{S_{NO_3} + K_{S,NO_3,H}}$ | Kaelin <i>et al</i> , 2009 |
| $b_{NOO} \frac{S_{O_2}}{S_{O_2} + K_{S,O_2,NOO}} + b_{NOO,ANAER}$ | Munz <i>et al</i> , 2011 |

2.4 Nitrification inhibition by FNA and FA

2.4.1 FA and FNA inhibition

In the biological nitrogen removal process, FA and FNA produce a negative effect. In 1976, Anthonisen *et al.* found that FA can inhibit both AOO and NOO, the range of FA concentration that begins to inhibit AOO is 10 to 150 mg/L, and the range of FA concentration that begins to inhibit NOO is 0.1 to 1 mg/L. FNA rather than NO_2^- inhibits NOO. The inhibition of nitrifying organisms was initiated between 0.22 and 2.8 mg/L.

According to Yarbrough *et al.* (1980), nitrite is inhibitory to a wide range of physiological types of bacteria. A non-competitive Monod-type kinetic expression was established to express nitrite inhibition by Wett & Rauch (2003), as well as a competitive Monod-type kinetic expression by van Loosdrecht *et al.* (1999) and Ni *et al.* (2008). Partial nitrification can be maintained if the activity of NOO is properly inhibited. In fact this is possible and has been verified in continuous operation (Zimmerman *et al.*, 2004). The inhibition of NOO is mainly due to the presence of high concentrations of nitrite in the bulk liquid that inactivates NOO due to its toxicity. In recent decades, inhibition has been extensively studied to evaluate the nitrite concentration effect on NOO's reaction rate (Seung, 2002; Munz, 2011) whereas there is limited information about the response of growth and decay for NOO especially in a full-scale operation and at which stage the inhibition acts on. At present, a non-competitive and/or competitive

Monod-type expression seem to be applied to express the reduction of nitrite oxidation rate when NOO is exposed to nitrite (Dunn *et al.*, 1985; Wett & Rauch, 2003; Manser *et al.*, 2005; Ni *et al.*, 2008; Jubany *et al.*, 2009). Based on this phenomenon it is possible to deduce that NOO's growth corresponds to the apparent reaction rate. However, nitrite may also accelerate decay.

Some reports stated that NOO activity is temporary. Suthersan & Ganczarczyk and Turk & Mavinic (1989) reported that AOO or NOO has time endurance.

2.4.2 Physiological reason for FA and FNA toxicity

The physiological reason of ammonia and nitrite toxicity had been researched by some studies. Most researchers considered that ammonia and nitrite toxicity are associated with energy generation and destroy bacterial membranes ((Fromm and Gillette, 1968; Anthonisen 1976; Russo, 1985; Parsonage 1985; Almeida 1995; Rebelo *et al.*, 2000; Camargo and Alonso, 2006). It is reported that nitrite affect energy generation and destroys it in a wide range of bacterial types. The possible poisoning mechanism is that ammonia and nitrite transport across the cell membranes and decrease intracellular pH. When intracellular pH was changed, for reducing the pH gradient the proton motive force needs to be generates. Thus, ATP synthesis can be affected. Since ATP is the only energy for maintaining the bacterial growth and protein synthesis including enzymes, when production ability of ATP becomes weak, the organisms function becomes weak or dies. An explain that the gill sodium pump ($\text{Na}^+\text{-K}^+\text{-ATP}$) activity was been affected

by NH_4^+ and NO_2^- also was documented (Pilar *et al.*, 2002; Eddie, 2007).

Additionally, NH_4^+ and NO_2^- increasing offspring mortality (Vorhees *et al.*, 1984) and mutagenicity (Luca *et al.*, 1987) using vivo and vitro experiments was reported. The documented reason of nitrite toxicity is the effect on multiplication, especially the chromosome. When the concentration of NH_4^+ or NO_2^- is higher than a certain set value, the deformity ratio of chromosome increase obviously. The type of chromosome includes fracture, exchange, ring chromosome, polyploidy and so on by changing the purine bases, so that nitrite can inhibit synthesis of amino acids that are used for synthesizing enzymes that can repair the injury of DNA.

2.5 Other effect factors on nitrifiers activity

Except FNA and FA, other main factors that affect nitrite accumulation in the nitrification process are pH, temperature, dissolved oxygen (DO). Some reports on nitrification in activated sludge processes typically included the remark that industrial wastewater may have inhibited nitrification if not fully then at least partially. Even though zinc, heavy metals, benzene, sulphide, quinone-like compounds, detergents, cyanide, azides and some organics are known to inhibit the nitrifier growth (Tomlinson *et al.*, 1966; Hill *et al.*, 1975; Hockenbury and Grady, 1977; Sharma & Ahlert, 1977; Rozich *et al.*, 1985; Blum & Speece, 1991; Nowak *et al.*, 1995; Kong *et al.*, 1996; Anette *et al.*, 1998, Mandoni *et al.*, 1999; Carrera *et al.*, 2004; Vadivelu *et al.*, 2006; Chen *et al.*, 2009; Chérif *et al.*, 2009; Breda *et al.*, 2014; Achlesh *et al.*, 2014; María *et al.*, 2010).

2.5.1 Temperature effect

In the nitrification process, temperature is important and creates a sensitivity for nitrifiers' growth rate. Although it was reported that nitrification has been shown to occur in wastewater temperature from 4 to 45°C, normally, 35-42°C is used in experiments (U.S. EPA, 1993a). Upper temperature limits for stable optimum nitrification is about 30°C with decreasing rates of nitrification on either side of this optimum. Nitrification rates approach zero as temperatures of wastewater approach 45°C. The optimum temperature is 35°C for *Nitrosomonas* and 38 °C for *Nitrobacter*. In

1965, Knowles *et al.* reported an equation for K_T , the half-saturation coefficient in nitrification process shown in Eq. 2.26.

$$\mu = \mu_{\max} \frac{N}{K_T + N} \quad (2.26)$$

$$K_T = 10^{0.05T - 1.148}$$

The most commonly accepted relationship expression between maximum nitrifier growth rate and temperature (ranging from 5 to 30°C) is shown in Eq. 2.27. The relationship could be illustrated graphically in Fig 2.3.

$$\mu_{\max} = 0.47e^{0.098(T-15)} \quad (2.27)$$

Where, μ : maximum specific growth rate of microorganism (g nitrifiers/g nitrifiers in system.d), T: water temperature (°C)

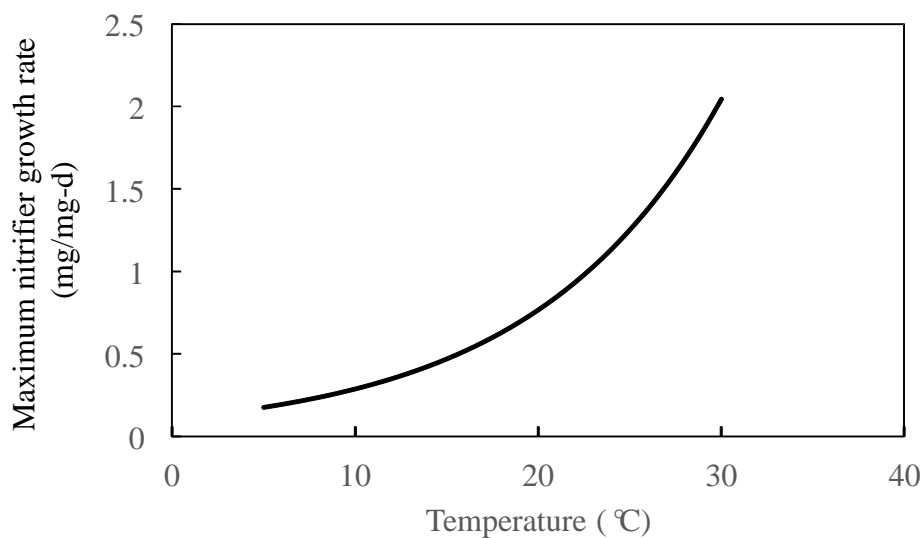


Figure 2. 3 The relationship between μ_{\max} and Temperature

2.5.2 DO effect

Since nitrifiers including AOO and NOO are obligate aerobes. This means that their activity can be kept under aerobic/oxic conditions. Nitrifiers are significantly affected by DO concentration. In ASM, DO Monod-type functions act on both growth and decay stages as shown in Eq. 2.4, 2.5, 2.24, and 2.25. Some oxygen half saturation values were summarized in Table 2.6. Apparently DO can effect nitrifiers' both growth rate and decay rate on a site-specific basis, depending on temperature, organic loading rate, SRT and diffusional limitations. Generally DO 2.0 mg/L has been considered to be a limitation boundary for nitrifiers' growth, but the limitation value was vague. AOO and NOO have different boundary for DO effect. A simultaneous nitrification and denitrification via nitrite in 0.4 – 0.8 mg/L of DO were carried out by Guo *et al.* in 2009, while Rongsayamanont, *et al.* (2014) inhibited the activity of NOO and achieved high partial nitrification by entrapped cells at bulk DO of 2 mg/L.

Table 2. 6 Some reported oxygen half-saturation values in nitrification process

| Organism | K _o , mg-O ₂ /L | Reference |
|----------|---------------------------------------|----------------------------|
| AOO | 0.3 | Loveless and Painter, 1968 |
| | 0.25 | Peeters et al., 1969 |
| | 0.50 | Laudelout et al. 1974 |
| | 1.0 | IWAPRC, 1986 |
| | 0.4 | Hezen et al.,2000 |
| NOO | 1.84 | Peeters et al., 1969 |
| | 0.72 | Laudelout et al. 1976 |
| | 1.0 | IWAPRC, 1986 |
| | 0.4 | Hezen et al.,2000 |

2.5.3 pH effect

In biological process, undoubtedly pH is a very important factor not only for bacterial activity but also bacterial survival. In nitrification process, a neutral to slight alkaline pH is suggested. When pH deviated the proper value, bacterial activity was inhibited with respect to the maximum specific growth rate. Hall (1974) reported complete nitrification could be achieved between 7.0 and 9.4. Conversely when pH is below 6.3 nitrification process cannot be conducted. A pH switching inhibition function was suggested in Eq. 2.28.

$$I = \exp\left(-3 \frac{pH - pH_{UL}}{pH_{UL} - pH_{LL}}\right)^2, \text{ if } pH \leq pH_{UL} \quad (2.28)$$
$$I = 1, \text{ if } pH > pH_{UL}$$

Where, I: pH inhibition function ($0 < I \leq 1$)

pH: pH in system (-)

pH_{UL}: limited value of pH inhibition occurs (-)

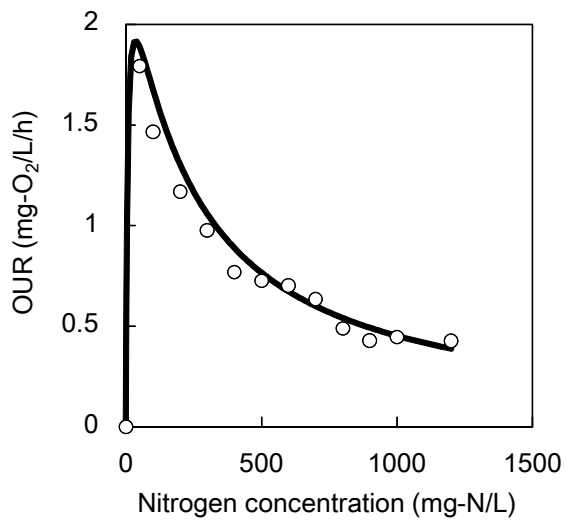
pH_{LL}: the pH value of keeping 5% maximum reaction rate (-)

In nitrification processes, since NH_4^+ and NO_2^- in substrates are toxic to nitrifiers in high concentrations in the form of FA and FNA, the effects of pH contributed significantly to FA and FNA concentrations (Makinia,2010).

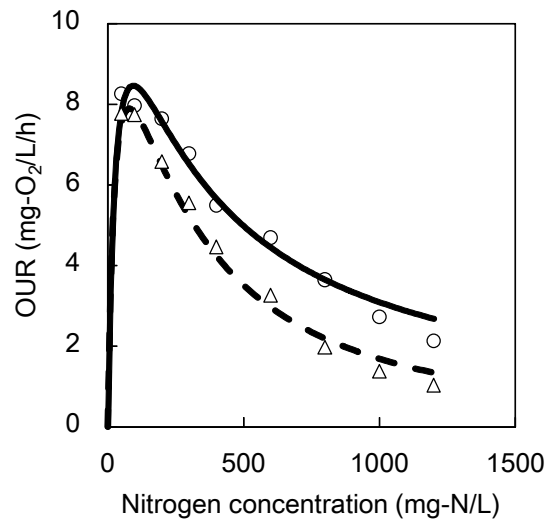
A very clear relationship map cannot be obtained strictly from the previously obtained research data, however NOO maximum specific growth rate at low SRT is relatively high from the Fig. 2.4 One of the supposed reasons of different values under different SRT was that bacterial species composition changed with SRT operation.

This is because each species of bacteria has a maximum growth rate (μ_{\max}) that is decided by bacterial characteristic itself. In the reactor, when SRT was maintained longer than maximum growth rate of a certain species of bacteria, bacteria can be kept in reactor, unless, it could be washed out of reactor if the operation time was long enough.

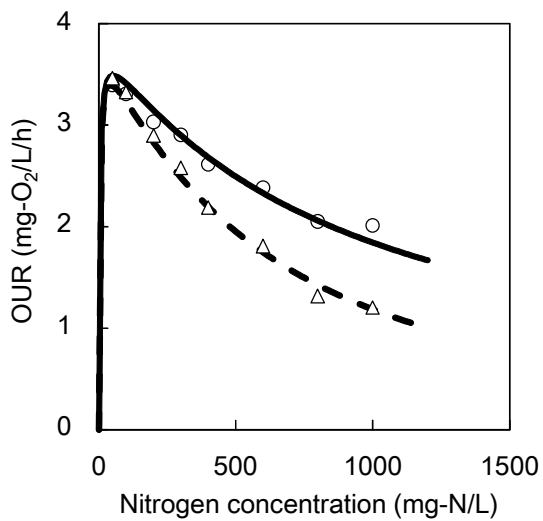
In different periods (2010. Mar., 2011. Dec., and 2012.Oct.) of NOO training experiment, short-time batch tests (each test took 15 minutes) using NO_2^- or NO_3^- and NH_4^+ as substrates were operated for kinetics check. The N molecule ratio of nitrite and ammonia was kept at 1. Non-competitive Monod-type was utilized to simulate the pilots obtained from batch tests shown in Fig. 2.5. The kinetics values were shown in Table 2.7. From the change of kinetics values, it can be summarized that bacterial kinetics change in operation period probably due to change of bacterial species.



Batch test in Mar. of 2010



Batch test in Dec. of 2011



Batch test in Oct. of 2012

- Batch tests with nitrite
- △ Batch tests with nitrite and ammonia (NH₄-N)/(NO₂-N)=1

Figure 2. 5 the different OUR responses of NOO under different training date

Table 2. 7 Kinetics values from three times batch tests in different periods

| No. | Date | K _S | K _{I-FNA} | K _{I-FA} |
|-----|---------|-------------------------|--------------------|-------------------|
| | | mg-NO ₂ -N/L | mg-FNA/L | mg-FA/L |
| 1 | 2010.03 | 6 | 0.018 | - |
| 2 | 2011.12 | 35 | 0.022 | 26.55 |
| 3 | 2012.10 | 3 | 0.050 | 62.32 |

Since NOO is a mix species as was mentioned in Chapter 2. *Nitrobacter spp.* and *Nitrospira spp.* are common species in wastewater sludge. According to the research of Huang et al. (2010), comparing to *Nitrobacter*, *Nitrospira* was dominant being better adapted to the low DO and shorter sludge retention times (SRT). To investigate kinetics values of NOO under inhibition conditions containing reversible and irreversible inhibition, NOO under 2 or 3 kinds of SRT (40-day, 20-day and 10-day) would be operated for a stable situation where batch test and bacterial species will be operated and analyzed in future researches.

3. Nitrite oxidising organism exogenous decay verification using live/dead staining under high nitrite concentration

3.1 Objective

Biological reactions may be inhibited by high concentration of substrate, reaction products, environmental variables (pH and temperature) or other external inhibitory compounds that were mentioned and discussed in chapter 2. Inhibition of biological reactions can cause reduced enzyme activity leading to sudden process failure and/or shift/selection of bacterial population. The inhibitory compounds may affect the enzymatic system leading to different forms of competitive, non-competitive or uncompetitive reversible enzyme inhibition. In present inhibition research, the reversible inhibition was focused on and developed well. Some functions mentioned in chapter 2 were also developed to express this kind of inhibition. In other situations, the concentration or nature of the inhibitory compound could be such as to result in toxicity leading to irreversible inhibition. Batstone *et al.* (2002) redefined toxicity and inhibition (Speece, 1996) as biocidal and biostatic inhibition respectively where inhibitory compounds and/or factors could act on the growth stage as biostatic inhibition whilst exogenous decay resulting in microbial death due to biocidal inhibition (poisoning).

Nitrification is a very important step in the biological nitrogen removal process, where NH_4^+ is oxidised to NO_2^- by AOO and NO_2^- to NO_3^- by NOO. In this process, NH_4^+ and NO_2^- exist as substrates and productions where functions were shown in Eq. 2.2 and 2.3. According to the research of Yarbrough *et al.* (1980), nitrite is inhibitory to a wide range of physiological bacterial types. Anthonisen *et al.* (1976) summarised the NH_4^+ and NO_2^- inhibition on nitrifying bacteria and pointed out free ammonia (FA) and free nitrous acid (FNA) were dominant inhibitors rather than NH_4^+ and NO_2^- . A competitive or non-competitive Monod-type kinetic expression was modelled to express such reversible inhibition (Wett & Rauch, 2003; Loosdrecht *et al.*, 1999). On the other hand, an irreversible inhibition was also mentioned in some researches (Mason *et al.*, 1986; van Loosdrecht & Henze, 1999; Manser *et al.*, 2006; Hao *et al.*, 2009).

In this study, as a continuation to clarify the biocidal effect on NOO, the death caused by FNA was monitored using a staining reagent to distinguish the living cells from the biomass. The cell numbers were counted in a set of batch tests where different FNA concentrations were kept. Based on the change (increment or decrement) the biocidal kinetics were estimated and compared with the OUR responses.

3.2 Materials and Methods

3.2.1 Enrichment of NOO sludge

Nitrifying activated sludge was collected from a domestic wastewater treatment plant using an MBR process with 100-day sludge retention time (SRT) and intermittent aeration (Kitakyushu, Japan). NOO in the sludge was enriched at 50-day SRT in a 5-L reactor with synthetic wastewater containing NaNO_2 (500 mg-N/L), NH_4Cl (1.0 mg-N/L), KH_2PO_4 (0.13 mg-P/L) and Na_2HPO_4 (1.67 mg-P/L). The pH, temperature and DO in the reactor were controlled at 7.3, 35 ± 0.5 °C and more than 5 mg- O_2 /L respectively. After 240 days of the operation, the enriched NOO sludge was used for the batch tests. Nitrite and nitrate concentrations were measured using ion chromatography (ICS-1000, Dionex, USA). The standards of nitrite and nitrate was supplied by three kinds of concentrations of 1, 5, 10 mg-N/L. 1.5 mM KOH was supplied as eluent solution, the retention time was kept at 15 minutes for one sample analysis. Ammonium nitrogen and sludge COD were analysed according to Standard Methods (APHA, 1995).

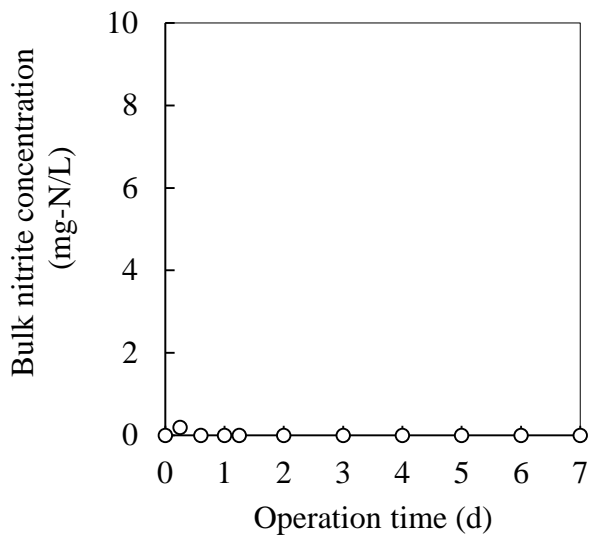
According to a mathematical model modified from Activated Sludge Model (Henze *et al.*, 2000), the dominant microorganisms in the enriched sludge was estimated to be NOO (60%) whereas small amount of ammonium oxidising microorganisms (AOO, 5%), ordinary heterotrophic microorganisms (OHO, 5%) and inert particulates (30%) were also present, which were generated as a cryptic growth from the decayed NOO biomass. The structure

of the mathematical model is discussed in later section.

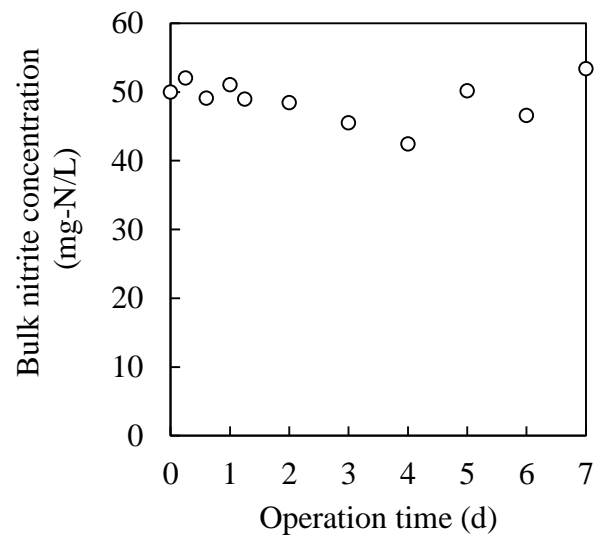
3.2.2 Inhibition test

NOO sludge was taken from the reactor and centrifugally washed with deionised water 3 times to make sure no nitrite was present in the liquid. The sludge (SS = 142.5 mg/L, VSS = 57.5 mg/L and COD = 134 mg-COD/L) was put into 4 units of 250 mL flask equipped with an aerator and its OUR, cell counting were measured for 200 hours. Using a computer-programmed syringe pump (SP-2PC, As One, Japan), the bulk NaNO_2 concentrations was maintained at about 0, 50, 500 and 2,000 mg-N/L (0, 0.029, 0.288, 1.152 mg-N-FNA/L) respectively, the measured nitrite concentrations during experimental operation were show in A-D of Fig. 3.1. The pH, DO and the temperature during these experiments were kept at 7.0 ± 0.1 , 5.0 ± 0.5 mg- O_2 /L and 35 ± 0.1 °C respectively.

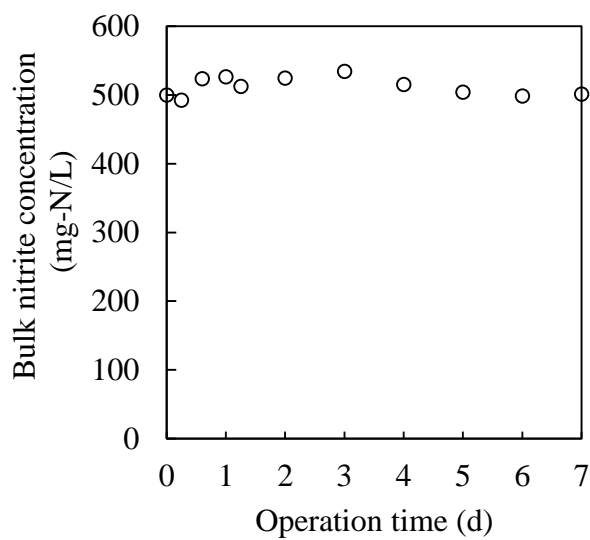
For the OUR measurement 100 mL of NOO sludge was taken from the flasks and placed in a Winkler-bottle. Pure oxygen gas was injected to set DO concentration beyond 20 mg- O_2 /L. After leaving the sludge for 15 minutes, the DO concentration in the Winkler-bottle was monitored at one-minute intervals with a DO meter (TOX-999B, Toko, Japan). Based on the slope of DO versus time, the OUR in the individual tests was determined.



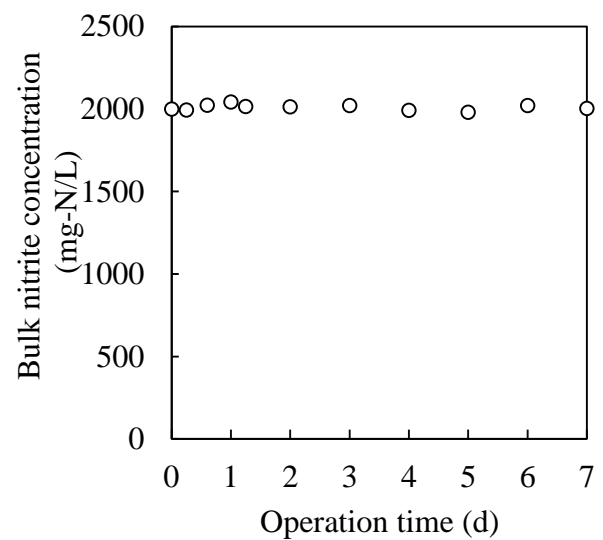
A: Nitrite concentration changes at 0 mg-NaNO₂-N/L operation



B: Nitrite concentration changes at 50 mg-NaNO₂-N/L operation



C: Nitrite concentration changes at 500 mg-NaNO₂-N/L operation

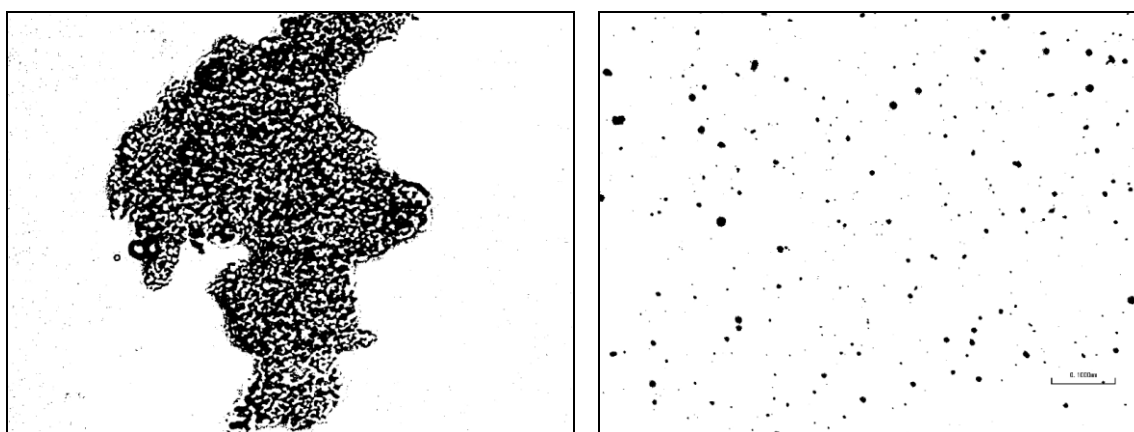


D: Nitrite concentration changes at 2000 mg-NaNO₂-N/L operation

Figure 3. 1 Nitrite concentrations change during experimental operation

3.2.3 Bacteria staining

To distinguish living and dead bacteria from the sludge, LIVE/DEAD[®] BacLight[™] bacterial viability kit (L-7012, Molecular Probes, USA) was used. The kit consisted of green fluorescent nucleic acid stain (SYTO[®] 9) and red-fluorescent nucleic acid stain (Propidium Iodide (PI)). In principle the SYTO[®] 9 (green fluorochrome) could penetrate into cells from their intact cell membrane ('living cell') because of small molecule whilst larger molecule PI (red fluorochrome) only penetrated damaged membrane ('dead cell'). When SYTO[®] 9 only was used, all bacterial cells were stained green. On the other hand, when both stains were used, PI penetrated into the 'dead' cell reduced the fluorescence from the SYTO[®] 9 resulting in cells labelled in red. In this way, the living cells (green) and the dead cells (red) could be individually counted (Hao *et al.*, 2009).



A: No treatment by ultrasonic wave B: Treatment by ultrasonic wave

Figure 3. 2 Comparison of before and after treatment by ultrasonic wave

For the preparation of staining experiments, 5 mL NOO sludge was taken

from the flasks and centrifugally washed 3 times for 3 minutes at 10,000rpm with 0.85% NaCl solution, then dispersed by ultrasonic wave (UD-200, TOMY, Japan). Since the presence of cell clusters in the sludge sample hindered the accuracy of the cell counting in microscopy, prior to the monitoring a preliminary experiment to optimise the degree of ultrasonication was conducted, the comparison of before and after treatment by ultrasonication was shown in Fig. 3.2. As shown in Fig. 3.3, it appeared that 30-45 seconds of ultrasonication showed the highest ratio of living bacteria to the total visualised cells with reasonable confidence interval. When no ultrasonication or longer treatment were performed, both experiments showed lower ratios which were attributed to poor cluster dispersion and considerable cell disruption respectively.

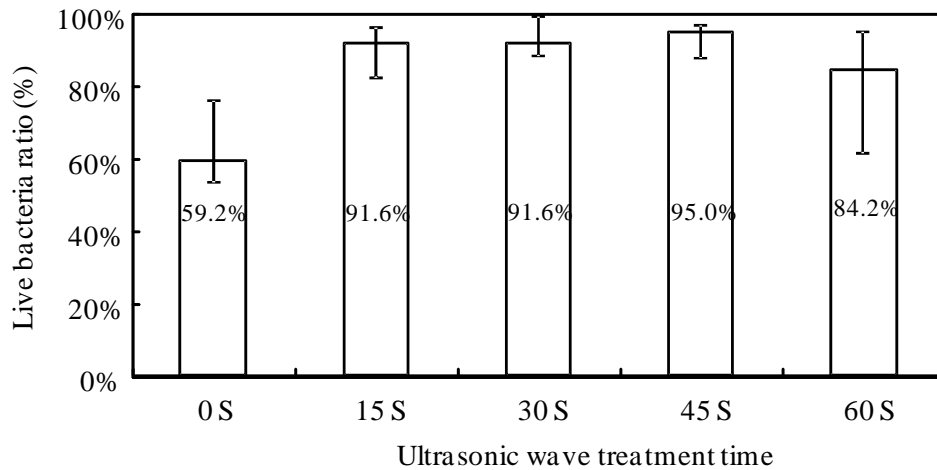


Figure 3. 3 Ratio of living bacteria to the total counted cells under different ultrasonication.

In addition when loading too much power input (more than level 3), the

countable cells decreased accordingly (data not shown). Based on the results, 45-second ultrasonication at level 3 was applied to the pre-treatment.

The dispersed sludge samples (977 μL in each testing) were transferred into 1 mL plastic tubes together with 1.5 μL of SYTO[®] 9 and 1.5 μL of PI, and incubated in the dark for 15 minutes at room temperature. Then, glass slides with stained sludge samples (10 μL on each slide) were prepared to observe and photograph with a fluorescence microscope (Nikon ECLIPSE 80i, Japan; Nikon DS-Fi2, Japan) using fluorescence filters of GFP-B (excitation at 460–500 nm and emission at LP515 nm for green fluorescence) and CY3 (excitation at 545 \pm 30 nm and emission at LP590 nm for red fluorescence) respectively (Lopez *et al.*, 2005; Hao *et al.*, 2009). The stained cell areas (μm^2) were visualised and measured with a binarised image analysing software (Quick Grain, Inotech Inc., Japan).

To calculate the average area for all population based on measured data and control the error to within a suitable range, the average area for all populations was calculated by Eq. 3.1, in which \bar{x} is the average for all samples, x_i is the value of sample No. i , U is sample standard deviation, and $F_{n-1}^1(\alpha)$ is the value under $(1-\alpha)$ confidence interval that can be obtained from appendix of statistics book.

$$\bar{x} - U \sqrt{\frac{F_{n-1}^1(\alpha)}{n}} \leq \mu \leq \bar{x} + U \sqrt{\frac{F_{n-1}^1(\alpha)}{n}}, \quad U = \sqrt{\frac{\sum (x_i - \bar{x})^2}{n-1}} \quad (3.1)$$

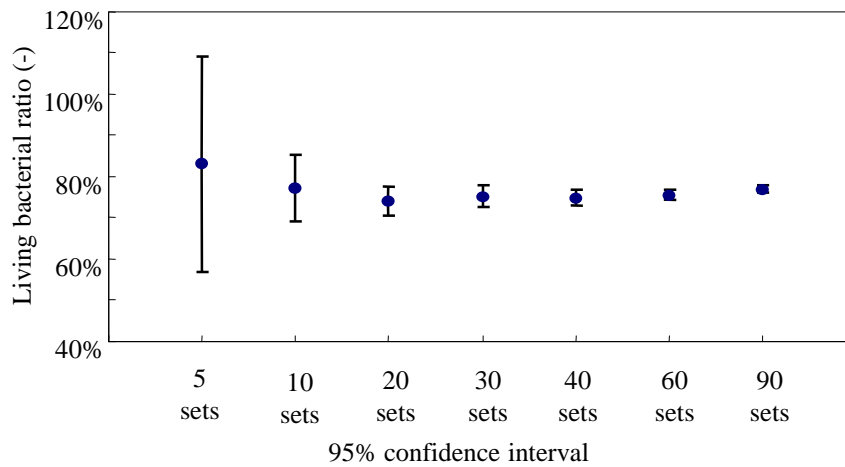
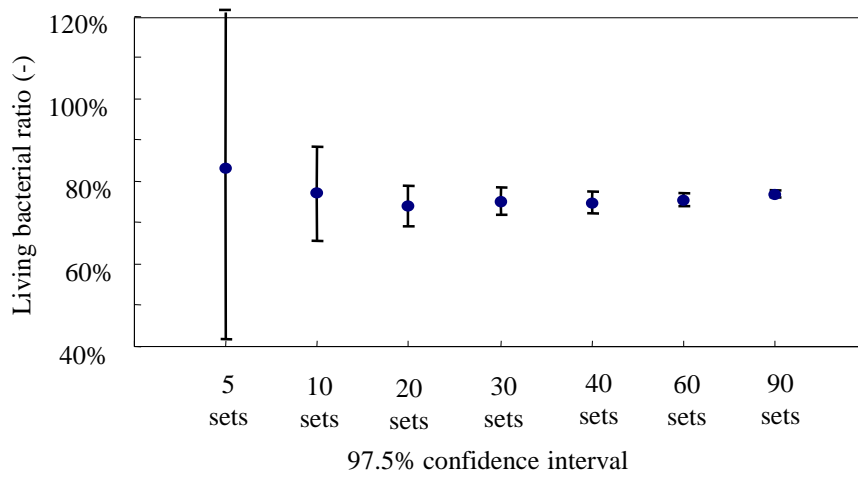
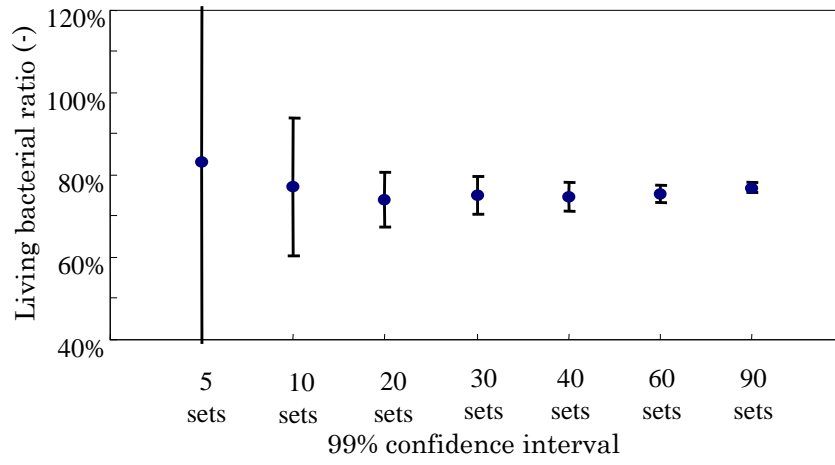


Figure 3. 4 Living bacterial ratio calculation under different sample numbers and confidence intervals.

In this experiment, 5, 10, 20, 30, 40, 60 and 90 sets of samples under 99%, 97.5%, and 95% confidence interval were calculated for a proper sample number shown in Fig. 3.4. Using 30 photo images per sludge sample, the areas were averaged and its 95%-confidence interval was statistically determined finally due to acceptable error bar (below 3%) and sample number. As the dominant microorganisms in the sample was supposed to be NOO, it was assumed that the visualised area corresponded to NOO biomass.

3.3 Results

3.3.1 Exogenous decay by FNA poisoning

When nitrite at 0, 50, 500, 2,000 mg-N/L were present in the cultivation vessels, two distinct NOO responses were observed as shown in Fig. 3.5. At 50 mg-N/L of nitrite the living NOO biomass increased exponentially at specific growth rate of 0.26 d^{-1} , whilst it decreased along with time where more than 500 mg-N/L or no nitrite as present. Comparing to the ordinary decay under without nitrite (specific decay rate, $b_{\text{NOO}} = 0.072 \text{ d}^{-1}$), the decrease of the biomass at 500 mg-N/L was remarkably quick (0.24 d^{-1}). The high decay was accelerated when higher nitrite was dosed (0.62 d^{-1}), indicating an exogenous decay took place due to poisoning by high FNA.

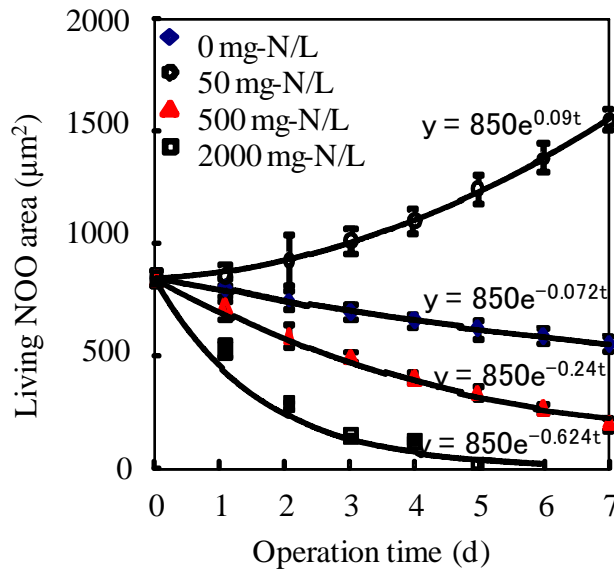


Figure 3. 5 Change of NOO stained in green (living cells with intact cell membrane) along with time

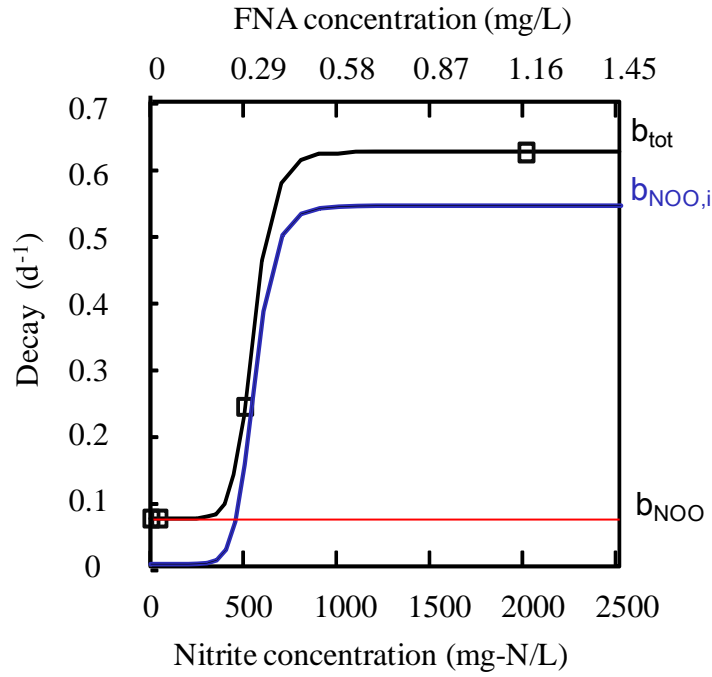


Figure 3. 6 Decay versus nitrite concentration

The specific decay rates at 0, 500, 2,000 mg-N/L were plotted against the nitrite concentration in the cultivation vessel as shown in Fig. 3.6. As the total specific decay (b_{tot}) was considered to be the consequence of the ordinary endogenous decay (b_{NOO}) and biocidal inhibition ($b_{NOO,i}$, exogenous decay), the impact of $b_{NOO,i}$ was extracted to Eq.(3.2). The set of inhibition kinetics in the equation (K_I and n) were used to draw the curve in Fig. 3.6. Due to limited datasets with three plots only, in this study it was assumed that the biocidal inhibition substantially appeared at a threshold level somewhere below 500 mg-N/L of nitrite.

$$b_{tot} = b_{NOO} + b_{NOO,i} = b_{NOO} + b_{NOO,i \max} \frac{S_{FNA}^n}{K_I^n + S_{FNA}^n} \quad \text{Eq.(3.2)}$$

Where, b_{tot} : total specific decay rate (d^{-1}), b_{NOO} : endogenous specific decay rate (d^{-1}), $b_{NOO,i}$: exogenous specific decay rate from FNA (d^{-1}) K_I : inhibition coefficient ($mg-N-FNA/L$), n : inhibition coefficient (-), S_{FNA} : FNA concentration ($mg-N-FNA/L$).

3.3.2 Cellular disintegration

The high nitrite concentration also accelerated the decomposition of 'dead cells'. Contrary to initial expectation, the NOO biomass stained in red (dead cells) decreased along with time under 500 $mg-N/L$ and 2,000 $mg-N/L$ respectively, which almost corresponded to the decrease of living NOO biomass, as shown in Fig. 3.7. The causative reason of the decrease was not clear at present but it could be explained that the penetrated high nitrite into the cells interfered the stain with the reagents and/or resulting in decrease of the fluorescence. Since the specific reaction rates to reduce the fluorescence were almost comparable to the $b_{NOO,i}$ at the given nitrite concentration, the poisoning might be attributed to reactions inside the cell as well as cell membrane.

Based on the results, the total stained area could be expressed with an exponential curve depending on the nitrite concentration as shown in Fig. 3.8, and the decay phenomena was thought to proceed in following two steps;

Step (1): Death of the living microorganisms (stained in green \rightarrow red)

Step (2): Disintegration of the dead microorganisms (stained in red \rightarrow loss of fluorescence, deformation of nucleic acids)

In step (1), the biomass could be assumed to retain almost its original structure apart from the degree of damage in cell membrane. On the other hand, since the biological activity was lost after the microbial death, the two kinds of particulates (living and dead biomass) should be classified into X_{NOO_Living} and X_{NOO_Dead} respectively. Next, as step (2) was considered to be a phase where the dead biomass lost its cellular structure, step (2) would produce compounds defined as slowly hydrolysable compounds (X_{CB}) and biological unbiodegradable particulate (X_U) respectively with a fixed stoichiometry, which was considered from Activated Sludge Model no.1 (Henze *et al.*, 2000). The X_{CB} would be the substrate for the ordinary heterotrophic biomass in their cryptic growth.

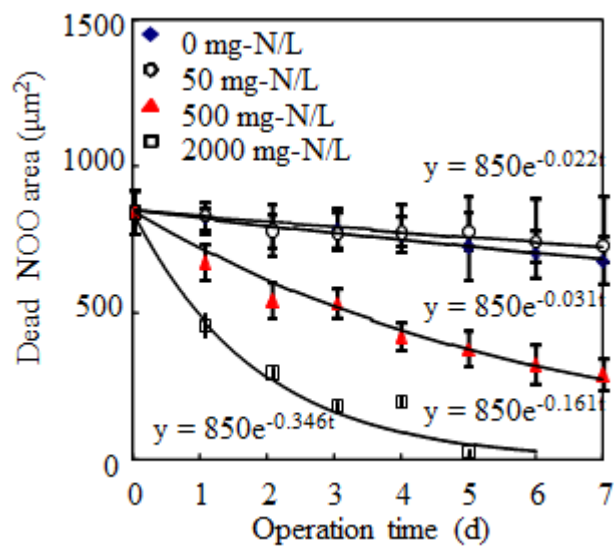


Figure 3. 7 Change of NOO stained in red (dead cells with damaged cell membrane) along with time

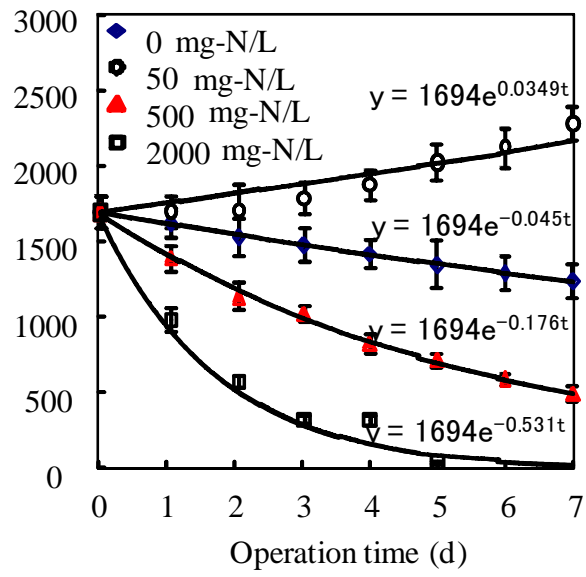


Figure 3. 8 Change of total NOO stained along with time

3.4 Discussion

3.4.1 Modelling growth/death of NOO in open culture

As the NOO enriched sludge was incubated in the open culture system, both OHO and AOO were supposed to grow from the decayed biomass. To express the entire reaction in the system, a Gujer matrix was made as shown in Table 3.1. For NOO, 4 kinds of unit reactions were listed (r1: growth, r2: ordinary endogenous decay, r3: exogenous decay by poisoning and r4: disintegration of the dead NOO biomass). When r4 took place, one unit of X_{NOO_dead} was produced with $1-f_U$ unit of X_{CB} and f_U unit of X_U respectively. During the reaction the nitrogenous fraction (i_N) in the biomass was partly changed to the biodegradable one as $X_{NOO,N}$. After the hydrolysis of X_{CB} by OHO at r5, substrate of S_B for OHO was uptaken at r6. OHO might be killed by high nitrite in the experiments but it was not included in the table for simplification. To harmonise the disintegration phenomena in the model, the disintegration of decayed OHO was also defined in r7 and r8. The organic nitrogen from the decay ($X_{NOO,N}$) was assumed to be a source of soluble degradable nitrogen ($S_{B,N}$) at r9 and was converted to ammonia/ammonium (S_{NH_x}) at r10, which were the same concept as ASM1. Based on the produced S_{NH_x} , AOO grew at r11 and eventually decayed at r12 and disintegrated at r1.

Table 3. 1 The Gujer Matrix for growth, decay and poisoning of the NOO enriched sludge

| r | component | S _{NO2} | S _{NO3} | S _{O2} | X _{NOO_Living} | X _{NOO_Dead} | X _{CB} | X _U | S _B | X _{OHO_Living} | X _{OHO_Dead} | X _{B,N} | S _{B,N} | S _{NHx} | X _{AOO_Living} | X _{AOO_Dead} |
|----|--------------------------------|---------------------|---------------------|---------------------------------|-------------------------|-----------------------|-------------------------------|----------------------------|--|-------------------------|-----------------------|---|---|---------------------|-------------------------|-----------------------|
| | process | | | | | | | | | | | | | | | |
| 1 | NOO growth | -1/Y _{NOO} | +1/Y _{NOO} | $-\frac{1.14-Y_{NOO}}{Y_{NOO}}$ | +1 | | | | | | | | | I _{N,Bio} | | |
| 2 | NOO ordinary decay (death) | | | | -1 | +1 | | | | | | | | | | |
| 3 | NOO poisoning (by FNA) | | | | -1 | +1 | | | | | | | | | | |
| 4 | NOO disintegration | | | | | -1 | 1-f _U | f _U | | | | I _{N,Bio} -f _{U,N} | | | | |
| 5 | Hydrolysis of organics by OHO | | | | | | -1 | | +1 | | | | | | | |
| 6 | OHO growth | | | $-\frac{1-Y_{OHO}}{Y_{OHO}}$ | | | | | -1/Y _{OHO} | +1 | | | | I _{N,Bio} | | |
| 7 | OHO ordinary decay | | | | | | | | | -1 | +1 | | | | | |
| 8 | OHO disintegration | | | | | | 1-f _U | f _U | | | -1 | I _{N,Bio} -f _{U,N} | | | | |
| 9 | Hydrolysis of organic nitrogen | | | | | | | | | | | -1 | +1 | | | |
| 10 | Ammonification | | | | | | | | | | | | -1 | +1 | | |
| 11 | AOO growth | +1/Y _{AOO} | | $-\frac{3.42-Y_{AOO}}{Y_{AOO}}$ | | | | | | | | | | -1/Y _{AOO} | +1 | |
| | | | | | | | | | | | | | | +I _{N,Bio} | | |
| 12 | AOO ordinary decay | | | | | | | | | | | | | | -1 | +1 |
| 13 | AOO disintegration | | | | | | 1-f _U | f _U | | | | I _{N,Bio} -f _{U,N} | | | | -1 |
| | | Nitrite, mg-N/L | Nitrate, mg-N/L | Oxygen, mg-O ₂ /L | Active NOO mg-COD/L | Inactive NOO mg-COD/L | Slowly biodegradable mg-COD/L | Particulate inert mg-COD/L | Readily biodegradable Substrate for OHO mg-COD/L | Active OHO mg-COD/L | Inactive OHO mg-COD/L | Particulate biodegradable organic nitrogen mg-N/L | Soluble biodegradable organic nitrogen mg-N/L | Ammonia mg-N/L | Active AOO mg-COD/L | Inactive AOO mg-COD/L |

3.4.2 Simulation of OUR and VSS

Based on the above developed model, the changes of OUR and VSS concentration in the set of experiments were simulated in Fig. 3.9 using a process simulator GPS-X ver.6.3 (Hydromantis software Inc., Canada). Apart from the decay kinetics identified in the previous graphs, the stoichiometric parameters for growth and VSS/COD conversion factor were referred from literatures as listed in Fig. 3.6. The model could produce both OUR and VSS plots reasonably shown in Fig. 3.6. The simulation without addition of nitrite provided very low OUR with a gradual decrease of VSS concentration along with time, whilst there was an increase of OUR and VSS concentration at 50 mg-N/L. The model successfully demonstrated the substantial reductions of OUR and gradual decreases of VSS due to more decay at 500 mg-N/L and 2,000 mg-N/L respectively. The shape of the curves and the plots matched reasonably for both OUR and VSS.

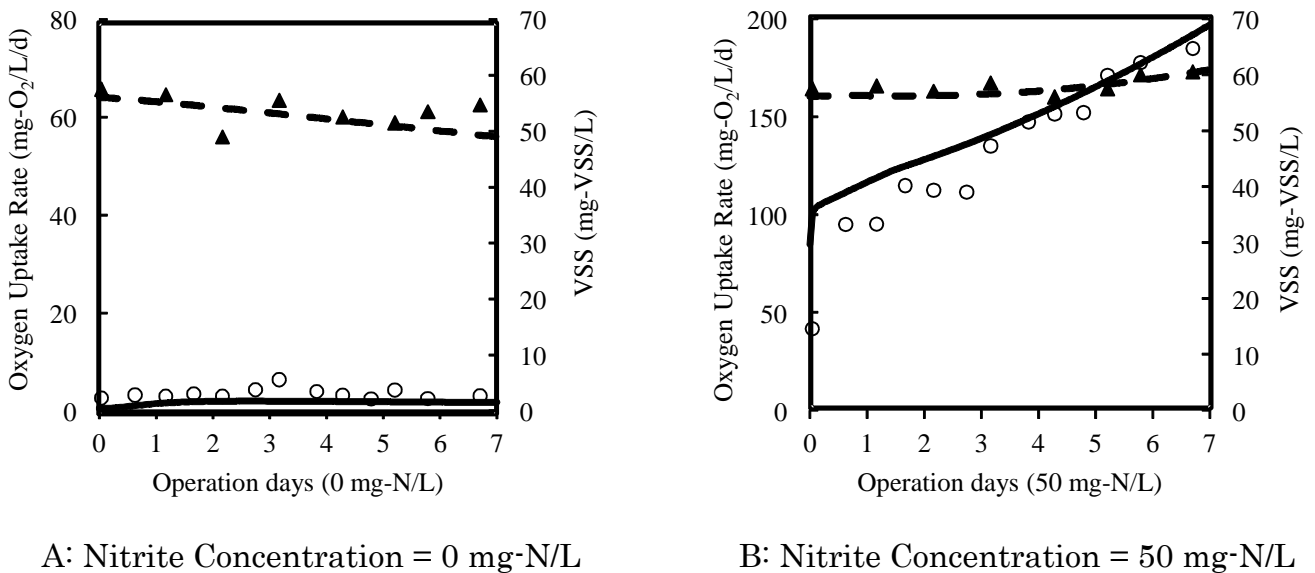
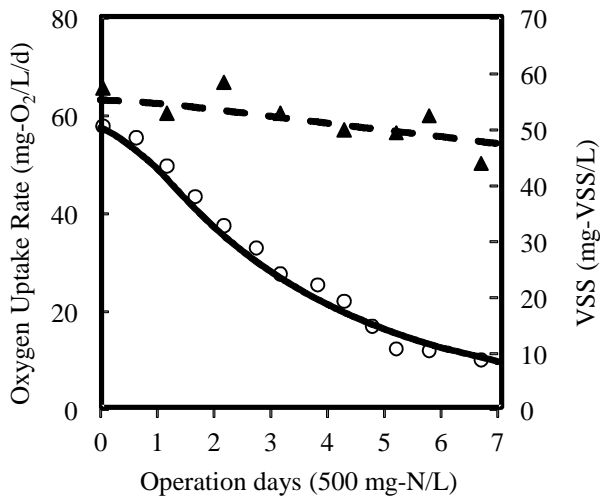
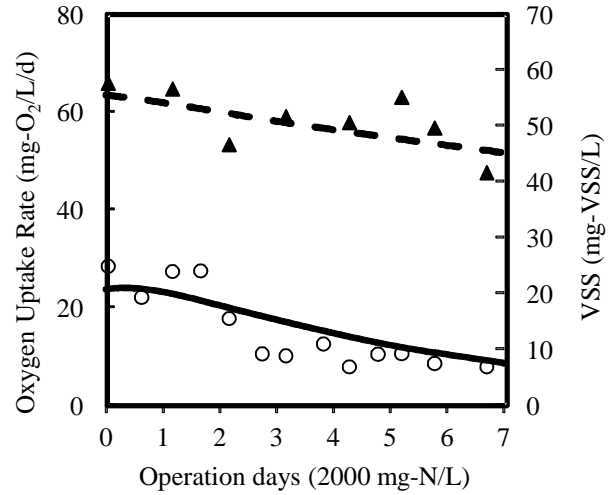


Figure 3. 9 Counted OUR and VSS and simulation results.



C: Nitrite Concentration = 500 mg-N/L



D: Nitrite Concentration = 2000 mg-N/L

Figure 3. 9 Counted OUR and VSS and simulation results (continued).

The experiment and the model provided an alternative concept that poisoning by high nitrite (FNA) reduced the nitrification from nitrite to nitrate. Until now most of the inhibition events have been interpreted as the consequence of competitive and/or non-competitive inhibition of nitrifiers. In such traditional understanding, it has been presumed that the active nitrifying biomass would retain in the system unless washout from the system, and the nitrification performance was expected to recover when the inhibitory concentration was reduced to an acceptable level. On the other hand this study suggested that the activity might be lost due to the disappearance of NOO biomass itself. To validate this expectation, a continuous experiment to feed high nitrite ammonia is an interesting option, which will be described in chapter 5.

Table 3. 2Kinetic and stoichiometric parameters for biological nitrite oxidation

| Symbol | Value | Item | Unit |
|-------------------------------|--------|--|---|
| <u>NOO parameters</u> | | | |
| Y | 0.03 | Yield of NOO | g-COD/g-N-nitrite (Ostace <i>et al.</i> , 2011) |
| f_U | 0.20 | Production of particulate inert | g-COD/g-COD (Henze <i>et al.</i> , 2000) |
| μ_{max} | 0.26 | Maximum specific growth rate | d ⁻¹ (at 35 °C) |
| K_S | 35.0 | Half-saturation coefficient on growth | mg-N-nitrite/L |
| b_{NOO} | 0.072 | Specific ordinary decay rate | d ⁻¹ (at 35 °C) |
| $b_{NOO,dis}$ | 0.0048 | Specific disintegration rate | d ⁻¹ (at 35 °C) |
| $b_{NOO,Inh\ max}$ | 0.552 | Specific maximum poisoning rate by FNA | d ⁻¹ (at 35 °C) |
| K_I | 0.317 | Half saturation coefficient on poisoning by FNA | mg-N-FNA/L |
| $n, FNA, decay$ | 10.0 | Power coefficient on poisoning by FNA | – |
| $b_{NOO,dis\ max}$ | 0.528 | Specific maximum disintegration rate by FNA | d ⁻¹ (at 35 °C) |
| K_{Ic} | 0.317 | Half saturation coefficient on disintegration by FNA | mg-N-FNA/L |
| n, FNA, c | 10.0 | Power coefficient on disintegration by FNA | – |
| <u>AOO parameters</u> | | | |
| Y | 0.208 | Yield of AOO | g-COD/g-N-nitrite (Henze <i>et al.</i> , 2000) |
| f_U | 0.08 | Production of particulate inert | g-COD/g-COD (Henze <i>et al.</i> , 2000) |
| μ_{max} | 6.0 | Maximum specific growth rate | d ⁻¹ (at 35 °C) (Henze <i>et al.</i> , 2000) |
| K_S | 6.0 | Half-saturation coefficient on growth | mg-N-nitrite/L(Henze <i>et al.</i> , 2000) |
| b_{AOO} | 0.04 | Specific ordinary decay rate | d ⁻¹ (at 35 °C) (Henze <i>et al.</i> , 2000) |
| $b_{AOO,dis}$ | 0.04 | Specific disintegration rate | d ⁻¹ (at 35 °C) (Henze <i>et al.</i> , 2000) |
| <u>OHO parameters</u> | | | |
| Y | 0.666 | Yield of OHO | g-COD/g-N-nitrite (Henze <i>et al.</i> , 2000) |
| f_U | 0.08 | Production of particulate inert | g-COD/g-COD (Henze <i>et al.</i> , 2000) |
| μ_{max} | 6.0 | Maximum specific growth rate | d ⁻¹ (at 35 °C) (Henze <i>et al.</i> , 2000) |
| K_S | 0.5 | Half-saturation coefficient on growth | mg-N-nitrate/L(Henze <i>et al.</i> , 2000) |
| b_{OHO} | 0.062 | Specific ordinary decay rate | d ⁻¹ (at 35 °C) (Henze <i>et al.</i> , 2000) |
| $b_{OHO,dis}$ | 0.062 | Specific disintegration rate | d ⁻¹ (at 35 °C) (Henze <i>et al.</i> , 2000) |
| <u>Hydrolysis process</u> | | | |
| r_{Hyd} | 3.0 | Maximum specific hydrolysis rate | d ⁻¹ (at 35 °C) (Henze <i>et al.</i> , 2000) |
| K_{Hyd} | 0.03 | Slowly biodegradable substrate half saturation coefficient | g-COD/g-COD(Henze <i>et al.</i> , 2000) |
| <u>Ammonification process</u> | | | |
| r_{AMM} | 0.08 | Ammonification rate | m ³ /g-COD/d (Henze <i>et al.</i> , 2000) |

3.5 Conclusions

Exogenous decay of nitrifying sludge under high nitrite concentration was studied using live/dead staining where the exogenous decay by high FNA resulting bacterial death was observed depending on FNA concentration. The following results were obtained in this study.

- The poisoning phenomena were visualised using live/dead staining under high nitrite concentration, and modelled applying inhibitory thresholds on the newly defined decay processes.
- The disintegration of the decayed biomass was accelerated when high nitrite was present. The decrease/increase of OUR activity and VSS concentration in the batch condition were also modelled.
- The model presented in this study was to express the loss of active NOO biomass due to poisoning, which was a distinct interpretation against the conventional models using competitive/non-competitive inhibition on growth stage. Therefore the study could be a critical platform to improve the understanding of microbial inhibition phenomena.

4. Nitrite oxidising organism reversible and irreversible inhibition by FNA and FA

4.1 Background

Biological nitrification-denitrification is commonly used to remove nitrogen from wastewater. In a typical nitrification-denitrification process, the ammonia ($\text{NH}_4^+\text{-N}$) is oxidised to nitrate ($\text{NO}_3^-\text{-N}$) and then denitrified to dinitrogen gas (N_2). To reduce the treatment cost for high strength ammonia wastewaters, alternative process configurations based on denitrification of nitrite ($\text{NO}_2^-\text{-N}$), an intermediate in nitrification, were evaluated (Joss *et al.* 2011). In operational regimes of these alternative process configurations, nitrite oxidisers are adequately inhibited to prevent oxidation of $\text{NO}_2^-\text{-N}$ to $\text{NO}_3^-\text{-N}$. For the successful design and operation of these processes, it is important to understand the nature and mechanism of reaction inhibition in these systems.

Biocidal and biostatic inhibition were redefined by Batstone *et al.* (2002) to express inhibition in biological reactions. Biostatic inhibition that is a reversible inhibition acting on growth stage was discussed in chapter 2. This kind of inhibition was described by competitive, non-competitive or

uncompetitive functions. Biocidal inhibition that is an irreversible inhibition acting on decay stage was verified in chapter 3. It was revealed by NOO Live/dead staining under high nitrite concentrations. The classification of biocidal and biostatic inhibition was considered to be important for modelling. The reversible biostatic inhibition influences the kinetic uptake and growth and therefore requires modified growth expressions that include inhibition terms. The irreversible biocidal inhibition influences the biomass decay rate and thus can be modelled by modifying the expressions for the decay rate. Based on this understanding the model for expressing the biostatic inhibition on the growth process could be expressed as shown in Eq. 4.1. With this expression the growth rate could reversibly change depending on the concentration of inhibitory compounds ($0 \leq I \leq 1$).

$$\text{Specific Growth Rate } \mu = \mu_{\max} \left(\frac{S}{K_S + S} \right) \times I_1 \times I_2 \cdots \times I_j \cdots \times I_k = \mu_{\max} \left(\frac{S}{K_S + S} \right) \times \prod_{j=1}^k I_j \quad (4.1)$$

The inhibition term I_j in Eq.(4.1) represents an inhibition function that varies between zero and one depending on the concentration of the inhibitory compound (S_{I_j}). Different types of reversible inhibitions models describing the inhibition term have been proposed based on the effect of inhibitory compound on the enzyme and enzyme-substrate complex (Andrew, 1968; Volskay *et al.*, 1988 and Neufeld *et al.*, 1980). The typical function for the inhibition term used in Activated Sludge Models (ASMs) and Anaerobic Digestion Model No.1 (ADM1) (Henze *et al.*, 2000; Batstone *et al.* 2002) is

representative of a non-competitive form of reversible inhibition. Some examples of the application of this function are the inhibition of DO on the denitrification process and ammonia inhibition in methanogenesis.

Another aspect of reversible inhibition as indicated by Speece (1996) relates to bacterial recovery from inhibition due to a rapid response of the enzymatic system (quick recovery) or a slow adaptation due to gradual proliferation of different microbial consortia having different kinetics (slow recovery). The current models for reversible inhibition do not account for bacterial recovery nor adaptation after a shock load. The actual physiological changes leading to bacterial recovery from the inhibition are probably quite complex and difficult to model. However, considering that the recovery process most likely involves the enzymatic adjustment in the system, both the quick and slow recovery processes could be associated to the growth process modelling purposes. Therefore, the inhibition term I_j shall include an appropriate term to account for the quick and slow recovery phenomenon.

For the biocidal irreversible inhibition affecting the decay process, contrary to the functional forms for reversible inhibitions, there is very limited information on the functional forms of inhibition terms in the specific decay rate described in the equation. Nevertheless based on mathematical insight, as the process is resultant from a stochastic irreversible inactivation of microorganisms that happens over the population in the system, the inhibition of the decay process may be expressed as in Eq.(4.2), where factors

affecting the inactivation ($k_j \cdot I_j$) are lineally added to the conventional first-order decay kinetic coefficient (b_D), which is also the probability of microbial inactivation. It is pronounced that there is very limited information on the functional forms of inhibition terms, however.

$$\text{Specific Decay Rate } b_{tot} = b_D + k_1 \cdot I_1 + k_2 \cdot I_2 \cdots k_j \cdot I_j \cdots k_k \cdot I_k = b_D + \sum_{j=1}^k k_j \cdot I_j \quad (4.2)$$

In formulating the above understanding, the reversible and irreversible inhibitions are associated to growth and decay processes respectively. This formulation appears to be logical and is expected to model most of the microbial responses. However, the primary problem in the application of this model is to properly distinguish the impact of each inhibitory compound on both the reversible and irreversible inhibition. For instance nitrite oxidizing organism (NOO) are inhibited by high substrate concentrations of both free nitrous acid (FNA) and free ammonia (FA) (Anthoniesen *et al.*, 1976 and Jubany *et al.*, 2009). Jubany *et al.* (2005) proposed a NOO growth model by only using a competitive FNA inhibition term in the growth process. They measured and reproduced NOO's oxygen uptake rate (OUR) profile from short term (0.5-1 day) batch tests for initial nitrite concentrations in 500-1,600 mg-N/L range. On the other hand Liu *et al.* (2011) highlighted that very high nitrite concentrations (1,000-2,000 mg-N/L) gave a remarkable poisoning effect and the long-term OUR response over 10 days could not be expressed by the conventional reversible inhibition functions due to consistent loss of NOO's activity. Accordingly they concluded that the decay

process accelerated by high nitrite (irreversible inhibition) should be taken into consideration for modelling. The observed discrepancy between the two studies was probably due to the differences in the initial nitrite concentration and the length of the batch experimental periods.

This study was undertaken to clarify the reversible and irreversible inhibition behaviour of FNA and FA on NOO using experimental data from batch tests. At first, a theoretical framework outlining the relevant switching functions to express the reversible inhibition with adaptation and irreversible inhibition from the shock loading was developed. Next a set of traditional short-term batch tests was carried out according to Jubany *et al.* (2005) to obtain inhibition kinetics on the growth process. The inhibition model developed from the short-term batch experiments was critically evaluated by applying it to data from a set of subsequent long-term batch tests. The model was also used to predict marginal ranges of FNA and FA concentration for complete NOO washout. The estimated inhibition ranges were compared with the values proposed by Anthoniesen *et al.* (1976).

4.2 Theoretical development

4.2.1 Structure of global switching function

Considering the fact that a hyperbolic formula has been widely applied to most biological switching functions, for simplification it was decided to retain its structure with minimum modifications for a global switching function as shown in (4.3). Here, unlike the conventional Monod-type equation that fixes n at 1, the global switching function f provided a Sigmoid-curve having a flexible mathematical property which enabled its curvature to change by manipulating the power coefficient n . As illustrated in Fig. 4.1, when $n > 1$, the increment of f was correspondingly strengthened around A . In this way the response of recovery from inhibition, the threshold of irreversible poisoning and the conventional growth switching function were expressed on the mutual platform.

$$f = \frac{C^n}{A^n + C^n} \quad (4.3)$$

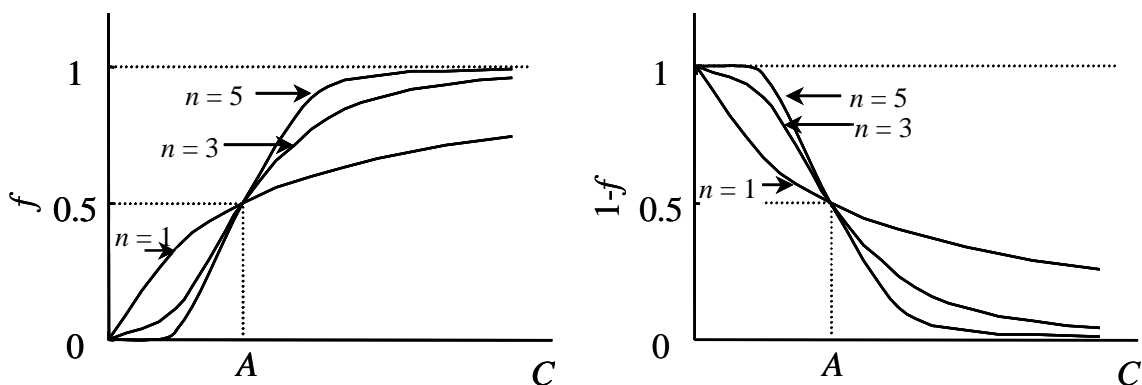


Figure 4. 1 Shape of global switching function f and dependency on the coefficient n .

4.2.2 Model for reversible inhibition with recovery

The functional form of the recovery factor was considered to be such that it lead to inhibition condition on initial exposure while slowly eliminating the inhibition leading to recovery. The expression used to describe the reversible inhibition with recovery, I_j is as shown in Eq. (4.4) based on (4.3). The model was representative of the non-competitive inhibition by the substance S_j with a time varying value at a sub-function f_j (recovery factor). Since the process of recovery should signify an increased tolerance to inhibitory compound, the use of a time dependent variable ($K_{Tj} \times \text{time}$) was thought to be the correct representative of the recovery process.

The implication of using this recovery function was that at $t = 0$ then $f_j = 1$, hence the original inhibition is not affected by the recovery. As the exposure to the inhibitory compound increased, the value of f_j decreased leading to non-inhibition on I_j after a certain period of time. In case of high S_j concentration, the time in which f_j reaching to zero was delayed, showing a need of more time until recovery. On the other hand, in the case where an inhibitory compound having high K_T was dosed, the time in which f_j reaching to zero was reduced, showing less time until recovery. It was pronounced that the dimension of K_T was a rate (mg/L/d) and therefore the value could be directly used as an index of recovery from the biostatic impact.

$$\begin{cases} I_j = \left(\frac{K_{I,j}}{K_{I,j} + S_j \times f_j} \right) \\ f_j = \left(\frac{S_j^n}{(K_{T,j} \cdot t)^n + S_j^n} \right) \end{cases} \quad (4.4)$$

4.2.3 Model for irreversible inhibition

The irreversible inhibition due to an inhibitory compound in Eq.(4.2) was also modelled using the global switching function of (4.3). Based on this, (4.5) was formulated and the irreversible inhibition factors were estimated. The applied sigmoid equation allowed irreversible inhibition to be initiated when the concentration of the inhibitory compound exceeded a threshold level (around the concentration at $K_{I,j}$). By manipulating the value of n , the steepness of the sigmoid curve between the bounded values of 0 and 1 could be controlled.

$$\begin{cases} k_j \cdot I_j = k_j \cdot f_j \\ f_j = \left(\frac{S_j^n}{K_{I,j}^n + S_j^n} \right) \end{cases} \quad (4.5)$$

4.3 Materials and Methods

4.3.1 Short-term OUR measurement procedure

NOO was trained using the same procedures as the ones described in 3.2.1 of chapter 3. 100 mL of NOO sludge was taken from the SBR after verifying no nitrite was present in the bulk liquid. The sludge was then put in a BOD-bottle and pure oxygen gas was injected to set DO concentration beyond 20 mg-O₂/L. The initial concentration of NaNO₂ was varied from 50 to 1,200 mg-N/L. The pH and the temperature during these experiments were kept same as that in the SBR. After exposing the sludge to the nitrite for 15 minutes, the DO concentration in the BOD-bottle was monitored at one minute intervals with a DO meter (TOX-999B, Toko, Japan). Based on the slope of DO in time, the OUR in the individual tests was determined. After completion of the tests, another set of experiments was carried out using fresh sludge with the presence of ammonia with a concentration equal to that of NaNO₂ ranging from 50 to 1,200 mg-N/L.

4.3.2 Long-term OUR measuring procedure

A respirometer (AER-8 Challenging Systems Inc, USA) was used to log the oxygen uptake at hourly intervals for over 10 days in the batch tests. The components of the respirometer were (1) a gas-tight 500-mL incubation vessel on the strong magnetic stirring base with supplied oxygen from an external gas cylinder, (2) a cell device measuring oxygen gas consumption, (3) an interface module to convert the oxygen gas consumption data to

digital form, and (4) a computer for data acquisition. Temperature of the incubation vessels and the cell base were maintained at $35\pm 0.2^\circ\text{C}$ in a temperature-controlled incubator. A small scrubber consisting of a caustic material was set in the incubation vessel to absorb CO_2 from the headspace gas. The oxygen gas consumption data was logged at regular intervals in the computer whilst the DO in the incubation vessels were maintained constant at over $6\text{ mg-O}_2/\text{L}$.

Based on the shape and area of the respirogram, relevant rate expressions for the growth (μ) and decay (b_{tot}) processes were elaborated based on Eq.(4.6), and corresponding parameters were estimated using a process simulator (GPS-X, Hydromantis Environmental Software Solutions, Inc., Canada) (Kappeler *et al.*, 1992; Henze *et al.*, 2000). Similar to the short-term tests, different concentrations of NaNO_2 was dosed to perform a six-parallel experiment ranging from zero to $2,000\text{ mg-N/L}$ as well as using the mixture of nitrite and ammonia. The test conducted without addition of nitrite (blank test) provided the estimated values for the X_{NOO} concentration in the sludge as 44 mg-COD/L and the inherent specific decay rate b_D as 0.08 d^{-1} , which was in the range reported in literatures ($0.08\text{-}0.22\text{ d}^{-1}$, Makinia, 2010)

$$\text{OUR} = \frac{1.14 - Y_{NOO}}{Y_{NOO}} \mu_{NOO} \cdot X_{NOO} + (1 - f_U) \cdot b_{tot} \cdot X_{NOO} \quad (4.6)$$

4.3.3 Calculation of FA and FNA

The fraction of non-ionised compounds, FNA ($[\text{HNO}_2]$, S_{FNA}) and FA ($[\text{NH}_3]$, S_{FA}) was estimated using Eq. (4.7) and Eq. (4.8) respectively. As concentrations of total nitrite ($[\text{NO}_2^-] + [\text{HNO}_2]$) and total ammonia ($[\text{NH}_4^+] + [\text{NH}_3]$) were obtained from the chemical analysis, inputting the corresponding equilibrium coefficient, K_a , the concentration of non-ionised fraction of nitrite and ammonia were estimated. The values of $K_{a, \text{Nitrite}}$ and $K_{a, \text{Ammonia}}$ were calculated based on $pK_{a, \text{nitrite}}$ and $pK_{a, \text{ammonia}}$ values of 3.24 and 8.95 at at 35°C respectively (Lide, 2006).

$$\text{HNO}_2 = \left(\frac{\text{H}^+}{K_{a, \text{Nitrite}} + \text{H}^+} \right) (\text{NO}_2^- + \text{HNO}_2) = \left(\frac{\text{H}^+}{K_{a, \text{Nitrite}} + \text{H}^+} \right) \cdot \text{Total Nitrite} \quad (4.7)$$

$$\text{NH}_3 = \left(\frac{K_{a, \text{Ammonia}}}{K_{a, \text{Ammonia}} + \text{H}^+} \right) (\text{NH}_3 + \text{NH}_4^+) = \left(\frac{K_{a, \text{Ammonia}}}{K_{a, \text{Ammonia}} + \text{H}^+} \right) \cdot \text{Total Ammonia} \quad (4.8)$$

4.4 Results

4.4.1 Reversible inhibition verification

The OUR datasets collected from the short-term batch tests were used to estimate the conventional inhibition kinetics for the growth process of NOO. As shown in Fig.4.2, when the enriched NOO culture was exposed to NO_2^- for 15 minutes (■), the maximum OUR value was observed to be 8.8 mg- O_2 /L/d. The observed maximum OUR value decreased gradually as the nitrite concentration was increased. At an initial concentration of 1,200 mg-N/L of nitrite, the maximum OUR was less than 50% of the maximum OUR observed at initial nitrite concentration of 100 mg-N/L. Both the conventional non-competitive and competitive models could reproduce the data plots reasonably well and showed almost identical curves as shown in the graph. For the simulation, since there was no clear experimental evidence whether NOO assimilated nitrite as ionised form (NO_2^-) or non-ionised form (HNO_2) or both, it was assumed that the both forms were simultaneously consumed by NOO. Consequently the substrate, C in (4.3) was expressed to be the sum of NO_2^- and FNA (total nitrite, S_{NO_2}). On the other hand, for the inhibition effect, the non-ionised concentration calculated from the pH and the total S_{NO_2} concentration were used in the expression. The calibrated values of the kinetic parameters for nitrite half-saturation and inhibition were estimated to be: $K_{S,\text{NO}_2} = 35$ mg-N- S_{NO_2} /L, K_{I,HNO_2} (non-competitive type) = 0.017 mg-N-FNA/L, K_{I,HNO_2} (competitive type) = 0.017 mg-N-FNA/L.

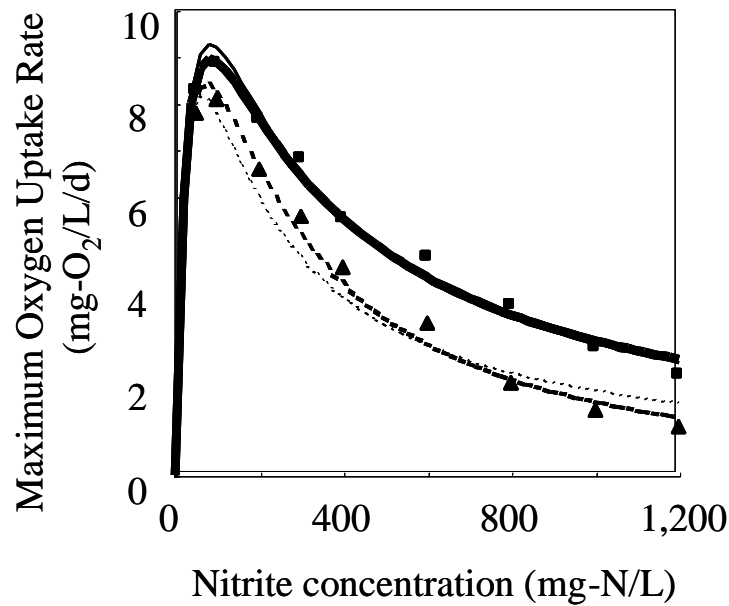


Figure 4. 2 Measured and simulated maximum OUR of NOO at pH = 7.3 fifteen minutes after collection of fresh sludge from the reactor.

(■: only nitrite, bold solid line: simulation using non-competitive type, thin solid line: simulation using competitive type; ▲: nitrite with ammonia, bold dotted line: simulation using non-competitive type, thin dotted line: simulation using competitive type)

When NOO were simultaneously exposed to both nitrite and ammonia (▲), the maximum OUR was slightly lower than the 8.8 mg-O₂/L/d (the maximum OUR observed without ammonia) and the decrease of maximum OUR at higher concentrations was remarkably enhanced. At 1,200 mg-N/L of nitrite with 1,200 mg-N/L of ammonia, the OUR became about half compared to that measured when only nitrite was present. According to the data plots, it seemed that higher ammonia concentrations reduced OUR more significantly. Based on the response, the inhibition of NOO by

non-ionised ammonia (FA) as well as FNA were modelled and simulated using non-competitive and competitive formulae as shown in the graph. Similar to the simulation results for nitrite only experiments, the two inhibition forms gave comparable curves. The calibrated values of the kinetic parameters for ammonia inhibition estimated to be; K_{LNH3} (non-competitive type) = 26.5 mg-N-FA/L, K_{LNH3} (competitive type) = 6.6 mg-N-FA/L.

Since the two kinds of inhibition forms for non-competitive (Eq.4.9) and competitive (Eq.4.10) on the growth process showed very close simulation curves on FNA inhibition as well as those on FNA + FA inhibition, it was decided to use non-competitive formula for further study because of its simplicity.

$$\mu = \mu_{\max} \frac{S_s}{K_s + S_s} \frac{S_I}{K_I + S_I} \quad (4.9)$$

$$\mu = \mu_{\max} \frac{S_s}{K_s \left(1 + \frac{S_I}{K_I} \right) + S_s} \quad (4.10)$$

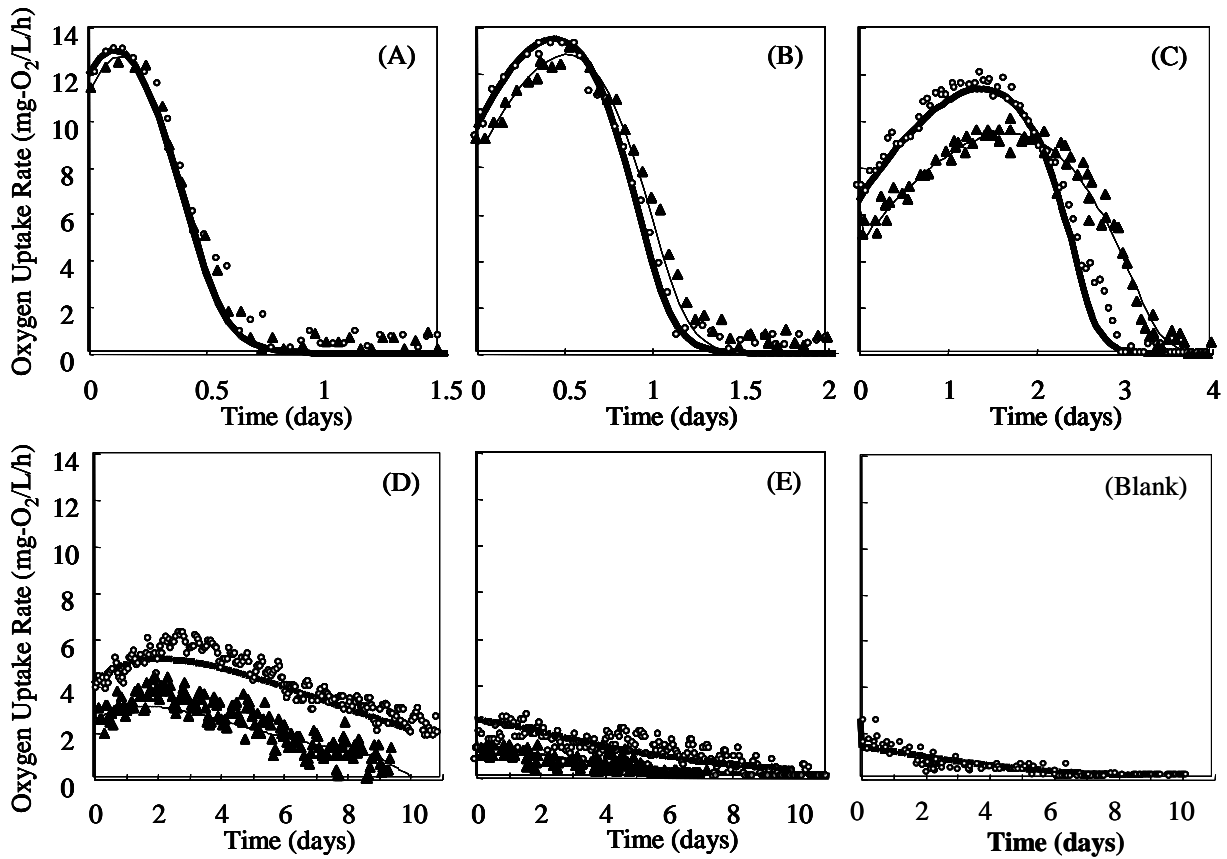


Figure 4.3 Experimental OUR plots and the simulated curves for the 6 datasets of the long-term batch tests at pH = 7.3.

(nitrite concentration: A: 125 mg-N/L, B: 250 mg-N/L, C: 500 mg-N/L, D: 1,000 mg-N/L, E: 2,000 mg-N/L; ○: addition of only nitrite, △: addition of nitrite with the same concentration of ammonia, bold line: simulation for FNA inhibition, thin line: simulation for FNA + FA inhibition, the last figure: blank test without nitrite)

Next, the OUR plots from the long-term batch tests are shown in Fig. 4.3 along with simulation curves using the concepts of the recovery from the shock loading and of the irreversible inactivation by poisoning (discussed in later sections). After addition of nitrite (and ammonia), the OUR was seen

to increase gradually with time and attained a peak. This behaviour was very prominent in all the experiments except the test conducted at 2,000 mg-N/L of nitrite and ammonia. The increase of OUR until attaining the peak, especially in the tests conducted at 125-1,000 mg-N/L of nitrite (and ammonia), could not be explained using the conventional inhibition models because the concentration of inhibitory compounds was still high in the system. Based on this, the period until attaining the peak OUR was considered to be due to biomass adaptation and is termed as the recovery period.

The time required to attain the peak OUR (recovery period) was directly correlated to the initial inhibitory compound concentration fed to the system (Fig.4.3 (A)-(E)), the recovery from each batch test of Fig 4.3 was mapped and shown in Fig. 4.4 based on Haldane-type inhibition curve ($t = 0$) and calculation by recovery function. This meant that a longer recovery time was needed when higher inhibitory compounds were present. The peak OUR appeared at 0.2 day for the test A conducted at 125 mg-N/L of S_{NO_2} whilst the peak time shifted to 0.5 day for the test B (S_{NO_2} : 250 mg-N/L), 1.5 days for test C (S_{NO_2} : 500 mg-N/L) and 2 days for test D (S_{NO_2} : 1,000 mg-N/L). In the case of very high concentration (S_{NO_2} : 2,000 mg-N/L), there was no prominent peak observed (test E). For this test, it was likely that high concentration caused considerable poisoning leading the death of active cells. In addition to the effect of FNA on recovery time, the presence of FA also increased the recovery time especially at high FA concentration.

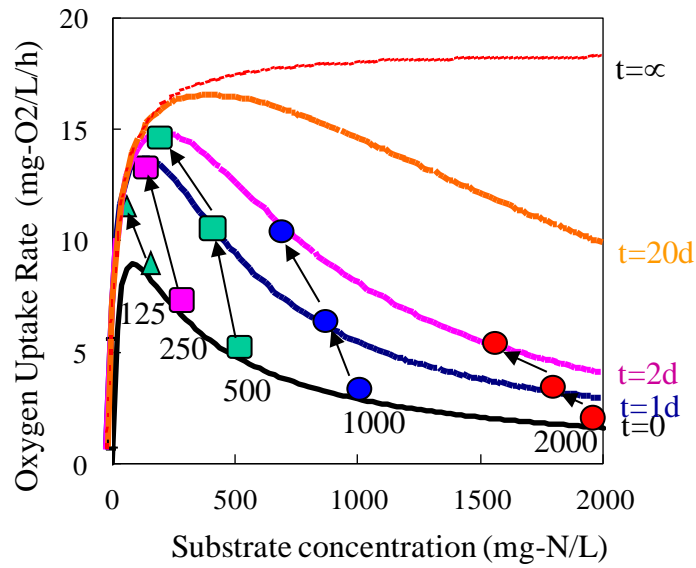


Figure 4. 4 NOO activity recovery phenomenon in long-term continuous batch tests

Over the tests, it appeared that both FNA and FA reduced the peak OUR depending on the concentration. Consequently under extremely high FNA and FA conditions (test D and E), these OURs did not reach the peak OUR of 13 mg-O₂/L/d which was observed for test A. Furthermore, the consistent decline of OUR after the peak indicated the poisoning was dominant over the periods.

To elucidate the complex responses, the inhibition coefficients for the five datasets, K_T in (4.4) for FNA and for FA were estimated first by visual inspection. Based on these first-guess values, the decrease in OUR after the peak was calibrated using additional decay processes in Eq.(4.2) and (4.5). After this first set of trials, the calibration was repeated several times until the entire curve shape and data plots matched. Through the calibration, the

sensitivity of power coefficient, n was found to be low as long as a high value (above 5) was used. The estimated K_T for FNA and for FA was 0.004 mg-N-FNA/L/d and 1.1 mg-N-FA/L/d respectively. Based on this, it appeared that the FNA toxicity concentration is about 300 times lower than FA, thus adaptation from FA shock loading should be easier than that from FNA for NOO. Thus the coefficient of K_T may be used as a quantification index to evaluate the adaptation phenomena kinetically, as no relevant metabolic theories were available at present.

The OUR plots having a convex inflection (\cap -shape) before the peak OUR could not be drawn using the conventional inhibition model with Monod-type switching function for substrate. This was because such substrate concentration-dependent composite functions had to have a concave inflection (\cup -shape). To highlight this deficiency of the conventional model, the simulation curve using the conventional non-competitive formula without the recovery function f is shown as a bold line on the top left graph in Fig. 4.5 together with the data plots conducted at 500 mg-N/L of only nitrite.

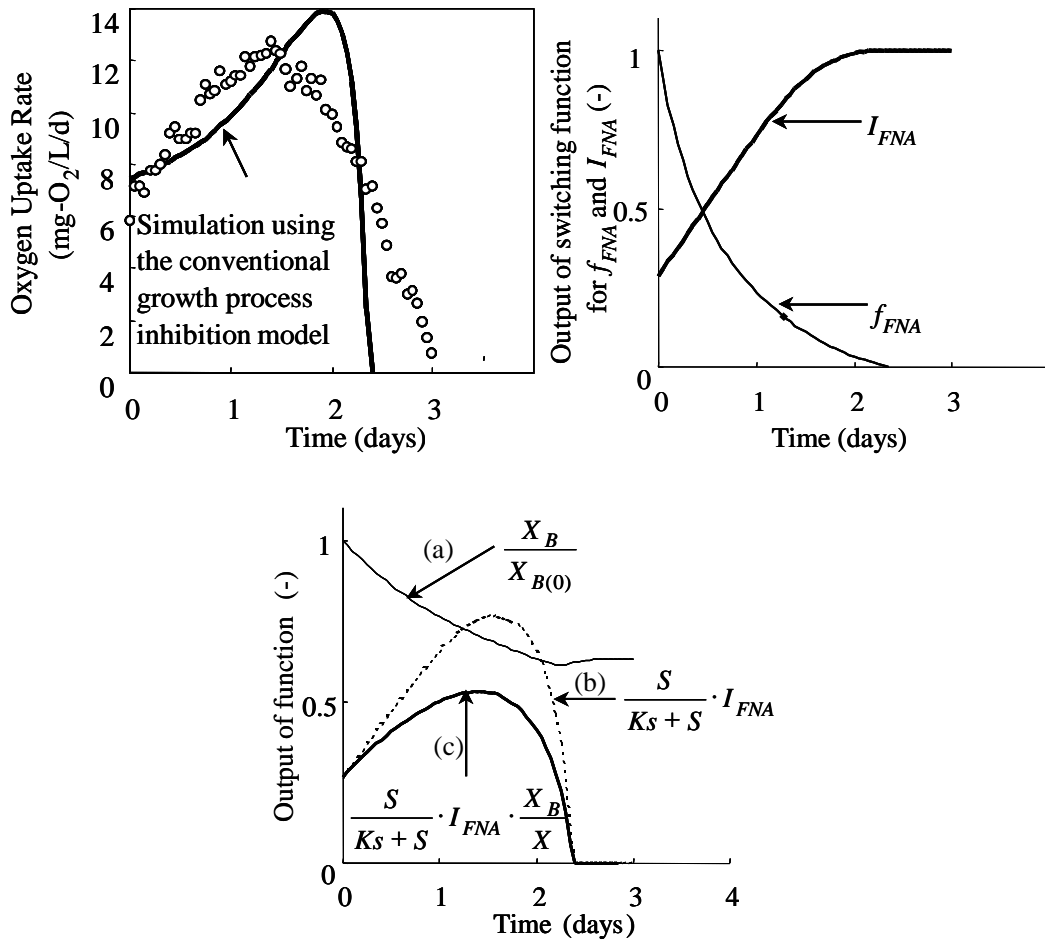


Figure 4. 5 Improper reproductivity of the inhibition model on growth process under long-term incubation (Initial nitrite = 500 mg-N/L, pH=7.3)

(top left: comparison of the simulation to the experimental OUR plots; top right: adaptation from the inhibition effect calculated by the new model (f_{FNA} : reduction of the inhibition effect with time, I_{FNA} : switching function to express the recovery from inhibition); bottom: the outputs of some selected functions, (a) dimensionless active biomass concentration, (b) dimensionless growth rate, (c) dimensionless reaction rate)

Apart from the comparable area of the graphs indicating the total oxygen uptake by NOO, the pattern of the simulated curve and the data plots were distinct. In order to fit the curve to the data plots during the recovery period,

(4.11) was introduced from Eq. 4.2 and (4.4). Based on the equation, the calibrated f_{FNA} and the calculated I_{FNA} were drawn on the top right graph in Fig. 4.5 as the thin and bold lines respectively. As the shape of curve for I_{FNA} resembles the unmatched conventional growth process inhibition model, use of only Eq. 4.11 form was not appropriate. To transform \smile -shape to \frown -shape on the graph, addition of a decay phenomenon leading to logarithmic decrease of active biomass concentration in time was essential as drawn on the down graph in Fig. 4.5.

$$\begin{aligned}\mu &= \mu_{\max} \cdot \left(\frac{S_{NO2}}{K_S + S_{NO2}} \right) \times I_{FNA} \times I_{FA} \\ &= \mu_{\max} \cdot \left(\frac{S_{NO2}}{K_S + S_{NO2}} \right) \cdot \left(\frac{K_{I,FNA}}{K_{I-FNA} + S_{FNA} \cdot f_{FNA}} \right) \cdot \left(\frac{K_{I,FA}}{K_{I-FA} + S_{FA} \cdot f_{FA}} \right)\end{aligned}\quad (4.11)$$

It was noted that, before the OUR peak, the conventional model underestimated the OUR data plots. To approach the plots, it was clear that the degree of inhibition had to be reduced in the conventional model by applying the recovery phenomena. Similarly after the OUR peak, the decrement of OUR in time in the conventional model was clearly overestimated. To match with the OUR data plots during the periods, the reaction rate had to be reduced by reducing the active NOO concentration which was additional decay. To express the entire shape of the graph, the two modifications were simultaneously needed.

4.4.2 Irreversible inhibition verification

In order to match the curve and the data plots, the calibration of the decay process associated with poisoning as well as the model for the recovery from inhibition on the growth process were needed. This was particularly influential on reproducing the consistent decrease of OUR under high inhibitory compounds (*e.g.* test D and E) and the OUR curve after the peak (*e.g.* test A-C). For the calibration, the inhibitions of FNA and FA on decay process were modelled using Eq. (4.9) which was introduced from Eq.(4.2) and (4.5). In the first step of the calibration, the threshold concentrations to activate the poisoning (switching coefficient of f_j in (4.5), $K_{I,j}$) were defined. Considering that the reduction of OUR in the short-term batch tests was observed at beyond about 0.004 mg-N-FNA/L and 1.1 mg-N-FA/L respectively, these values were used as the kinetic coefficients for $K_{I,FNA}$ and $K_{I,FA}$. Similar to the modelling of reversible inhibition on growth process, the sensitivity of power coefficient n was also low as long as a high value (over 5) was used.

$$\begin{aligned} b_{tot} &= b_D + k_{FNA} \cdot I_{FNA} + k_{FA} \cdot I_{FA} \\ &= b_D + k_{FNA} \cdot f_{FNA} + k_{FA} \cdot f_{FA} \end{aligned} \quad (4.9)$$

The maximum specific poisoning rates for FNA (k_{FNA}) and FA (k_{FA}) were calibrated to be 0.4 d⁻¹ and 0.05 d⁻¹ respectively. Unlike the reversible inhibition function on the growth process having a time dependency, constant k_{FNA} and k_{FA} were enough to reproduce the OUR curves. This suggested that the physiological mechanism for these two inhibitions were distinct as shown in Eq. 4.10. Here, a process rate for decay under the batch

condition could be generalised using Weibull distribution as a probability density function (adapted from Weibull *et al.*, 1952; Taylor *et al.*, 1992; Arensberg *et al.*, 1995 and Gendig, *et al.*, 2003). In case of logarithmical decrease of active biomass concentration with time, which was ordinary decay, the shape parameter m was set at 1 and gave an ordinary rate expression as $b \cdot e^{-bt}$. On the other hand, if the failure rate (= decay rate) in the process increased along with time (*e.g.* due to aging), m should be calibrated to be greater than 1 ($m > 1$) in order to reproduce the event on the model.

$$\begin{cases} \frac{dX_B}{dt} = -r_{\text{Decay}} \\ \frac{1}{X_{B(0)}} \cdot r_{\text{Decay}} = m \cdot b \cdot (b \cdot t)^{m-1} \exp(-(b \cdot t)^m) \end{cases} \quad (4.10)$$

Over the test periods, since both of two specific poisoning rates were able to be fixed, $m = 1$ could be applied. Based on this result, the poisoning by FNA and FA on the microorganisms was thought to happen randomly and independently with a constant probability over time as long as the concentration exceeded the threshold levels. In addition, due to a low yield coefficient for NOO ($Y = ca. 0.03 \text{ g-COD/g-N}$, Ostace *et al.*, 2011; WEF manual of practice No. 34, 2010), the development of new biomass during the long-term tests was limited and hence the initially seeded NOO should be the dominant and consistently received the inhibitions throughout the test period. Therefore, the successful reproduction of the OUR using the set of

fixed coefficients indicated that the so-called aging phenomena in Weibull distribution, which represented an acceleration of the deterioration on specific activity per NOO was thought to be minor. Accordingly the conventional mechanistic concept to express NOO as a single state variable (X_{NOO}) could be retained. This was quite a convenient finding because of no need for consideration of an age-distribution problem in the system for the poisoning model (no need to define numerous state variables for X_{NOO} having their inherent age), apart from modelling of the quick adaptation from the shock loading where residence time of all cells have to be tracked individually.

4.4.4 Model structure and kinetics values

Based on the above experimental results and theoretical consideration, a complete model structure for the inhibition, recovery and poisoning was developed. The structure of the model and the suggested parameters values are listed in Table 4.1 and 4.2 respectively.

It should be noted that oxygen (S_{O_2}) was assumed to be consumed in the poisoning processes in the model. If the inhibitory compounds completely killed NOO, S_{O_2} should not be consumed but some biodegradable fractions (X_{CB}) should be produced. Nevertheless, considering that the sludge was enriched as a mixed culture where very small amounts of heterotrophs were present to consume the compounds through the cryptic growth of NOO (data not shown) and for model simplification purpose, the assumption was

applied to the model.

Table 4. 1 The Gager Matrix for biological nitrite oxidation

| m | Component → | S_{NO2} | S_{NO3} | S_{O2} | X_{NOO} | X_U | Rate (mg-COD/L/d) |
|-----|------------------|-------------------|-------------------|--------------------------------|--|-------------------------------|---|
| | Process ↓ | | | | | | |
| 1 | Growth | $-\frac{1}{Y}$ | $+\frac{1}{Y}$ | $-\frac{1.14-Y}{Y}$ | +1 | | $\mu_{\max} \left(\frac{S_{NO2}}{K_S + S_{NO2}} \right) \times I_{FNA,1} \times I_{FA,1} \times X_B$ |
| 2 | Inherent decay | | | $-(1-f_U)$ | -1 | $+f_U$ | $b_D \times X_B$ |
| 3 | Poisoning by FNA | | | $-(1-f_U)$ | -1 | $+f_U$ | $k_{FNA} \times I_{FNA,3} \times X_B$ |
| 4 | Poisoning by FA | | | $-(1-f_U)$ | -1 | $+f_U$ | $k_{FA} \times I_{FA,4} \times X_B$ |
| | | Nitrite mg-N/L | Nitrate mg-N/L | Oxygen mg-O ₂ /L | Active nitrite oxidizing organism, mg-COD/L | Particulate inert mg-COD/L | $I_{FNA,1}$ and $I_{FA,1}$: see (4.4) $I_{FNA,3}$ and $I_{FA,4}$: see (4.5) |

Table 4. 2 Kinetic and stoichiometric parameters for biological nitrite oxidation

| Symbol | Value | Item | Unit |
|--|----------------------|--|---|
| <u>Conventional parameters</u> | | | |
| Y_{NOO} | 0.03 | Yield of NOO | g-COD/g-N-nitrite (Ostace <i>et al.</i> , 2011) |
| f_U | 0.20 | Production of particulate inert | g-COD/g-COD (Henze <i>et al.</i> , 2000) |
| $\mu_{max,NOO}$ | 0.32 | Maximum specific growth rate | d ⁻¹ (at 35 °C) |
| $K_{S,NO2}$ | 35 | Half-saturation coefficient on growth | mg-N-nitrite/L |
| $b_{D,NOO}$ | 0.08 | Inherent specific inherent decay rate | d ⁻¹ (at 35 °C) |
| <u>Inhibition parameters on growth stage</u> | | | |
| $K_{I, FNA, growth}$ | 0.017 | Inhibition coefficient for FNA on growth | mg-N-FNA/L (Non-competitive type) |
| $K_{T, FNA}$ | 4.4×10 ⁻⁸ | Inhibition coefficient for FNA on recovery | mg-N-FNA/L/d (at 35 °C) |
| n | 5 | Power coefficient for FNA on recovery | – |
| $K_{I, FA, growth}$ | 26.5 | Inhibition coefficient for FA on growth | mg-N-FA/L (Non-competitive type) |
| $K_{T, FA}$ | 4.4×10 ⁻⁵ | Inhibition coefficient for FA on recovery | mg-N-FA/L/d (at 35 °C) |
| $n, FNA, growth$ | 5 | Power coefficient for FA on recovery | – |
| <u>Inhibition parameters on decay stage</u> | | | |
| k_{FNA} | 0.4 | Specific FNA poisoning decay rate | d ⁻¹ (at 35 °C) |
| $K_{I, FNA, decay}$ | 0.0044 | Half saturation coefficient on poisoning | mg-N-FNA/L |
| $n, FNA, decay$ | 5 | Power coefficient on FNA poisoning | – |
| k_{FA} | 0.05 | Specific FA poisoning decay rate | d ⁻¹ (at 35 °C) |
| $K_{I, FA, decay}$ | 1.1 | Half saturation coefficient on poisoning | mg-N-FA/L |
| $n, FA, decay$ | 5 | Power coefficient on FA poisoning | – |

4.5 Discussion

4.5.1 Marginal inhibition condition

Anthonisen *et al.* described a relationship between pH and FA or FNA for AOO and NOO in 1976 shown in Fig. 7.1.

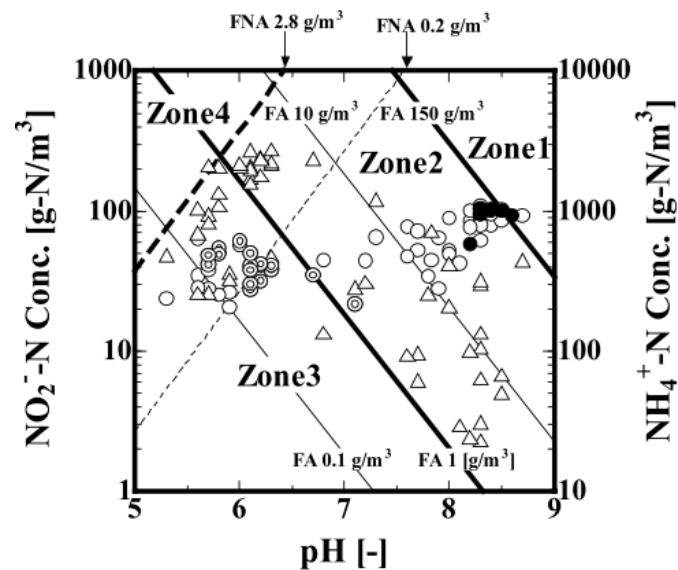


Figure 4. 6 Dependence of free ammonia (FA) and free nitrous acid (FNA) on pH in the solution described by Anthonisen *et al.* (1976).

In Fig. 4.6 , Zone 1 shows FA inhibition of Nitrobacter and Nitrosomonas, Zone 2 shows FA inhibition of only Nitrobacter, Zone 3 shows complete nitrification and Zone 4 shows FNA inhibition of Nitrobacter, Symbols: open circles, $\text{NH}_4^+\text{-N}$; double circles, $\text{NH}_4^+\text{-N}$ from 0 to 70 g/m^3 ; closed circles, $\text{NH}_4^+\text{-N}$ from 180 to 240 g/m^3 ; open triangles, $\text{NO}_2\text{-N}$; solid lines, FA of 0.1,1,10 and 150 g/m^3 , respectively; dotted lines, FNA of 0.2and 2.8 g/m^3 .

FA inhibits the activity of nitrite oxidoreductase (Yang & Alleman 1992). Anthonisen *et al.* (1976) reported that for FA concentration above 1.0 mg/L ,

there is inhibition of the activity of NOO. Mauret *et al* (1996) reported in the mixed culture experiment that the FA concentration threshold for the inhibition of NOO was 6.6 - 8.9 mg NH₃-N/L. Bae *et al* (2001) and Jianlong & Ning (2004) achieved nitrite accumulation in the conditions of pH 8 (30°C, DO = 1.5mgL⁻¹) and pH 7.5 (30°C, DO = 1.5mgL⁻¹). Turk & Mavinic (1989) proved that AOO and NOO could endure FA 40 mg NH₃-N/L.

A marginal inhibition condition resulting in non-growth condition for NOO was calculated using (4.14) developed from Eq. 4.1, 4.2, 4.7 and 4.8. The calculated lines were overlaid on the experimental plots and the inhibition boundaries obtained by Anthonisen *et al.* (1976).

The marginal condition was obtained by a set of nitrite concentrations, ammonia concentration and pH. When the pH and ammonia (or nitrite) concentration were fixed, the critical FNA (or FA) concentration could be determined from the equation depending on the microbial kinetics. Using the parameter values listed in Table 4.2, it appeared that about 0.0044 mg-N-FNA/L was the critical concentration (FNA_{cri}) without the presence of FA (Fig.4.7, top graph). If FA was present in the system, the marginal line correspondingly shifted to alkaline side. Similarly when more FNA was present, the marginal line moved to more acidic side (Fig.4.7, bottom graph).

$$\text{Marginal inhibition condition, } 0 = \mu - b_{tot} = g(S_{NO2}, FNA, FA) = h(S_{NO2}, S_{NH3}, pH) \quad (4.14)$$

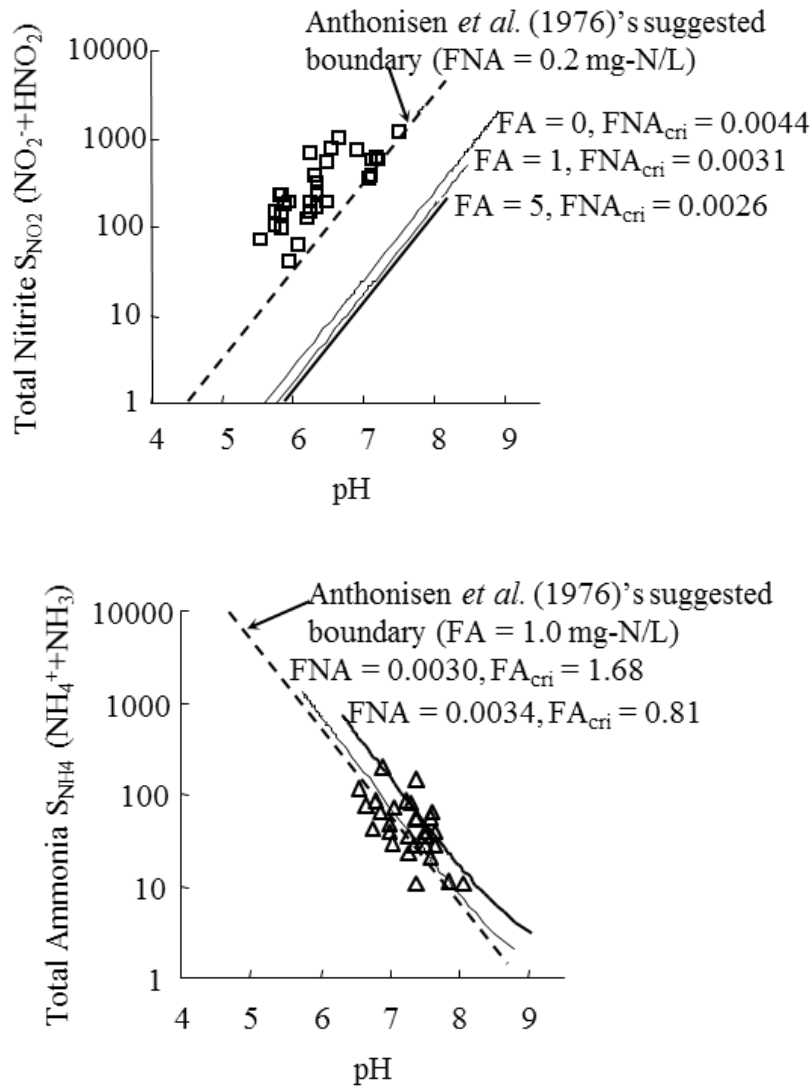


Figure 4. 7 Marginal lines of FNA and FA inhibition concentrations with pH (top: marginal line by FNA, bottom: marginal line by FA; plots indicated NOO's activity deterioration NOO served by Anthonisen *et al.* (1976))

Compared to Anthoniesen's boundaries that showed the NOO (Nitrobacter) inhibition zone and non-inhibition zone, it seemed that the FNA_{cri} obtained in the batch tests was considerably lower than their estimated boundary where a deterioration of Nitrobacter's reaction took place (at FNA = 0.2 mg-N/L) whilst the FA_{cri} was fairly close to the boundary (FA = 1.0 mg-N/L)

when small FNA was present simultaneously. On the other hand, in case of using the calibrated parameter from the benchmark dataset ($K_{I, FNA, decay}$: 0.33 mg-N-FNA/L), the marginal line was very close to their suggested boundary at FNA = 0.2 mg-N/L (not shown). Since Anthoniesen's boundaries were defined as an initiation point of NOO activity deterioration, direct linkage with (4.14) was technically difficult. Nevertheless, the equation could provide mathematical insight for the response of NOO. For instance, instead of using zero on the left side of Eq. 4.14, using a reciprocal SRT would give another set of marginal condition corresponding to a continuously operated system at a given SRT.

The actual decay phenomenon of NOO under starvation conditions seems to be further complicated as a recent research using OUR tests pointed out that there would be two types of decay (cell decay: associated to cell death, and activity decay: reduction of specific activity of active bacteria) (Hao *et al.*, 2009). At present it is not clear which decay type governed the poisoning observed in this study. In addition, apart from cell decay, there is no relevant information whether the 'activity decay' retains for long periods of time without any microbial recovery. To reveal the problem in the next task, the concept of the recovery function and the additional decay function developed here may be applied to simulate the two types of decay (Loosdrecht and Henze, 1999).

4.6 Conclusions

Kinetic modelling for the inhibition of nitrite oxidizing organisms was studied using batch respirometric tests. The inhibition by non-ionised nitrite and non-ionised ammonia was classified into two types as reversible form (growth inhibition) and non-reversible form (poisoning) depending on the inhibitory concentrations. The developed model was successfully validated using a WERF benchmark dataset conducted under a chemostat mode. The following results were obtained in this study.

- The traditional reversible inhibition model focusing on only the growth process could not properly reproduce the microbial oxygen uptake rate when the incubation was extended to several days. This was because an adaptation from the shock loading and poisoning took place almost simultaneously.
- The poisoning phenomena were modelled applying inhibitory thresholds on the newly defined decay processes whilst the traditional inhibition model on the growth process was modified by incorporating a recovery function from shock loading.

5. Benchmark simulation to verify an inhibition model on decay stage for nitrification

5.1 Background

Since the early work of Anthonisen *et al.* (1976) indicating that the high free nitrous acid (FNA) and free ammonia (FA) inhibit the biological reactions for ammonium oxidising organism (AOO) and Nitrite oxidising organism (NOO), various kinds of kinetic inhibition models have been proposed and mentioned in chapter 2. Most commonly the traditional Haldane-type switching function or its modification have been employed to model the substrate inhibition.

On the other hand, unlike instantaneous enzymatic reactions, microorganisms in biological wastewater treatment systems adapt to the shock loading, probably due to changes in the biochemical reaction in the cells (Speece, 1996). In fact, Liu *et al.* (2011) observed that K_I of NOO quickly increased along with time and finally the inhibition disappeared after several hours in the 10-day batch experiments. This recovery was seen over the experiments with the initial nitrite concentration ranging from 125 to 2,000 mg-N/L at pH 7.3. Another interesting phenomenon was that the bulk oxygen uptake rate decreased consistently under high nitrite in spite of

corresponding decrease of FNA by nitrification, indicating that an irreversible inhibition (poisoning) took place. The irreversible inhibition was verified and modelled in chapter 3. These points suggest that the use of traditional Haldane-type inhibition functions are not appropriate to express the biological reaction and may give potential technical problems for plant simulation. First, the phenomenon for the non-reversible biomass inactivation have to be addressed rather than the reversible biomass inactivation expressed by non-competitive and/or competitive function shown in Eq. 4.9 and Eq. 4.10. Second, if K_I changes along with time, time-dependent adaptation phenomena have to be incorporated into the equations. This means a residence time distribution (RTD) has to be considered for the individual cell particles in the wastewater treatment plant. Accordingly, the calculation procedure becomes significantly complicated. Unless it is a perfect plug-flow system, all particles have to be tracked to solve the model. For instance, kinetically recovered biomass in the secondary clarifier returning to the aeration tank where the inhibition effect is provided. Third, even if the plant response can be simulated based on the traditional approach using the Haldane-type inhibition functions as mentioned in the above section, the obtained K_I would be solely apparent, which is the mixed output of plant hydraulic conditions and inherent K_I of the microorganism.

To cope with the technical difficulty a modified NOO inhibition model including poisoning threshold was recently presented as shown in Table 5.1

and Eq. 5.1 developed from Eq. 4.5 (adapted from Liu *et al.*, 2011). In the model the Haldane-type inhibition on the growth stage was neglected since it lasted limited duration. Instead of the inhibition, a poisoning effect was added on the decay stage. To initiate the loss of biological activity under high inhibitory substances (FNA and FA), these thresholds were newly defined in the rate expression using a switching function with power coefficient to enhance the effect.

Table 5. 1 NOO inhibition model including toxicity threshold

| | S_{NO_2} | S_{NO_3} | S_{O_2} | X_{NOO} | X_U | Rate expression |
|-------------------|----------------|----------------|---------------------|-----------|--------|--|
| Growth | $-\frac{1}{Y}$ | $+\frac{1}{Y}$ | $-\frac{1.14-Y}{Y}$ | +1 | | $\mu_{\max} \frac{S_{NO_2}}{K_S + S_{NO_2}} X_{NOO}$ |
| Inherent Decay | | | $-(1-f_U)$ | -1 | $+f_U$ | bX_{NOO} |
| Poisoning | | | $-(1-f_U)$ | -1 | $+f_U$ | $\sum_{i=1}^j b_i X_{NOO}$ |

$$b_i = b_{i\max} \frac{S_i^n}{K_i^n + S_i^n} \quad (5.1)$$

Where S_{NO_2} : total nitrite nitrogen including ionised and un-ionised forms (mg-N/L), S_{NO_3} : total nitrate nitrogen including ionised and un-ionised forms (mg-N/L), S_{O_2} : oxygen (mg-O₂/L), Y : nitrifier biomass yield coefficient (g-COD/g-N), f_U : production of inert (0.2 g-COD/g-COD), X_{NOO} : NOO (mg-COD/L), X_U : inert particulates (mg-COD/L), μ_{\max} : maximum specific

growth rate of NOO (d^{-1}), K_S : half saturation coefficient (mg-N/L), b : specific decay rate of NOO (d^{-1}), b_i : specific poisoning rate (d^{-1}), $b_{i \max}$: maximum specific poisoning rate (d^{-1}), S_i : inhibitory substance (mg/L), i : number of inhibitory substances (-), K_I : half saturation coefficient (mg/L), n : power coefficient (-).

Since the model was developed through batch experiments, it was necessary to justify the model structure under continuous operation. For this purpose, the datasets collected by Zimmerman *et al.* (2004) in a WERF benchmark project were utilised. These datasets corresponded to different SRTs and pHs in the reactor. The corresponding effluent qualities were simulated after individual evaluation of response for NOO and AOO. In addition to the verification of the model, a possible reason for an unexpected event leading to a sudden decrease in NOO biomass during one of the experiments was also explored.

5.2 Materials and Methods

5.2.1 Data extraction from WERF benchmark datasets

The four datasets in Water Environment Research Foundation (WERF) published by Zimmerman *et al.* (2004) obtained from chemostat operations with SRTs of 20-day, 10-day and 5-day were used as a benchmark for the model verification. In three operations the bioreactors were seeded with activated sludge containing nitrifiers and high-strength ammonia synthetic wastewater was used as influent substrate. Another set of reactors was operated at 20-day SRT using dewatered solids wastewater and experimental conditions were same as the one using synthetic wastewater. The bulk pH in the reactor was dynamically changed by changing the alkalinity in the influent during operation to observe its effect on nitrification and denitrification. The 20, 10 and 5-day SRTs using synthetic wastewater and 20-day SRT using dewatered solids wastewater continuous tests were operated for 260, 252, 76, and 250 days respectively. The temperature and DO in the bioreactor were maintained at 20 ± 2 °C and 8.0 ± 2 mg-DO/L, whereas the pH in the reactor changed in the range of 5.8–8.2, 6.1–8.8, 6.9–8.8, and 6.3–9.4 respectively. Influent and effluent ammonia concentrations, effluent nitrite and nitrate concentrations, influent and effluent TVS concentrations and effluent alkalinities were measured regularly in each operation. The datasets were electrically scanned and exported to a Microsoft Excel spread sheet.

The AOO and NOO volumetric reaction rates (r_{AOO} and r_{NOO} respectively) were calculated according to the effluent nitrite and nitrate concentrations from the datasets using Eqs. 5.4 and 5.5.

$$r_{\text{AOB}} = D \cdot (S_{\text{NH4-inf}} - S_{\text{NH4-eff}}) \quad (5.4)$$

$$r_{\text{NOB}} = D \cdot S_{\text{NO3-eff}} \quad (5.5)$$

Where r_{AOO} : volumetric AOO reaction rate (mg-N/L/d), D : dilution rate (d^{-1}), $S_{\text{NH4-inf}}$: influent total ammonium concentration (mg-N/L), $S_{\text{NH4-eff}}$: effluent total ammonium concentration (mg-N/L), r_{NOO} : volumetric NOO reaction rate (mg-N/L/d), $S_{\text{NO3-eff}}$: effluent total nitrate concentration (mg-N/L). The schematic representation of the system is illustrated in Figure 5.1.

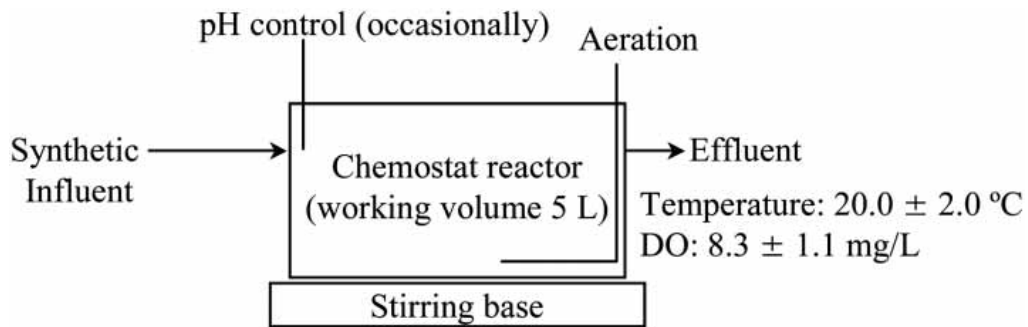


Figure 5. 1 Reactor configuration

5.2.2 Dynamic simulation

The corresponding experimental conditions of the datasets were operated on GPS-X (Hydromantis Environmental Software Solutions, Inc., Canada) simulation software and the response of effluent qualities were compared to the data plots. FNA and FA were calculated from Eqs. 5.5 and 5.6

(Anthonisen *et al.* 1976).

$$\left[\begin{array}{l} FNA = \frac{S_{NO_2}}{K_a + 10^{pH}} \\ K_a = \exp\left(-2300/(273+T)\right) \end{array} \right. \quad (5.5)$$

$$\left[\begin{array}{l} FA = \frac{S_{NH_4} \times 10^{pH}}{K_a + 10^{pH}} \\ K_a = \exp\left(6344/(273+T)\right) \end{array} \right. \quad (5.6)$$

Where T : temperature ($^{\circ}$ C).

Based on the inhibition model mentioned in Table 5.1, the volumetric reaction rates for AOO and NOO were individually calculated using the bulk nitrogenous concentrations (S_{NH_4} and S_{NO_2}). These rates were compared with the rates extracted from the datasets. After calibrating the individual response of each microorganism, continuous simulations were conducted by using the reactions by both AOO and NOO. As no information for initial AOO and NOO concentrations were available in the WERF report, initial AOO and NOO concentrations were assumed to be both 5 mg-COD/L. For the 5-day experimental dataset, as only the effluent ammonia and nitrite were monitored in the initial phase whilst the nitrate was not produced, the produced nitrite in the period was calculated from the decrement of ammonia concentration between the influent and effluent. To calibrate nitrifier biomass yield coefficient, a typical ratio of COD to activated sludge

VSS was used as a conversion factor of 1.42 (Speece and McCarty, 1964). Until reasonable matching of the calculated curves and data plots, individual kinetic coefficients were carefully calibrated through visual inspection. Since a preliminary calibration revealed that inhibition for AOO was rather limited in the operating conditions, NOO was mainly focused on during the model verification unless specified.

In addition to the model verification, with respect to the dataset for 10-day SRT, an unexpected loss of nitrification after 170 day was reported in the publication. In the period nitrite oxidation suddenly deteriorated although the bulk concentration for FNA, FA and pH were certainly within an acceptable level where nitrite conversion was observed until the day. Since the authors of the report could not explain the reason of the event based on kinetic inhibition concept, a microbial lysis (*e.g.* due to infection by Bacteriophage and/or *Bdellovibrio* spp.) was assumed to be the third decay ($= k_3 \cdot X_{\text{NOO}}$) in order to meet the simulation.

5.3 Results

5.3.1 Individual evaluation by benchmark datasets using synthetic wastewater

For the 20-day SRT experiment, operating conditions were shown in Fig. 5.2, the r_{AOO} consistently increased until day 30 after start-up, and peaked at day 40-50 due to acculturation of AOO biomass in the reactor shown in Fig. 5.3. This resulted in the decrease of FA, which was also affected by the intentional decrease of pH 6. In this period, nitrite nitrogen correspondingly increased up to 700 mg-N/L while the conversion of nitrite to nitrate was limited to be below 100 mg-N/L. Since the accumulation of FA lasted for only 20-30 days, AOO's growth could be simulated without considering the inhibition effect of FA. On the other hand, the lower r_{NOO} was mainly attributed to the NOO poisoning by the FA that reduced its overall specific growth rate. Nevertheless the r_{NOO} exponentially elevated after the significant decrease of FA, but it was strongly slowed by the FNA until day 100. After day 100, although slight ammonium remained in the effluent, no nitrite was detected. After day 180, complete nitrification was observed due to enrichment of AOO biomass from the excess substrate. The effluent nitrite concentration was reasonably simulated using the model. Without incorporating the poisoning phenomena, the r_{NOO} was remarkably overestimated in the initial phase.

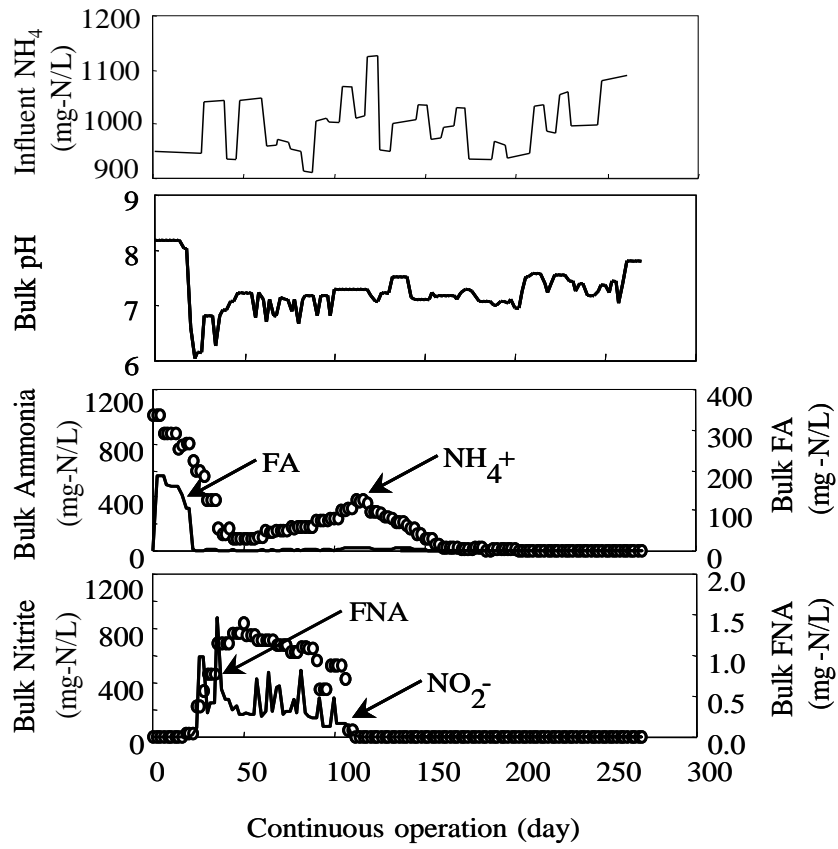


Figure 5. 2 Operating condition for SRT 20 d (synthetic wastewater)

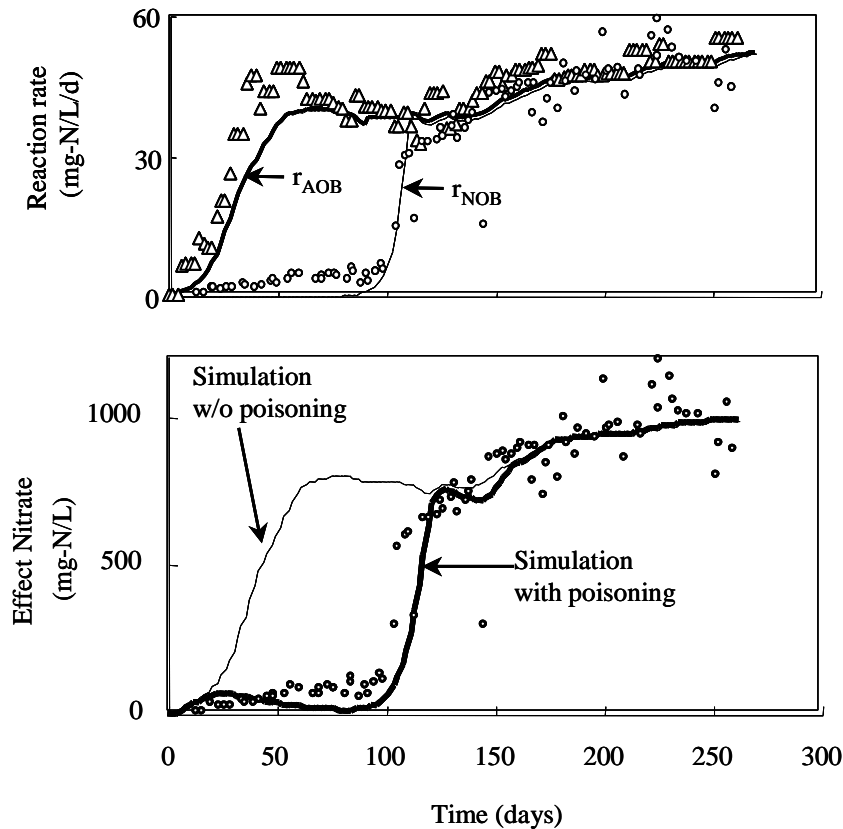


Figure 5. 3 Nitrifier reaction rate (top) and effluent nitrate (bottom) for SRT 20 d operation (synthetic wastewater)

Next, for the 10-day SRT experiment, operation conditions shown in Fig. 5.4 a consistent increase of r_{AOO} was observed and calculated in the initial 50 days due to high specific growth rate of AOO (Fig. 5.5). These rates were slightly reduced by the presence of FA. In addition to this, since the bulk pH was also reduced from 9 to 6 by nitrification, FA concentration dropped and FNA was seen to accumulate in the reactor. The accumulation of FNA significantly delayed the reaction of NOO as well as AOO in this period. Again without the poisoning phenomenon, the delay of nitrataion could not be reproduced. From day 50 to day 100, the r_{AOO} decreased consistently due to reduced influent ammonium load. Because of the low r_{AOO} , inhibition due

to FNA was minimised and the r_{NOO} increased in this period. Between day 130 and day 140, FA accumulated slightly due to an imbalance of influent ammonium load and r_{AOO} . This caused the pause of increment for r_{NOO} . Nevertheless after progressing the growth of NOO, complete nitrite conversion to nitrate was achieved after 140 days.

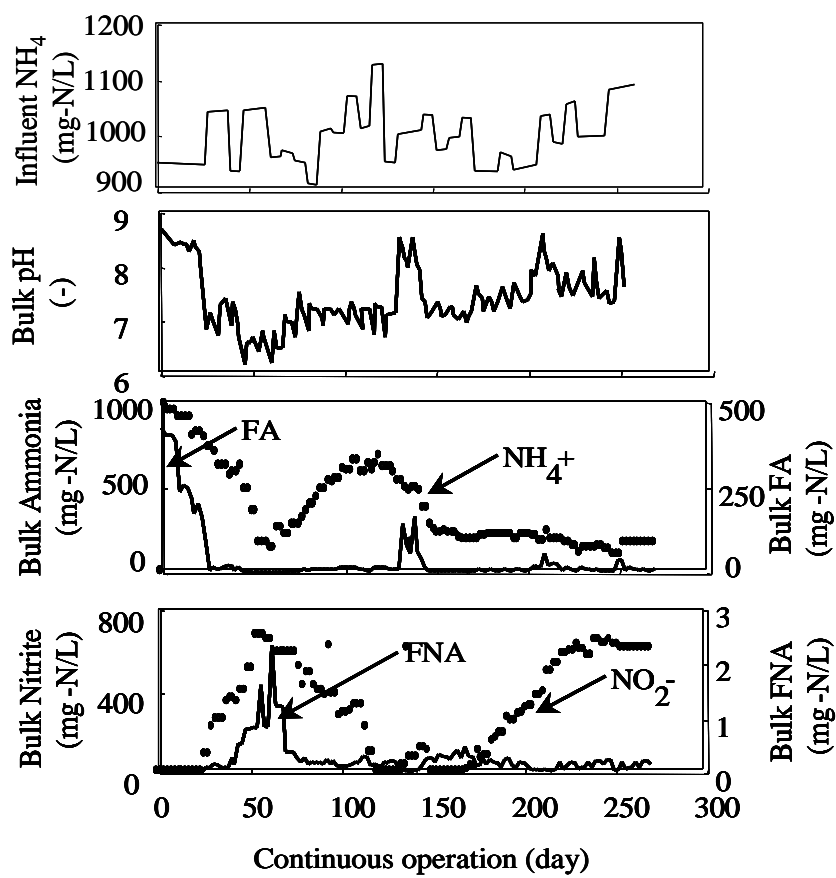


Figure 5. 4 Operating condition for SRT 10 d (synthetic wastewater).

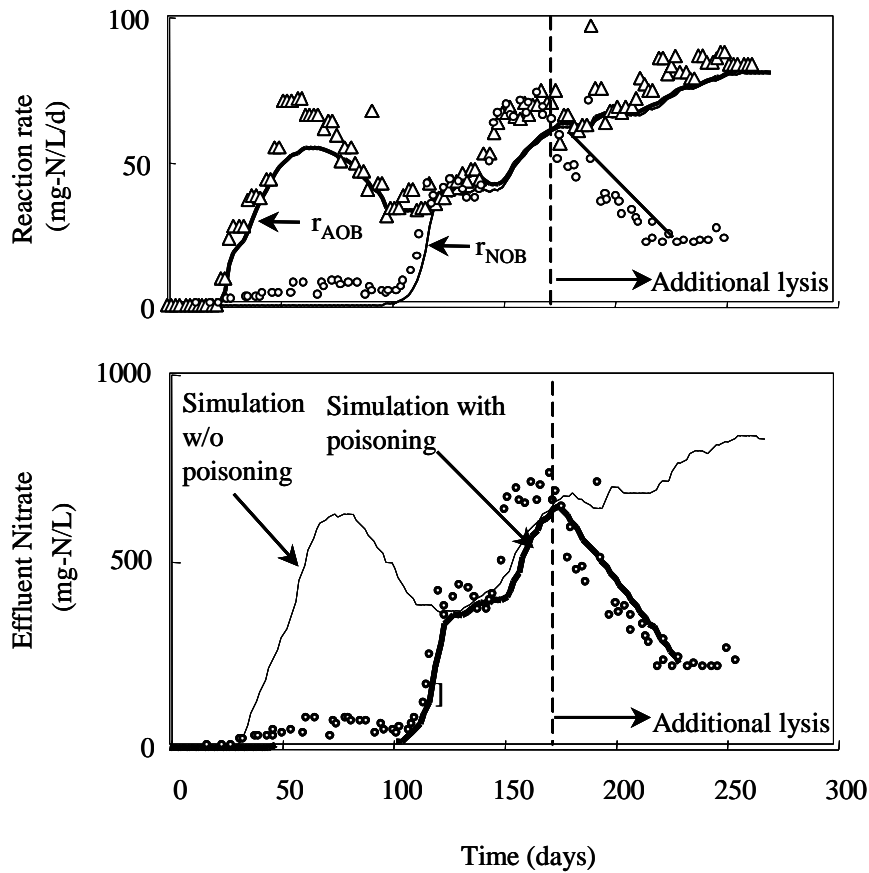


Figure 5. 5 Nitirifier reaction rate (top) and effluent nitrate (bottom) for SRT 10 d operation (synthetic wastewater).

With respect to the 5-day SRT experiment, operating conditions shown in Fig. 5.6, the initial reduction of ammonium conversion to nitrite was attributed to presence of high FA and inhibition on AOO. This lasted until reduction of FA by changing the bulk pH. Based on this period, the FA inhibition kinetics were calibrated. Through the intentional control for pH reduction, FA concentration reached acceptable level for AOO and significant production of nitrite started from day 30. Because of high FA and FNA, NOO were not possible to grow in the system and washed out finally. After that, the

response of r_{AOO} corresponded to the influent ammonium load and could be reproduced without considering FNA inhibition in the period. The AOO and NOO reaction rate and effluent nitrite concentration were simulated and shown in Fig 5.7.

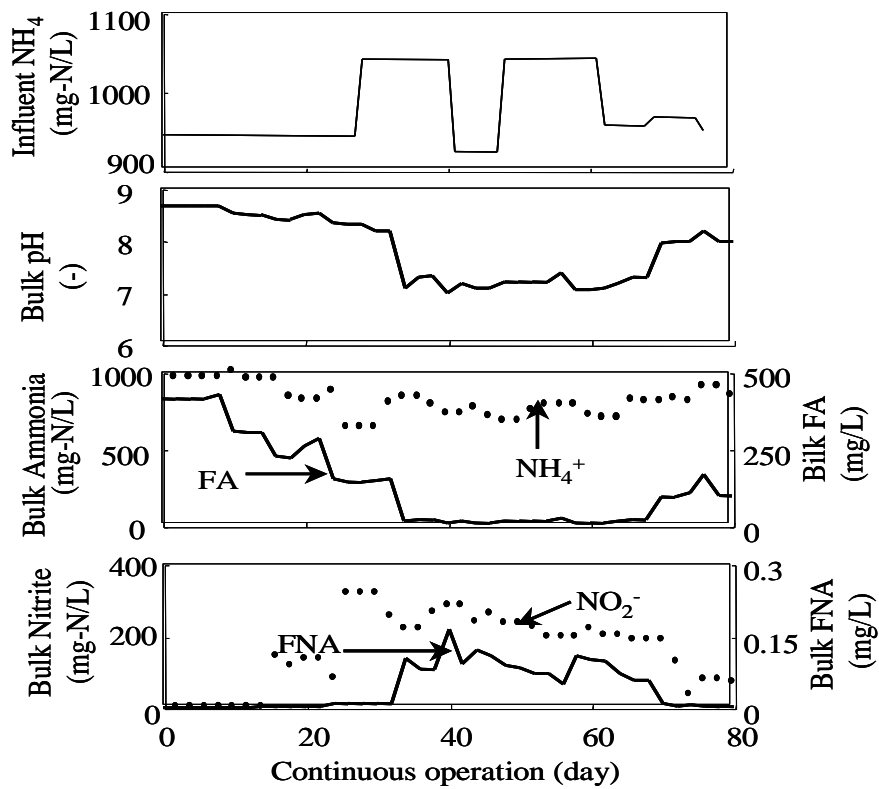


Figure 5. 6 Operating condition for SRT 5 d (synthetic wastewater).

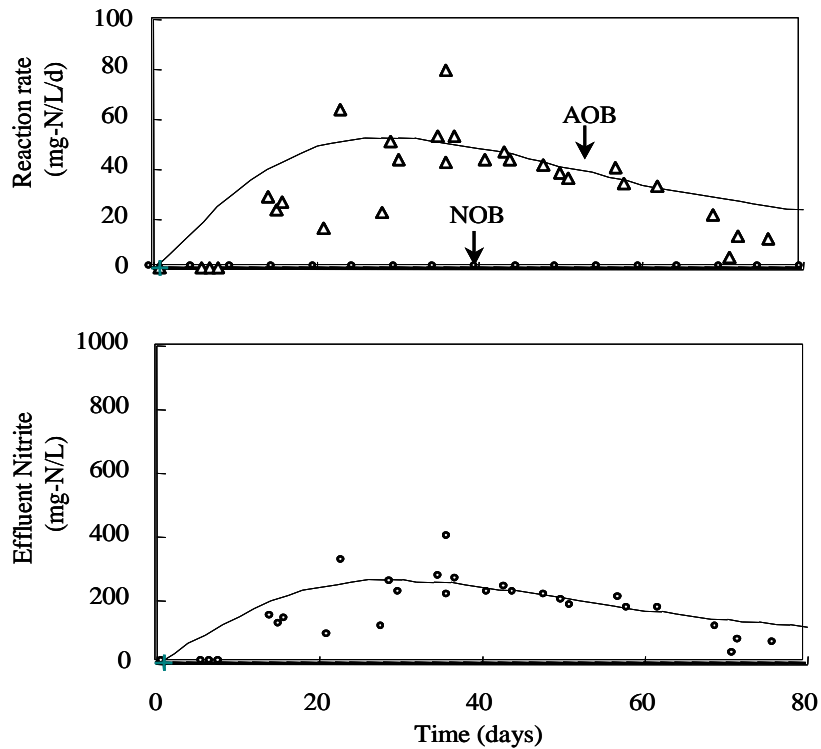


Figure 5. 7 Nitrifier reaction rate (top) and effluent nitrate (bottom) for SRT 5 d operation (synthetic wastewater).

5.3.2 Individual evaluation by benchmark datasets using dewater solid wastewater

In this experiment, the r_{AOO} consistently increased until day 20 after the start-up and peaked at day 50 due to acculturation of AOO biomass in the reactor (Fig. 5.8). This resulted in the decrease of FA, which was also affected by the intentional decrease of pH to 6.2. In this period, nitrite nitrogen correspondingly increased up to 800 mg-N/L while the conversion of nitrite to nitrate was limited to be below 50 mg-N/L. Since the accumulation of FA lasted for only 20-30 days, AOO's growth could be simulated without considering the inhibition effect of FA. On the other hand, the lower r_{NOO} was

mainly attributed to the NOO poisoning by the FA that reduced its overall specific growth rate. Nevertheless the r_{NOO} exponentially elevated after the significant decrease of FA, but it was strongly slowed by the FNA until day 100. After day 100, although a slight of ammonium remained in the effluent, no nitrite was detected. After day 100, complete nitrification was observed due to enrichment of AOO biomass from the excess substrate. The effluent nitrite concentration was reasonably simulated using the model shown in Fig. 5.9. Without incorporating the poisoning phenomena, the r_{NOO} remarkably overestimated in the initial phase.

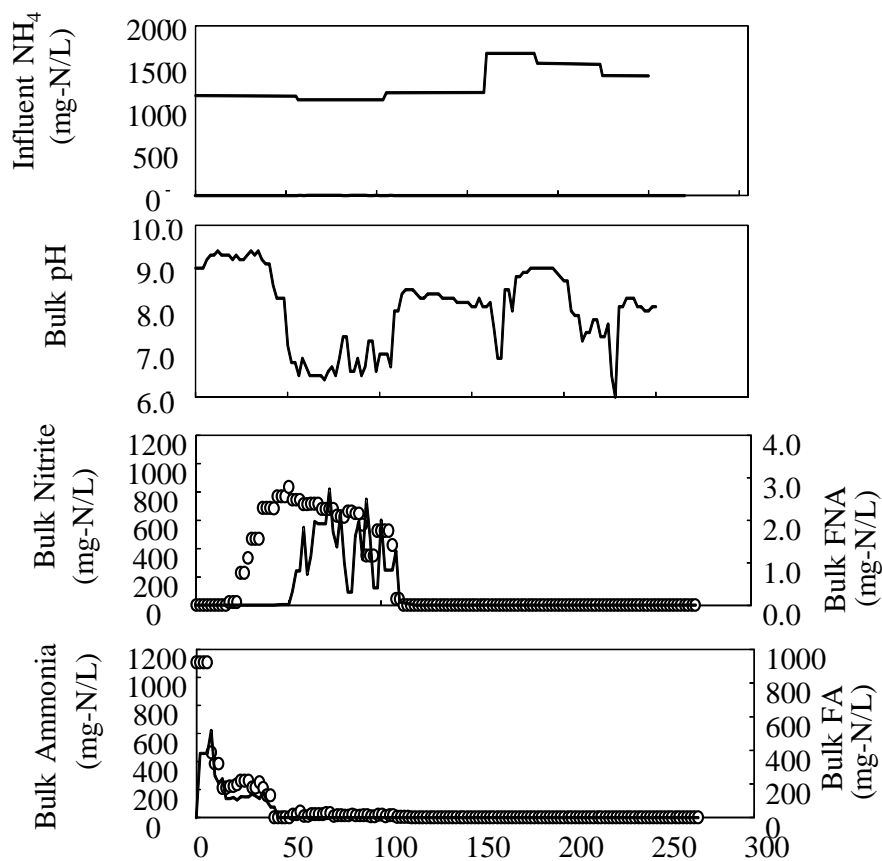


Figure 5. 8 Operating condition for SRT 20 d (dewater solid wastewater)

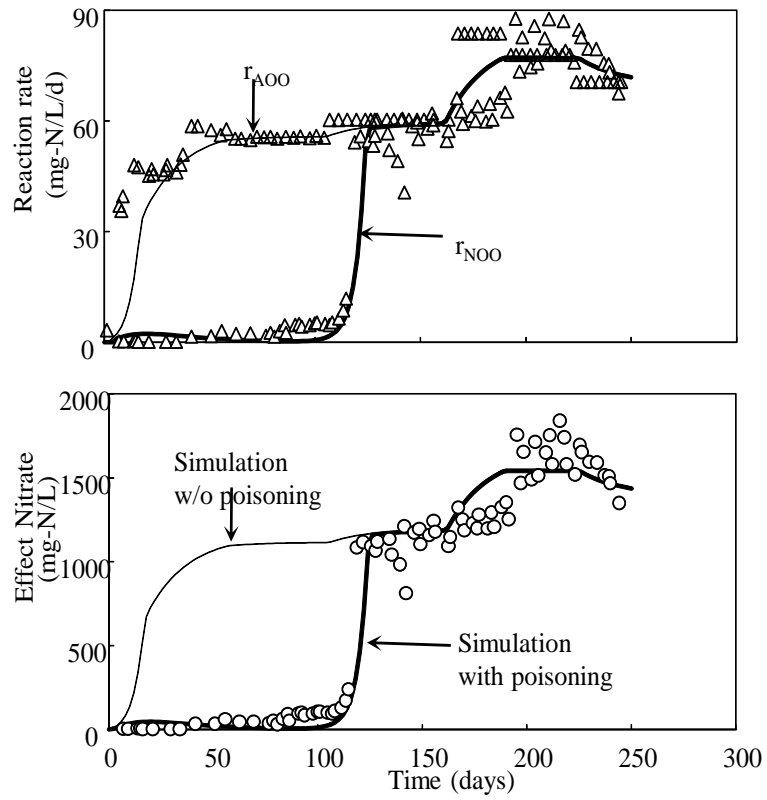


Figure 5. 9 Nitrifier reaction rate (top) and effluent nitrate (bottom) for SRT 20 d operation (dewater solid wastewater).

5.4 Discussion

5.4.1 Model verification in the nitrification process

To complete the model verification, the simulation using the reactions by both AOO and NOO were conducted as shown in Fig. 5.10-12. The effluent of ammonium, nitrite and nitrate were reasonably reproduced from the model for the three datasets. The coefficients for the model are summarised in Table 5.2. Biomass yield coefficients for AOO and the maximum specific growth rates were close to literature values ($Y_{\text{AOO}} = 0.25$, $Y_{\text{NOO}} = 0.03$, $Y_{\text{Nitrifier}} = 0.80 \text{ d}^{-1}$) (Stensel *et al.*, 1992 and Henze *et al.*, 2000). However the TVS concentrations were remarkably underestimated in the period after day 120 for the 20-day experiment. As biomass in the system during the period was relatively stable since complete nitrification was achieved, the discrepancy was considered to be attributed to the influent TVS fraction in the synthetic inorganic wastewater having high calcium salts used by Zimmerman *et al.* (2004).

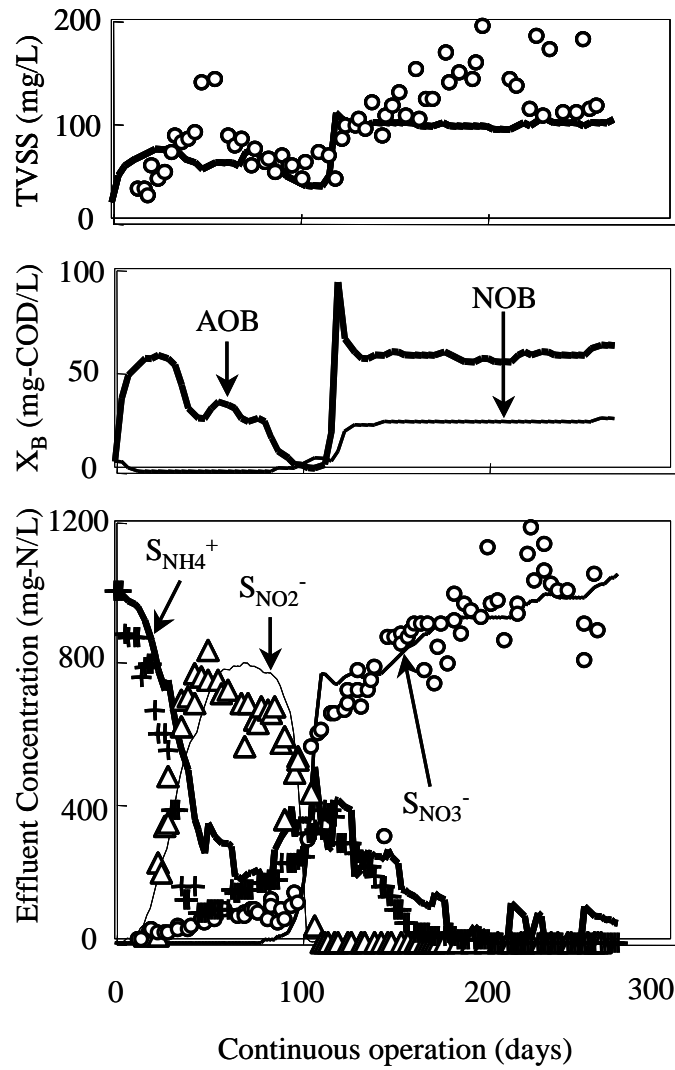


Figure 5. 10 Benchmark simulation result at 20-day SRT (+: Ammonium, Δ : Nitrite, O: Nitrate).

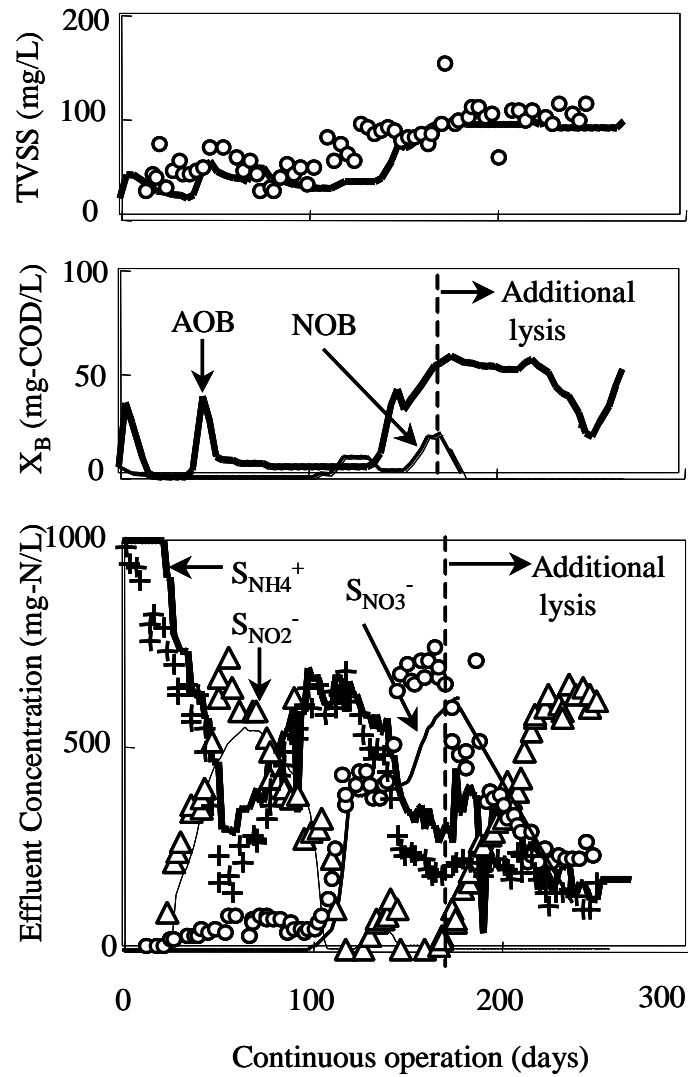


Figure 5. 11 Benchmark simulation result at 10-day SRT (+: Ammonium, Δ : Nitrite, O: Nitrate).

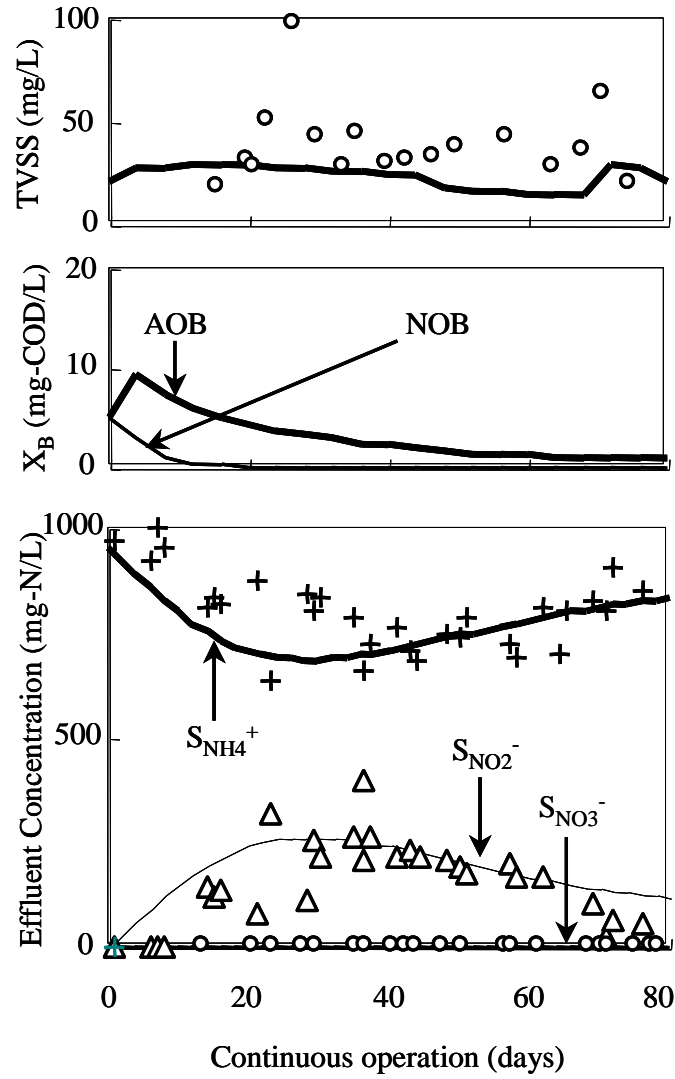


Figure 5. 12 Benchmark simulation result at 5-day SRT (+: Ammonium, Δ : Nitrite, O: Nitrate)

Table 5. 2 Coefficient list for the inhibition model

| | Symbol | Synthetic wastewater | | | Dewater solid WW | Unit | References |
|-------------------------|-------------|----------------------|---------------|----------------|---------------------|-----------------|--|
| | | 20-day SRT | 10-day SRT | 5-day SRT | 20-day SRT | | |
| AOO | Y | 0.24 | ← | ← | ← | g-COD/g- N | Henze <i>et al.</i> (2000) (as dominant nitrifier biomass) |
| | μ_{max} | 1.0 | ← | ← | ← | d ⁻¹ | |
| | K_S | 2.0 | ← | ← | ← | mg-N/L | |
| | b | 0.15 | ← | ← | ← | d ⁻¹ | |
| FNA | k_{max} | 2.0 | 0.8 | Not used | 2.0 | d ⁻¹ | |
| Poisoning for AOO | K_I | 0.57 | 0.1 | ditto | 0.57 | mg-N/L | |
| | n | 5 | ← | ditto | 5 | – | |
| FA | k_{max} | Not used | 3 | 0.82 | Not used | d ⁻¹ | |
| Poisoning for AOO | K_I | ditto | 180 | 25 | ditto | mg-N/L | |
| | n | ditto | 5 | 5 | ditto | – | |
| NOO | Y | 0.029 | ← | ← | ← | g-COD/g- N | |
| | μ_{max} | 0.35 | ← | ← | ← | d ⁻¹ | |
| | K_S | 35 | ← | ← | ← | mg-N/L | |
| | b | 0.08 | ← | ← | ← | d ⁻¹ | |
| FNA | k_{max} | 0.15 | ← | ← | ← | d ⁻¹ | |
| Poisoning for NOO | K_I | 0.33 | 0.20 | ← | 1.2 | mg-N/L | |
| | n | 5 | ← | ← | ← | – | |
| FA | k_{max} | 0.4 | 0.8 | Not | 0.4 | d ⁻¹ | |
| Poisoning for NOO | | | | identifie d | | | |
| | K_I | 11 | ← | ditto | 11 | mg-N/L | |
| | n | 5 | ← | ditto | 5 | – | |
| Additional lysis (?) | K_3 | – | 0.37 | – | – | d ⁻¹ | |

Calibration of the half saturation coefficients was needed to meet the dynamic responses and the same values could be used over the three datasets. The specific decay rate were not calibrated and literature values were used (Henze *et al.*, 2000; Liu *et al.* (2011)). With respect to the poisoning coefficients, it seemed that inhibition impact of FA was stronger than FNA for NOO as its k_{\max} was more than 2.5 times higher than FA. This suggests that the partial nitrification process would be robust as compared to complete nitrification process. Comparing the poisoning coefficients of NOO at 20-day SRT to those at 10-day SRT, the $k_{i\max}$ for FA at 20-day SRT was 50% of that at 10-day SRT whereas the K_I for FNA at 20-day SRT was 160 % higher. Although the exact reason is not clear at present, it may due to difference in the participating species of NOO at different SRT.

5.5 Conclusion

Four sets of long-term continuous benchmark datasets were simulated using developed model containing reversible inhibition on growth stage and irreversible inhibition on decay stage to verify the correctness of new model. the following conclusions were obtained in this study.

- The research systematically clarified the inhibition effects of FA and FNA on nitrifiers. Although Haldane-type inhibition is traditionally used to model the inhibition of ammonia oxidation and nitrite oxidation process.
- It appears that an alternative poisoning model with poisoning concentration threshold could express the nitrifier's response more accurately.
- Since the model assumed a non-reversible inactivation of the microorganism, further experimental validation involving characterisation of active/inactive cells could strengthen the concept. Apart from substrate inhibition of nitrifiers, an additional mechanism of microbial lysis due to predator infection may need further investigation.
- FNA and FA poisonings occur on NOO while dewatered biosolids supernatant containing high strength ammonia concentration.

- With influent conditions (pH and concentration) changing, although the same source of bacteria was used in the operation, a slight change in the parameters values may be due to a response from different bacterial species in combination.

6 Bioaugmentation with nitrifiers developed from different substrates

6.1 Background

When operation conditions changes in biological processes, reactions will be affected by shock loads resulting in a sudden reduction of bacterial activity. In biological nitrification processes, AOO and NOO are sensitive on environmental conditions that were discussed in chapter 2. However, in real operation processes, the conditions sometimes change out of anthropogenic control. For instance to expand the bacterial training scale, the trained bacteria need to be moved to a new environment, during the transportation or the beginning of training in new conditions, the environment cannot be kept as same as the original one absolutely. In those kinds of situations, it is important to know the bacterial activity recovery ability.

To verify and evaluate the adaption ability in new conditions, bioaugmentation datasets that were obtained from nitrifiers developed in different conditions high-strength ammonia synthetic waste water, dewatered biosolid supernatant containing high ammonia concentration and tricking filter were selected in WERF published by IWA (Zimmerman *et al.*, 2004). Kinetics values were obtained from simulations using the same model developed in chapter 3 and compared among the kinetic values from simulations.

6.2 Material and Methods

6.2.1 Seed nitrifiers training

For bioaugmentation experiments, seed nitrifiers were developed from commercially available nitrifiers trained in high ammonia concentration synthetic wastewater (about 1000 mg-NH₄-N/L) as was introduced in Part I of chapter 5. To be sure the bioaugmentation procedures, a low ammonia concentration (about 25 mg-NH₄-N/L) synthetic wastewater obtained by diluting the high-strength wastewater was utilized to verify the bioaugmentation feasibility (Zimmerman *et al.*, 2004). The characteristics of high ammonia concentration wastewater used are shown in Table 6.1

Table 6. 1 Synthetic wastewater characteristics

| Constituent | Concentration (mg/L) |
|---|----------------------|
| MgSO ₄ -7H ₂ O | 20000 |
| FeSO ₄ -7H ₂ O | 2500 |
| ZnSO ₄ -7H ₂ O | 200 |
| MnSO ₄ -H ₂ O | 30 |
| CaCl ₂ -2H ₂ O | 2000 |
| Na ₂ HPO ₄ | 2481 |
| KH ₂ PO ₄ | 1215 |
| NaHCO ₃ | 2453 |
| (NH ₄) ₂ SO ₄ | 4717 |

Seed nitrifying population for bioaugmentation were also developed from microorganisms indigenous to dewatered biosolids supernatant. This supernatant typically contains a high ammonia concentration.

Bioaugmentation procedures were verified in diluted supernatant (Zimmerman *et al.*, 2004). Typical characteristics of undiluted dewatered biosolids supernatant are shown in Table 6.2.

Table 6. 2 Typical dewatered biosolids supernatant characteristics

| parameter | Concentration (mg/L) |
|-----------|----------------------|
| Mg | 12.9 |
| Fe | 3.04 |
| Zn | 0.292 |
| Mn | 0.087 |
| Ca | 55.1 |

6.2.2 Bioaugmentation analyses

Batch bioaugmentation analyses were conducted using the MLSS and final clarifier effluent from a non-nitrifying activated sludge with seed nitrifiers developed from the high-strength ammonia synthetic wastewater and dewatered biosolids supernatant operated at a 20-day SRT and also with biomass from an operating nitrifying tricking filter facility. Environmental conditions (e.g. temperature and pH) between the seed bioreactors (used to develop the supplemental nitrifiers) and the bioaugmentation reactors (to which supplemental nitrifiers were added) were not significantly different. For nitrifiers developed from high-strength ammonia synthetic waste, the difference in temperature and pH between the seed and bioaugmentation reactors was $\pm 2.1^{\circ}\text{C}$ and ± 0.5 standard units respectively. For nitrifiers developed from dewatered biosolids supernatant, the difference in temperature and pH between the seed and bioaugmentation reactors was $\pm 4.5^{\circ}\text{C}$ and ± 0.8 respectively (Zimmerman *et al.*, 2004).

6.2.3 Model structure

Since the nature culture bacterial organisms were considered in bioaugmentation process, the whole model was constructed including two-step nitrification containing ammonia and nitrite oxidation, OHO and ammoniaification shown in Table 4.1. In the model, a poisoning process was added for AOO, NOO and OHO.

In the growth stage, Monod-type functions were utilized, and in the decay stage, specific inherent decay rate (b) was the same as ASM (Henze *et al.*, 2000). To account for a poisoning event and for a complete model, poisoning expression was added as shown in Table 5.6. A Monod-type threshold function was mentioned in chapter 4 was used.

6.3 Results

6.3.1 Bioaugmentation with nitrifiers developed from high-strength ammonia synthetic waste at 20-day SRT

A set of bioaugmentation analyses were conducted using seed nitrifiers developed from high-strength ammonia synthetic waste at 20-day SRT, using low-strength ammonia synthetic wastewater, clarified activated sludge and non-nitrifying activated sludge as substrates. The experimental conditions were shown in Table 6.3. In Table 6.3 Run No.1 was conducted in the seed bioreactor without supplemental nitrifiers.

Table 6. 3 Bioaugmentation analyses with nitrifiers developed from high-strength ammonia synthetic waste at 20-day SRT

| Run No. | 1 | 2 | 3 | 4 | 5 |
|---|-----------------|------------------------------|------|----------------------------|------------------|
| substrate | Seed bioreactor | Low-strength synthetic waste | | Clarified activated sludge | Activated sludge |
| Substrate volume, L | N/A | 5.75 | 3.50 | 3.50 | 3.50 |
| Supplemental nitrifier volume, L | N/A | 0.25 | 0.50 | 0.50 | 0.50 |
| Total volume, L | 5.00 | 6.00 | 4.00 | 4.00 | 4.00 |
| X_{Nest} (VSS _N), mg/L | 109 | 6.8 | 15.4 | 14.2 | 15.0 |
| NH ₃ -N removal rate, mg/L/h | 5.78 | 0.66 | 0.72 | 0.94 | 0.86 |
| q_{Nest} , mgNH ₃ -N oxidized/mg VSS _N /d | 1.28 | 2.34 | 1.12 | 1.59 | 1.38 |
| OUR, mg/L/h | N/A | N/A | 2.97 | 2.96 | 10.59 |
| Specific oxygen uptake, mgO ₂ /mgNH ₃ -N oxidized | N/A | N/A | 4.13 | 3.15 | N/A |

Simulation results (Run No.1-5)

According to a mathematical model modified from ASM (Henze *et al.*, 2000) shown in Table 5.6, the dominant microorganisms in the seed sludge were estimated to be AOO (50%), NOO (20%), OHO (20%) and inert particulates (10%), this corresponded to simulation results that were obtained and shown in Fig.6.1– 6.5. The parameters values were listed in Table 6.4.

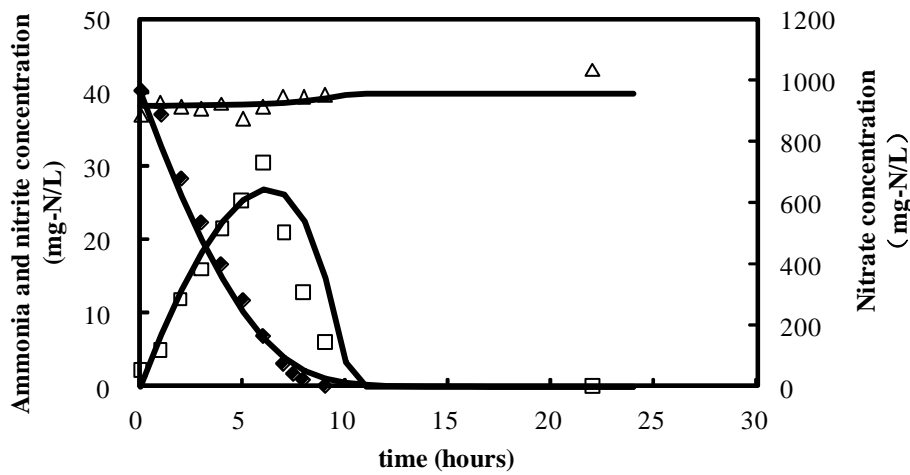


Figure 6. 1 Bioaugmentation with nitrifiers developed from high-strength ammonia synthetic wastewater at 20-day SRT in seed bioreactor.

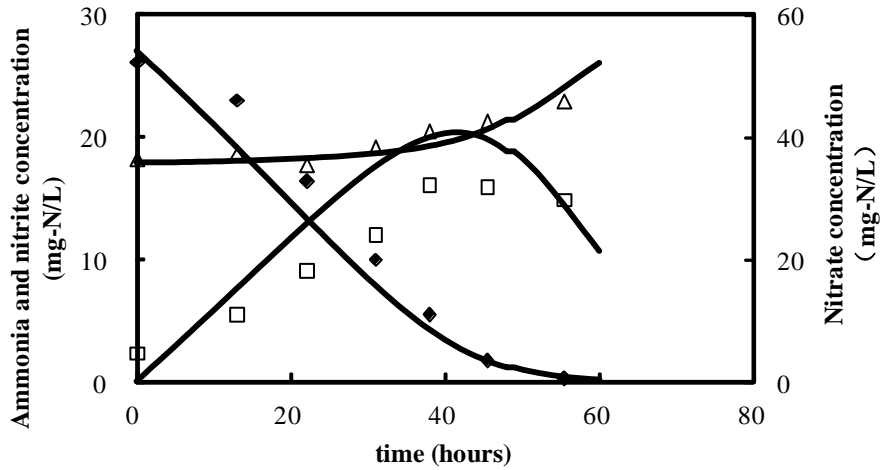


Figure 6. 2 Bioaugmentation with nitrifiers developed from high-strength ammonia synthetic wastewater at 20-day SRT under low-strength synthetic wastewater (test 1).

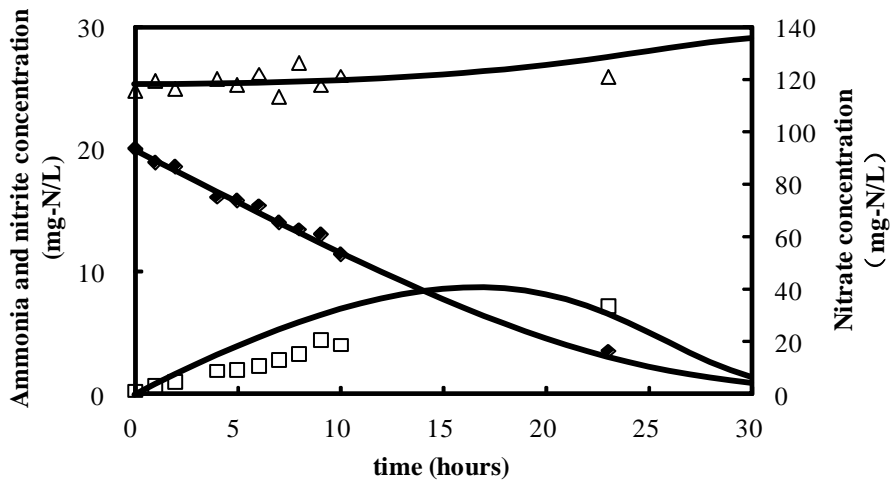


Figure 6. 3 Bioaugmentation with nitrifiers developed from high-strength ammonia synthetic waste at 20-day SRT under low-strength synthetic wastewater (test 2)

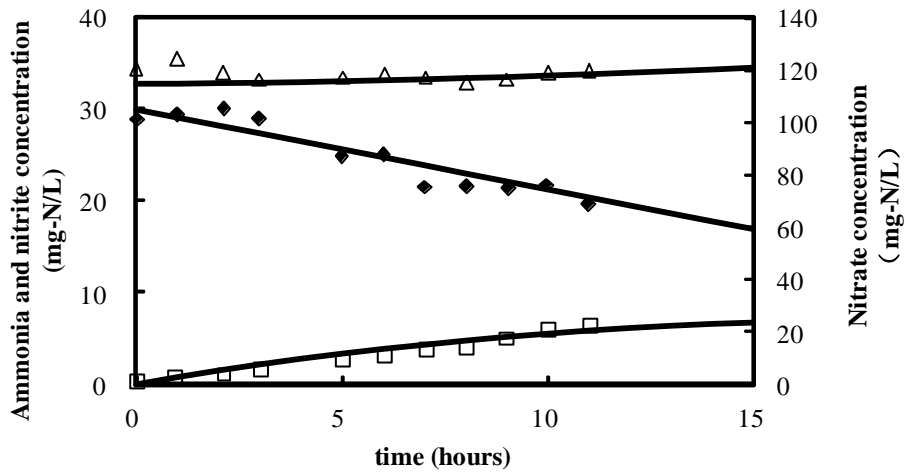


Figure 6. 4 Bioaugmentation with nitrifiers developed from high-strength ammonia synthetic waste at 20-day SRT using clarified activated sludge supernatant

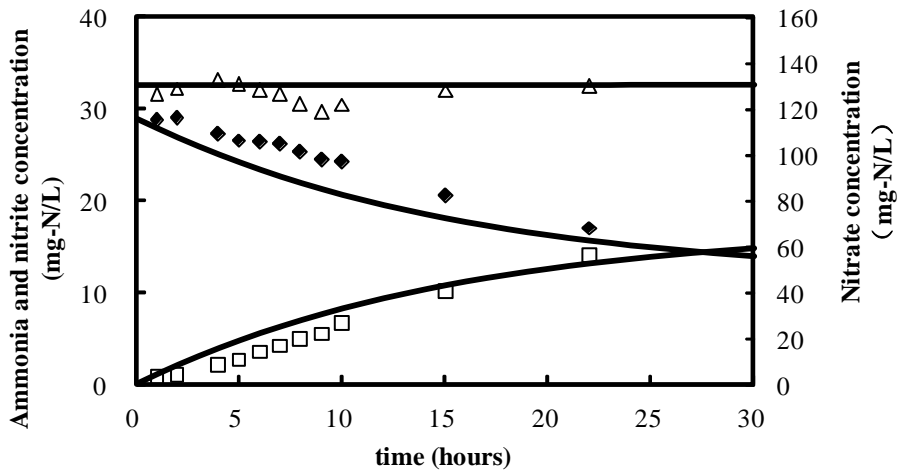


Figure 6. 5 Bioaugmentation with nitrifiers developed from high-strength ammonia synthetic waste at 20-day SRT using activated sludge supernatant

Table 6. 4 Parameters values from simulations

| | | NO.1 | NO.2 | NO.3 | NO.4 | NO.5 |
|-----------------|-----------------|-------------|------------|-------------|-------------|-------------|
| Parameter | Unit | | | | | |
| Y_{AOO} | g-COD/g-N | 0.208 | 0.208 | 0.208 | 0.208 | 0.208 |
| $\mu_{max,AOO}$ | d ⁻¹ | 0.4 | 0.5 | 0.35 | 0.35 | 0.35 |
| $K_{S,AOO}$ | mg-N/L | 6 | 6 | 6 | 6 | 6 |
| b_{AOO} | d ⁻¹ | 0.04 | 0.04 | 0.04 | 0.04 | 0.04 |
| Y_{NOO} | g-COD/g-N | 0.029 | 0.029 | 0.029 | 0.029 | 0.029 |
| $\mu_{max,NOO}$ | d ⁻¹ | 0.35 | 0.3 | 0.35 | 0.35 | 0.35 |
| $K_{S,NOO}$ | mg-N/L | 6 | 6 | 6 | 6 | 6 |
| b_{NOO} | d ⁻¹ | 0.04 | 0.04 | 0.08 | 0.04 | 0.04 |
| Y_{OHO} | g-COD/g-N | 6 | 6 | 6 | 6 | 6 |
| $\mu_{max,OHO}$ | d ⁻¹ | 20 | 20 | 20 | 20 | 20 |
| $K_{S,OHO,O2}$ | mg-O/L | 0.2 | 0.2 | 0.2 | 0.2 | 0.2 |
| $K_{S,OHO,NO3}$ | mg-N/L | 0.5 | 0.5 | 0.5 | 0.5 | 0.5 |
| b_{OHO} | d ⁻¹ | 0.62 | 0.62 | 0.62 | 0.62 | 0.62 |

Run No. 1 was operated in a seed reactor using high strength synthetic ammonia wastewater as a substrate as shown in Fig. 6.1. From the parameters values listed in Table 6.4, $\mu_{max,AOO}$ is 0.4 d⁻¹ and $\mu_{max,NOO}$ is 0.35 d⁻¹. Run No. 2 and 3 were conducted to verify bioaugmentation procedures by subjecting the supplemental nitrifier population to a familiar substrate, a

low-strength ammonia synthetic wastewater at similar temperature and pH shown in Fig. 6.2 and 6.3. Comparing to $\mu_{\max, \text{AOO}}$ and $\mu_{\max, \text{NOO}}$ of Run No. 1, there are no significant differences in Run 1, Run 2 and Run 3.

Run No.4 and 5 were conducted to determine if an acclimation period was required when the separately cultured nitrifier was introduced to an unfamiliar substrate. From the datasets in Fig. 6.4 and 6.5 and simulation parameter values shown in Table 6.4, there were no significant different between nitrifiers trained in a seed reactor those using low-strength familiar substrate. According to the parameters values from the simulation, a conclusion that bioaugmentation with nitrifiers developed from high-strength ammonia synthetic waste can be achieve in different substrates of low-strength ammonia synthetic wastewater, clarified activated sludge, and non-nitrifying activated sludge at 20-day SRT although there are slight differences in some parameters values.

6.3.2 Bioaugmentation with nitrifiers developed from dewatered biosolids supernatant at 20-day SRT

Bioaugmentation analyses were conducted in diluted bioreactor supernatant containing ammonia wastewater, clarified activated sludge and non-nitrifying activated sludge. Results from the analyses utilizing nitrifiers developed from dewatered biosolids supernatant containing ammonia

wastewater at a 20-day SRT are summarized in Table 6.5 with the data from Run No.6 conducted in the seed bioreactor without supplemental nitrifiers.

Table 6. 5 Bioaugmentation analyses with nitrifiers developed from dewatered biosolids supernatant at 20-day SRT

| Run No. | 6 | 7 | 8 | 9 | 10 | 11 |
|---|-----------------|-------------------------------|------|----------------------------|------|------------------|
| substrate | Seed bioreactor | Diluted dewatered supernatant | | Clarified activated sludge | | Activated sludge |
| Substrate volume, L | N/A | 4.75 | 3.55 | 4.75 | 3.55 | 3.55 |
| Supplemental nitrifier volume, L | N/A | 0.25 | 0.45 | 0.25 | 0.45 | 0.45 |
| Total volume, L | 5.00 | 5.00 | 4.00 | 5.00 | 4.00 | 4.00 |
| X (VSS), mg/L | 558 | 34.5 | 59.0 | 31.3 | 61.4 | 77.2 |
| X _{Nest} (VSS _N), mg/L | 285 | 17.6 | 30.1 | 16.0 | 31.3 | 39.4 |
| NH ₃ -N removal rate, mg/L/h | 6.55 | 0.85 | 0.62 | 0.64 | 0.72 | 0.65 |
| q _{Nobs} , mgNH ₃ -N oxidized/mg VSS/d | 0.28 | 0.59 | 0.25 | 0.49 | 0.28 | 0.20 |
| q _{Nest} , mgNH ₃ -N oxidized/mg VSSN/d | 0.55 | 1.16 | 0.50 | 0.97 | 0.55 | 0.40 |
| OUR, mg/L/h | N/A | N/A | 2.32 | N/A | 2.97 | 10.74 |
| Specific oxygen uptake, mgO ₂ /mgNH ₃ -N oxidized | N/A | N/A | 3.74 | N/A | 4.13 | N/A |

Simulation results (Run No.6-11)

According to model shown in Table 4.1 and calculated initial AOO and NOO, the corresponding simulation results were obtained shown in Fig.6.6– 6.11.

The parameters values were listed in Table 6.6.

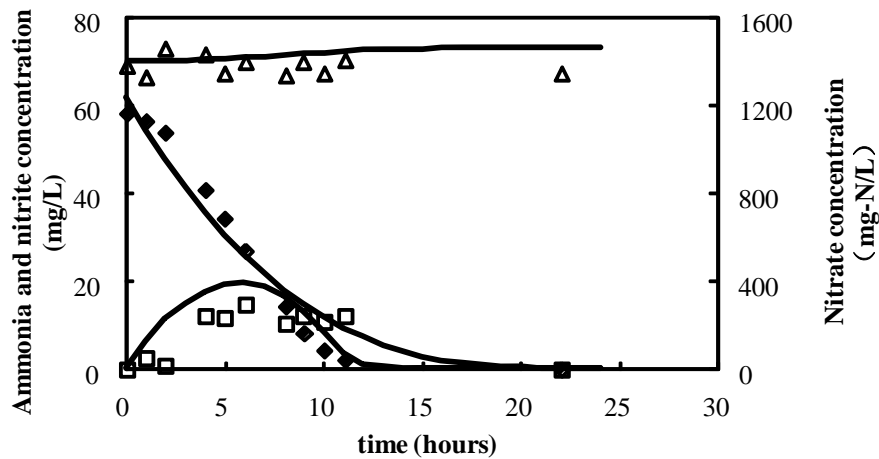


Figure 6. 6 Bioaugmentation with nitrifiers developed from dewatered biosolids supernatant at 20-day SRT in seed bioreactor.

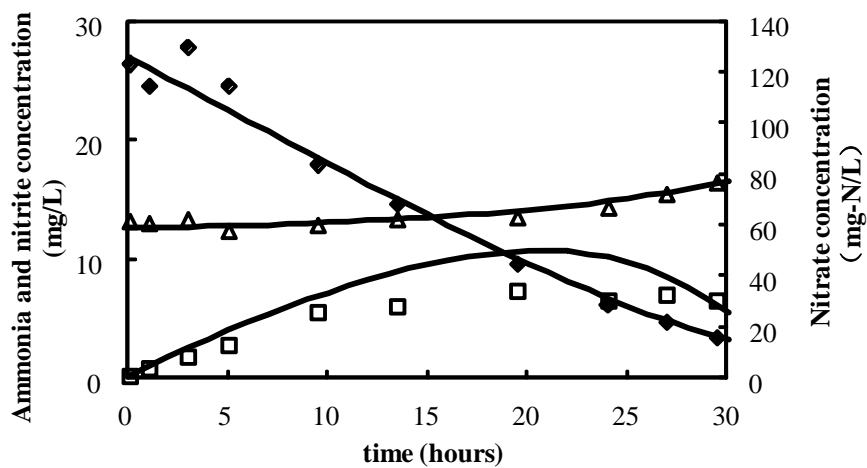


Figure 6. 7 Bioaugmentation with nitrifiers developed from dewatered biosolids supernatant at 20-day SRT using diluted dewatered supernatant as substrate (test 1).

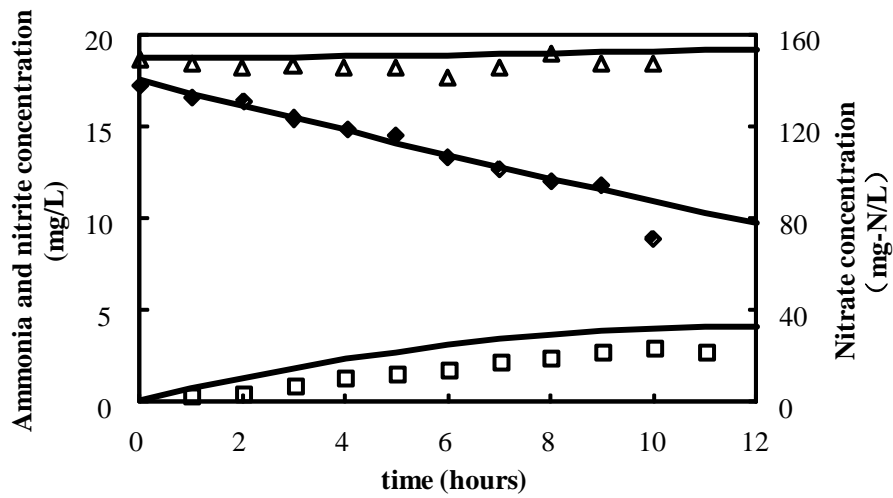


Figure 6. 8 Bioaugmentation with nitrifiers developed from dewatered biosolids supernatant at 20-day SRT using diluted dewatered supernatant as substrate (test 2).

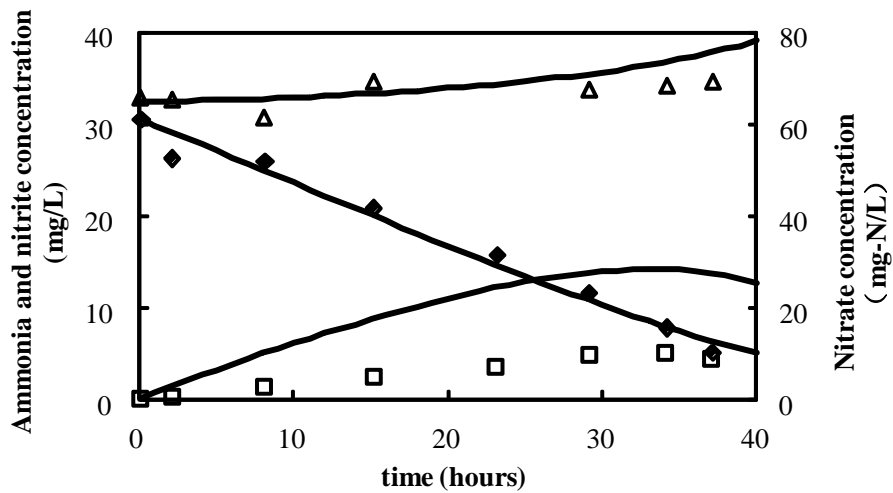


Figure 6. 9 Bioaugmentation with nitrifiers developed from dewatered biosolids supernatant at 20-day SRT using clarified activated sludge supernatant as substrate (test 1).

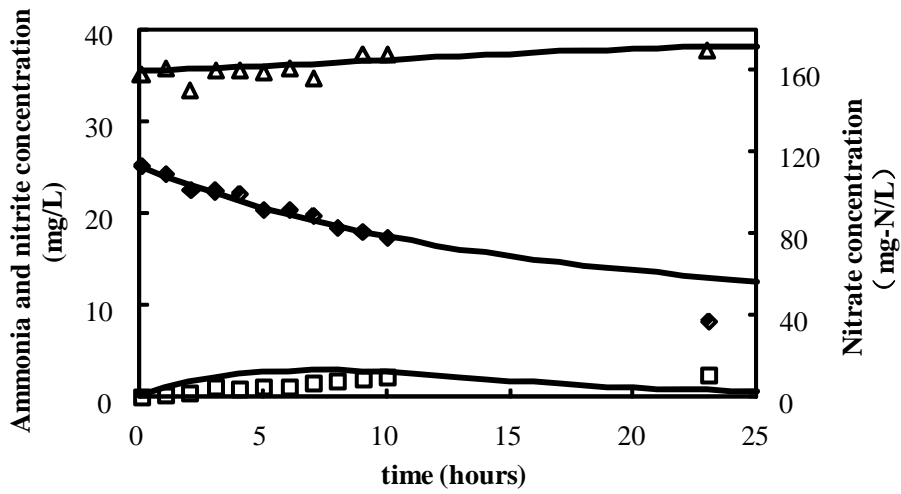


Figure 6. 10 Bioaugmentation with nitrifiers developed from dewatered biosolids supernatant at 20-day SRT using clarified activated sludge supernatant as substrate (test 2).

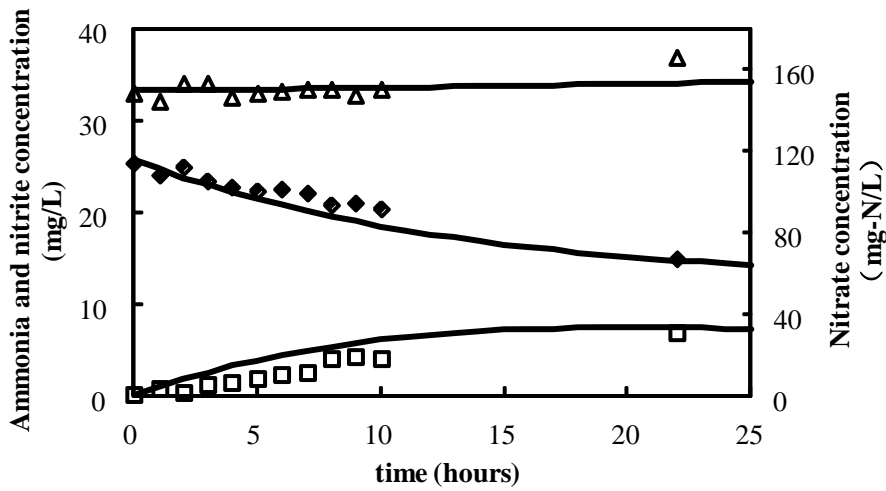


Figure 6. 11 Bioaugmentation with nitrifiers developed from dewatered biosolids supernatant at 20-day SRT using activated sludge supernatant as substrate.

Table 6. 6 Parameters values from simulations

| | | NO.6 | NO.7 | NO.8 | NO.9 | NO.10 | NO.11 |
|-----------------|-----------------|-------------|------------|-------------|-------------|------------|-------------|
| Parameter | Unit | | | | | | |
| Y_{AOO} | g-COD/g-N | 0.208 | 0.208 | 0.208 | 0.208 | 0.208 | 0.208 |
| $\mu_{max,AOO}$ | d ⁻¹ | 0.15 | 0.3 | 0.15 | 0.25 | 0.2 | 0.15 |
| $K_{S,AOO}$ | mg-N/L | 6 | 6 | 6 | 6 | 6 | 6 |
| b_{AOO} | d ⁻¹ | 0.04 | 0.04 | 0.04 | 0.04 | 0.04 | 0.04 |
| Y_{NOO} | g-COD/g-N | 0.029 | 0.029 | 0.029 | 0.029 | 0.029 | |
| $\mu_{max,NOO}$ | d ⁻¹ | 1 | 1 | 1 | 0.7 | 1 | 0.25 |
| $K_{S,NOO}$ | mg-N/L | 6 | 6 | 6 | 6 | 6 | 6 |
| b_{NOO} | d ⁻¹ | 0.04 | 0.04 | 0.08 | 0.04 | 0.04 | 0.04 |
| Y_{OHO} | g-COD/g-N | 6 | 6 | 6 | 6 | 6 | 6 |
| $\mu_{max,OHO}$ | d ⁻¹ | 20 | 20 | 20 | 20 | 20 | 20 |
| $K_{S,OHO,O2}$ | mg-O/L | 0.2 | 0.2 | 0.2 | 0.2 | 0.2 | 0.2 |
| $K_{S,OHO,NO3}$ | mg-N/L | 0.5 | 0.5 | 0.5 | 0.5 | 0.5 | 0.5 |
| b_{OHO} | d ⁻¹ | 0.62 | 0.62 | 0.62 | 0.62 | 0.62 | 0.62 |

Run No. 6 is an operation in a seed reactor with nitrifiers using dewatered biosolids supernatant containing high ammonia concentration wastewater as a substrate shown in Fig. 6.6. From the parameters values listed in Table 6.6, $\mu_{max,AOO}$ is 0.15 d⁻¹ and $\mu_{max,NOO}$ is 1.0 d⁻¹.

Run No. 7 and 8 were conducted to verifying bioaugmentation procedures by subjecting the supplemental nitrifier population to a familiar diluted

substrate, a low-strength ammonia dewater supernatant wastewater at similar temperature and pH shown in Fig. 6.7 and 6.8. Comparing to $\mu_{\max, AOO}$ and $\mu_{\max, NOO}$ of Run No. 6, there are no significant differences between Run 6 and Run 8, and the $\mu_{\max, AOO}$ value of Run 7 is more than the seed reactor because of bacterial activity recovery phenomenon .

Run No.9, 10 and 11 were conducted to determine if an acclimation period was required when the separately cultured nitrifier was introduced to an unfamiliar substrate. According to the datasets in Fig. 6.9, 6.10, and 6.11 and parameter values from simulation shown in Table 6.6, there were no significant differences from nitrifiers trained in seed reactor but a slight different in $\mu_{\max, NOO}$ of Run No.11.

According to parameters values of the Run 6, 8, 10, and 11 from simulation, a conclusion that bioaugmentation with nitrifiers developed from high-strength ammonia synthetic wastewater can be achieve in diluted dewatered supernatant, clarified activated sludge and activated sludge at 20-day SRT, although there are slight differences at $\mu_{\max, NOO}$ values of Run 9 and 11.

6.3.3. Bioaugmentation with nitrifiers from nitrifying tricking filter biomass.

Bioaugmentation analyses were conducted in low-strength synthetic waste, clarified activated sludge and non-nitrifying activated sludge. Results from the analyses utilizing nitrifiers developed from nitrifying tricking filter biomass at a 20-day SRT. Results are summarized in Table 6.7.

Table 6. 7 Bioaugmentation analyses with nitrifiers from nitrifying tricking filter biomass.

| Run No. | 13 | 14 | 15 | 16 | 17 | 18 | 19 |
|--|------------------------------|-------|----------------------------|-------|-------|------------------|-------|
| substrate | Low-strength synthetic waste | | Clarified activated sludge | | | Activated sludge | |
| Substrate volume, L | 5.730 | 5.864 | 5.730 | 5.864 | 5.685 | 5.767 | 5.883 |
| Supplemental nitrifier volume, L | 0.270 | 0.136 | 0.270 | 0.136 | 0.315 | 0.233 | 0.117 |
| Total volume, L | 6.000 | 6.000 | 6.000 | 6.000 | 6.000 | 6.000 | 6.000 |
| X (VSS), mg/L | 490 | 320 | 490 | 320 | 440 | 5.28 | 265 |
| NH ₃ -N removal rate, mg/L/h | 1.71 | 0.87 | 1.71 | 1.11 | 1.24 | 1.46 | 0.81 |
| q _{Nobs} , mgNH ₃ -N oxidized/mg VSS/d | 0.084 | 0.066 | 0.084 | 0.083 | 0.067 | 0.067 | 0.074 |

Simulation results (Run No.12-19)

According to model shown in Table 6.7 and calculated initial AOO and NOO, the corresponding simulation results were obtained shown in Fig. 6.13 – 6.19. The parameters values were listed in Table 6.8.

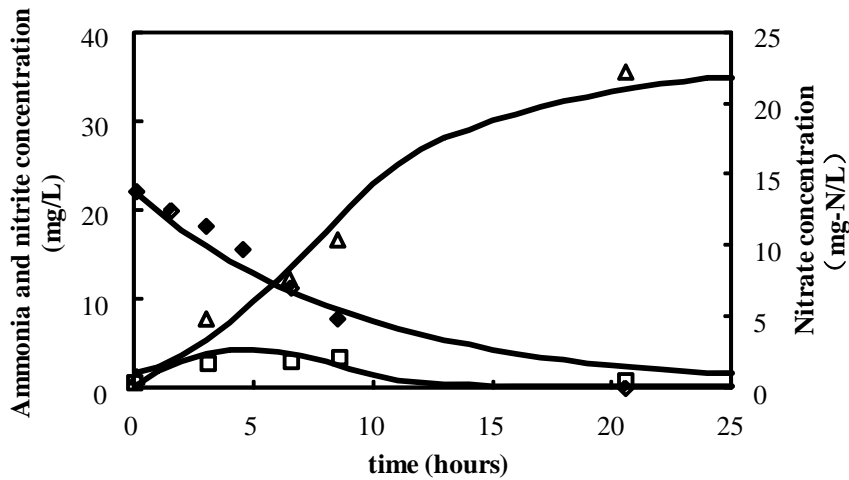


Figure 6. 12 Bioaugmentation with nitrifiers developed from nitrifying tricking filter biomass using low-strength synthetic waste as substrate (test 1).

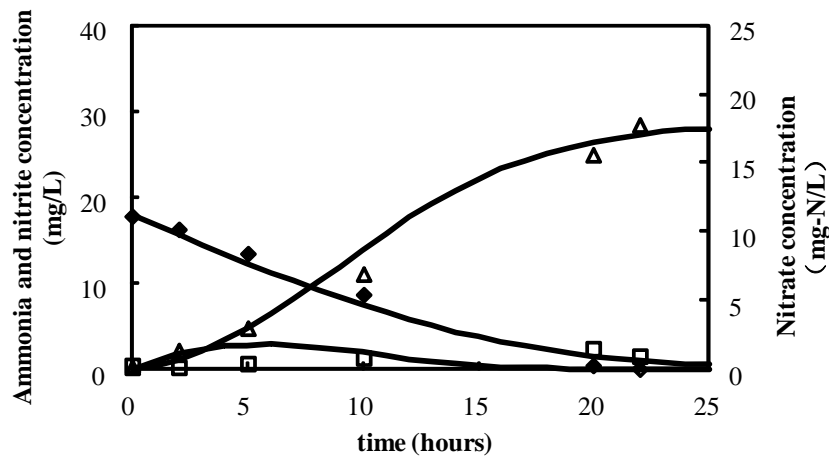


Figure 6. 13 Bioaugmentation with nitrifiers developed from nitrifying tricking filter biomass using low-strength synthetic waste as substrate (test 2).

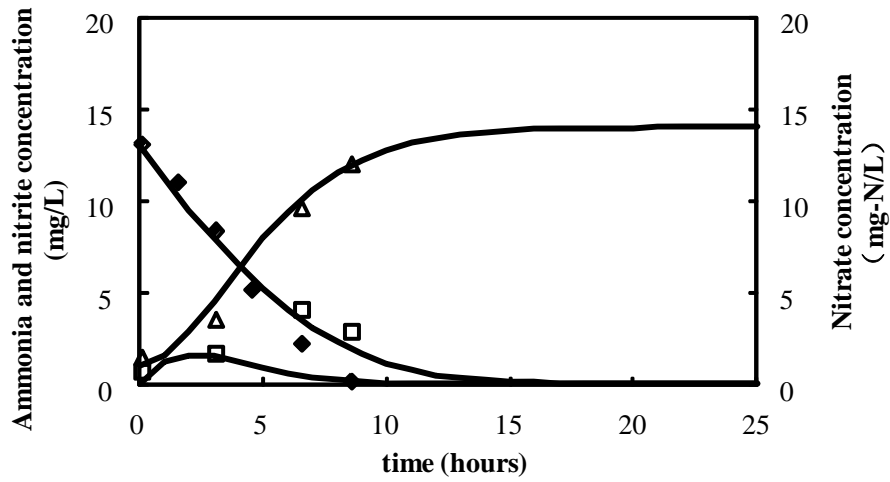


Figure 6. 14 Bioaugmentation with nitrifiers developed from nitrifying tricking filter biomass using clarified activated sludge supernatant as substrate (test 1).

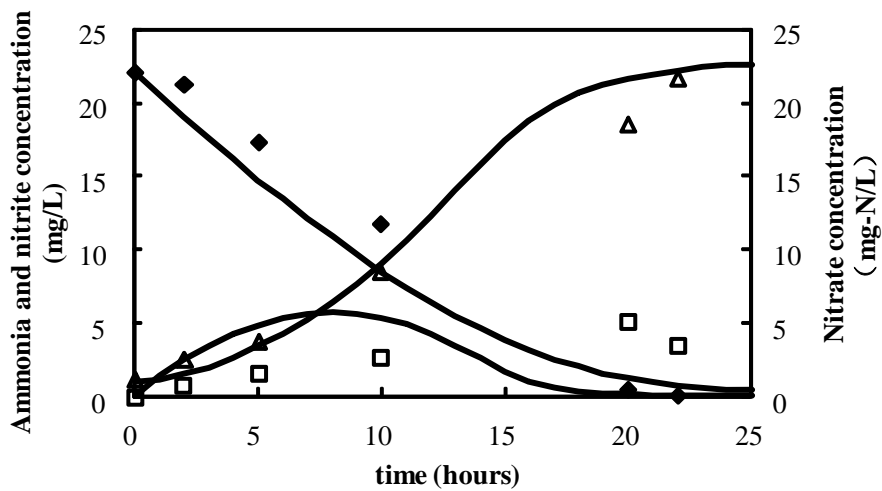


Figure 6. 15 Bioaugmentation with nitrifiers developed from nitrifying tricking filter biomass using clarified activated sludge supernatant as substrate (test 2).

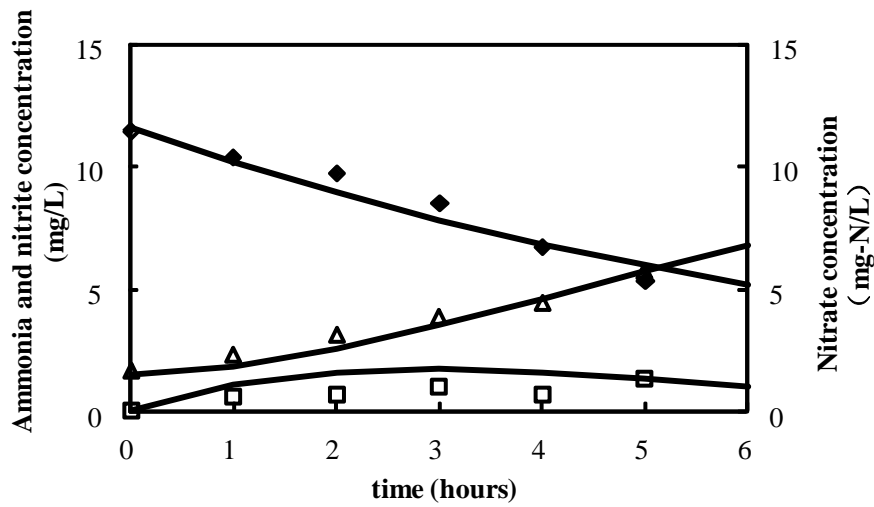


Figure 6. 16 Bioaugmentation with nitrifiers developed from nitrifying tricking filter biomass using clarified activated sludge supernatant as substrate (test 3).

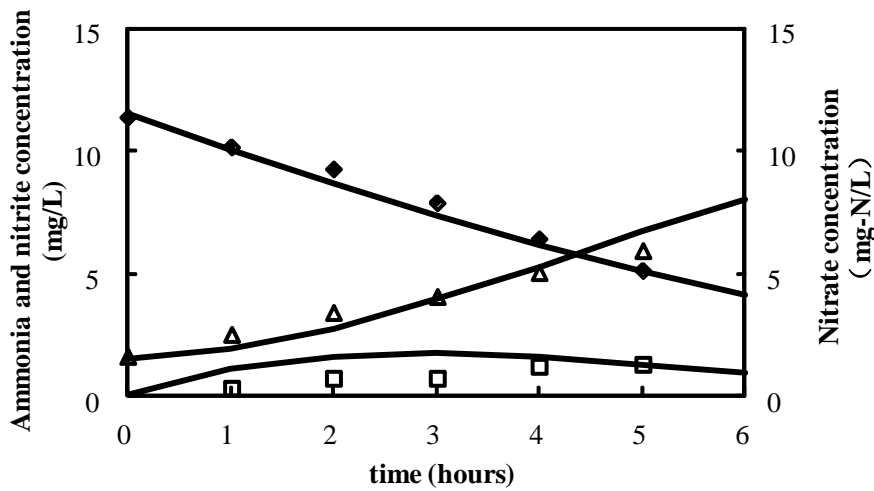


Figure 6. 17 Bioaugmentation with nitrifiers developed from nitrifying tricking filter biomass using activated sludge supernatant as substrate (test 1).

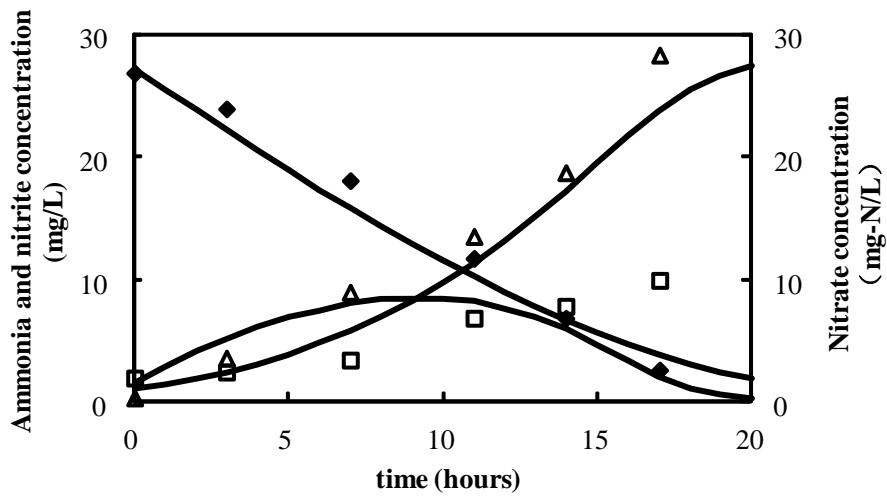


Figure 6. 18 Bioaugmentation with nitrifiers developed from nitrifying tricking filter biomass using activated sludge supernatant as substrate (test 2).

Nitrifiers from nitrifying tricking filter were utilized for bioaugmentation.

Run No. 13 and 14 were conducted in low-strength ammonia synthetic wastewater. Run No. 15, 16 and 17 were conducted in clarified effluent from non-nitrifying activated sludge (final clarifier effluent). Run No. 18 and 19 were conducted in non-nitrifying activated sludge. In Run No. 13 through Run No. 19, similar parameters values were obtained as shown in Table. 6.8. There were no apparent or acclimation period in operation period. Comparing the other two sets of bioaugmentation tests, the $\mu_{\max, AOO}$ values were much lower because AOO percentage was low in total bacterial amount. In this case most of the bacteria was considered to be OHO in the tricking filter. The $\mu_{\max, NOO}$ values were different due to its sensitivity characteristic.

Table 6. 8 Parameters values from simulations

| | | NO. 13 | NO. 14 | NO. 15 | NO. 16 | NO. 17 | NO. 18 | NO. 19 |
|------------------|-----------------|-------------|-------------|--------------|-------------|-------------|--------------|--------------|
| Parameter | Unit | | | | | | | |
| Y_{AOO} | g-COD/g-N | 0.208 | 0.208 | 0.208 | 0.208 | 0.208 | 0.208 | 0.208 |
| $\mu_{max,AOO}$ | d ⁻¹ | 0.06 | 0.05 | 0.055 | 0.06 | 0.05 | 0.052 | 0.042 |
| $K_{S,AOO}$ | mg-N/L | 6 | 6 | 6 | 6 | 6 | 6 | 6 |
| b_{AOO} | d ⁻¹ | 0.04 | 0.04 | 0.04 | 0.04 | 0.04 | 0.04 | 0.04 |
| Y_{NOO} | g-COD/g-N | 0.029 | 0.029 | 0.029 | 0.029 | 0.029 | | |
| $\mu_{max,NOO}$ | d ⁻¹ | 0.4 | 0.4 | 0.5 | 0.3 | 0.3 | 0.35 | 0.35 |
| $K_{S,NOO}$ | mg-N/L | 6 | 6 | 6 | 6 | 6 | 6 | 6 |
| b_{NOO} | d ⁻¹ | 0.04 | 0.04 | 0.08 | 0.04 | 0.04 | 0.04 | 0.04 |
| Y_{OHO} | g-COD/g-N | 6 | 6 | 6 | 6 | 6 | 6 | 6 |
| $\mu_{max,OHO}$ | d ⁻¹ | 20 | 20 | 20 | 20 | 20 | 20 | 20 |
| K_{S,OHO,O_2} | mg-O/L | 0.2 | 0.2 | 0.2 | 0.2 | 0.2 | 0.2 | 0.2 |
| K_{S,OHO,NO_3} | mg-N/L | 0.5 | 0.5 | 0.5 | 0.5 | 0.5 | 0.5 | 0.5 |
| b_{OHO} | d ⁻¹ | 0.62 | 0.62 | 0.62 | 0.62 | 0.62 | 0.62 | 0.62 |

According to parameters values from simulations, a conclusion that bioaugmentation with nitrifiers developed from nitrifying tricking filter can be achieve in low-strength synthetic waste, clarified activated sludge and activated sludge can be obtained, although there are slight differences in some paremeters values.

6.4 Conclusion

Bioaugmentation procedures were verified by evaluating acclimation and ammonia removal in several kinds of substrate, low-strength synthetic wastewater, diluted dewatered biosolids supernatant, clarified activated sludge wastewater, and supernatant of activated sludge. The following conclusions were obtained by simulation process.

1. In all operations, a discernible acclimation period was not observed, bioaugmentation procedures were verified.
2. From the simulation, similar values of parameters were obtained in each sets of bioaugmentation operation. The maximum specific growth rate of AOO had a narrow range while NOO had a wider range probably due to higher sensitivity on environmental conditions.
3. The results can contribute to bacterial training and purification process for environmental bacterial reagent production.

7. Conclusion

Biological reactions often experience inhibition from high concentrations of substrates, reaction products and other external inhibitory compounds. The inhibitory compounds may affect the enzymatic system leading to different forms of competitive, non-competitive or uncompetitive reversible inhibition. In other situations, the concentration of inhibitory compound could result in poisoning leading to irreversible inhibition. There are several mathematical models to express reversible inhibition, however recovery and adaptation phenomenon are not well described by these models. Furthermore, the modelling approaches for irreversible inhibitions are not well developed.

In this study, an irreversible inhibition function was developed and evaluated using nitrite oxidising organism (NOO) as a research subject under different nitrite concentrations and pH. A set of batch tests was carried out at pH 7.0 where the nitrite concentration was automatically kept almost constant over the experimental periods for 7 days. During the experiments oxygen uptake rate (OUR) and microscopic cell-counting using bacterial staining (live/dead method) were performed at 24-hr interval. The OUR at 50 mg-N- NaNO_2 /L linearly increased with an increase of 'living cells' whilst the OUR and the living cells without nitrite decreased logarithmically showing the decay took place. On the other hand, when the nitrite concentration was set at over 500 mg-N/L, both OUR and living cells decreased at higher specific decay rates than that without nitrite. In the

conditions the number of cells stained as 'dead' (cells with damaged cell membrane) increased along with time but did not correspond to the loss of living cells, suggesting a deformation of cell particulates after death. Threshold functions depended on nitrite concentration were developed to express the newly defined decay processes and disintegration processes. Based on the response the behaviours for NOO and other cryptic growing microorganisms were expressed on Gujer-matrix and these kinetics were estimated. The decrease/increase of OUR activity and VSS concentration in the batch condition were also simulated by newly constructed model. The model presented in this study was to express the loss of active NOO biomass due to poisoning, which was a distinct interpretation against the conventional models using competitive/non-competitive inhibition on growth stage. Therefore the study could be a critical platform to improve the understanding of microbial inhibition phenomena.

Nitrite and ammonia may exist in the nitrification process in N-removal of wastewater treatment, and free nitrous acid (FNA) and free ammonia (FA) was identified as reversible inhibitors for NOO and ammonia oxidising organisms (AOO) in previous researches. To evaluate and model for reversible and irreversible inhibition by FNA and FA, batch experiments were conducted using nitrite-N concentration in the range of 125 - 2000 mg-N/L (the N concentration ratio of nitrite and ammonia was kept at 1 in parallel experiments), and the OURs were measured as dynamic reaction responses. OUR responses revealed that the inhibition effect of free nitrous

acid (FNA) and free ammonia (FA) disappeared after several hours due to microbial adaptation from the shock loading. The traditional inhibition model on the growth process was modified by incorporating a recovery function from the shock loading. The OUR tests also indicated irreversible inhibition (poisoning) leading to a perpetual reduction in activity at higher doses of inhibitory compounds. For the reversible inhibition a time-dependent switching function was developed to express the degree of the adaptation. The irreversible poisoning phenomenon was defined as an additional first-order type decay/death process that was initiated when the inhibitory concentration exceeded the threshold level.

The modified model developed from the batch experimental data was able to reasonably reproduce the effluent nitrogenous concentration in the WERF benchmark datasets of over 250 days. In simulation process, some kinetic inhibition parameters were needed to calibrate depending on the nitrifying processes, probably due to the differences of dominant nitrifier species. Nevertheless the calculated marginal inhibition concentrations of non-ionised nitrite and ammonia were consistent with those presented in past studies. Although Haldane-type inhibition is traditionally used to model the inhibition of nitrite oxidation process. It appears that an alternative poisoning model with poisoning concentration threshold could express the nitrifier's response more accurately. Apart from substrate inhibition of nitrifiers, additional mechanism of microbial lysis due to predator infection may need further investigation. The traditional reversible inhibition model

focusing on only growth process could not properly reproduce the microbial oxygen uptake rate when the incubation was extended to several days. This was because an adaptation from the shock loading and poisoning took place almost simultaneously.

8. Reference

- Abeling U. and Seyfried C. F. (1992) Anaerobic-aerobic treatment of high-strength ammonia wastewater-nitrogen removal via nitrite. *Wat. Sci. Tech.* 26 (5-6), 1007-1015.
- Abuharfeil, N., Sarsour, E., Hassuneh, E. (2001). The effect of sodium nitrite on some parameters of the immune system *Food and Chemical Toxicology* 39, 119-124.
- Achlesh Daverey, Yi-Chian Chen, Shihwu Sung, Jih-Gaw Lin, (2014) Effect of zinc on anammox activity and performance of simultaneous partial nitrification, anammox and denitrification (SNAD) process
- Aiba S, Shoda M, Nagatami M (1968). Kinetics of product inhibition in alcohol fermentation, *Biotechnol. Bioeng.*, 10: 845-864.
- Ali, R. D. & Fikret, K. (2001). Salt inhibition kinetics in nitrification of synthetic saline wastewater *Enzyme and Microbial Technology* 28, 661-665.
- Almeida, J.S., Reis, M.A.M. & Carrondo, M.J.T. (1995). Competition between nitrate and nitrite reduction in denitrification by *Pseudomonas fluorescens*. *Biotechnol Bioeng* 52 (1), 176-182.
- Andrew, J.F. (1968). A mathematical model for the continuous culture of microorganisms utilizing inhibitory substrates. *Biotechnol. Bioeng.* 10, 707-723.
- Anette Æsøy, Hallvard Ødegaard, Greta Bentzen (1998) The effect of sulphide and organic matter on the nitrification activity in a biofilm process. *Water*

Science and Technology, Volume 37, Issue 1, 1998, Pages 115–122

Anthonisen, A. C., Loehr, R. C., Prakasam, T. B. S. & Srinarh, E. G. (1976).

Inhibition of nitrification by ammonia and nitrous acid. *J.W.P.C.F* 48 (5), 835-852.

APHA, (2005). Standard methods for the examination of water & wastewater,

21st ed. American Publishers Health Association, USA.

Arensberg, P., Hemmingsen, V.H., Nyholm, N. (1995). A miniscale algal

toxicity test. *Chemosphere*. 30 (11), 2103-2115.

A., Truper, H. G., Dworkin, M., Harder, W. K., Schleifer, H., Eds.;

Springer-verlag: Berlin, Germany.

Balmelle B., Ngugen M., Capdeville B., Cornier J. C. and Deguln A. (1992).

Study of factors controlling nitrite build-up in biological processes for water nitrification. *Wat. Sci. Tech.* 26 (5-6), 1017-1025.

Batstone, D.J., Keller, J., Angelidaki, I., Kalyuzhnyi, S.V., Pavlostathis, S.G.,

Rozzi, A., Sanders, W.T.M., Sirgrist. H., Vavilin, V.A. (2002). Anaerobic Didedtion Model No. 1. IWA Scientific and Technical Report No. 13.

Ben-Youssef, C., Zepeda, A., Texier, A. and Gomez, J. (2009). A two-step

nitrification model of ammonia and nitrite oxidation under benzene inhibitory and toxic effects in nitrifying batch cultures. *Chemical Engineering Journal*, **152**, 264-270.

Bess, B. Ward, Daniel, J. Arp, Martin, G. Klotz. 2011. Nitrification. ASM

press. IWA publishing.

Blum, D. J. W. and R.E. Speece. (1991). A database of chemical toxicity to

environmental bacteria and its use in interspecies comparisons and

- correlations. *Res. J. Wat. Poll. Con. Fed.*, 63:198.
- Bock, E., Koops, H. P., Ahlers, B., Harms, H., (1992) Oxidation of inorganic nitrogen compounds as energy source. In the prokaryotes, 2nd Ed., Balows,
- Boilos, L., Prevost, M., Barbeau, B., Coallier, J., Desjardins, R. (1999). Live/dead BacLight: application of a new rapid staining method for direct enumeration of viable and total bacteria in drinking water.
- Boon B. Laudelout H. (1962). Kinetics of nitrite oxidation by nitrobacter Winogradskyi. *Biochemical Journal*. 85(3):440-447.
- Breda Novotnik, Tea Zuliani, Janez Ščanc̣ar, Radmila Milac̣ic̣, (2014) Inhibition of the nitrification process in activated sludge by trivalent and hexavalent chromium, and partitioning of hexavalent chromium between sludge compartments. *Chemosphere* 105, 87–94.
- Camargo, J.A., Alonso, A., (2006). Ecological and toxicological effects of inorganic nitrogen pollution in aquatic ecosystems: a global assessment. *Environ. Int.* 32, 831–849.
- Carrera, J., Jubany, I., Carvallo, L., Chamyb, R., Lafuente, J. (2004). Kinetic models for nitrification inhibition by ammonium and nitrite in a suspended and an immobilised biomass systems. *Process. Biochem.*, 39, 1159-1165.
- Carvallo L., Carrera J., Chamy R. (2002). Nitrifying activity monitoring and kinetic parameter determination in a biofilm airlift reactor by respirometry. *Biotechnology letters*. 24(24):2063-2066.
- Cecen F. and Gonenc I. E. (1994) Nitrogen removal characteristics of

- nitrification and denitrification filters. *Wat. Sci. Tech.* 29 (10-11), 409-416.
- Chandran, K., Hu, Z., Smets, B.F., (2008). A critical comparison of extant batch respirometric and substrate depletion assays for estimation of nitrification biokinetics. *Biotechnol. Bioeng.* 101, 62–72. Ahn, J.H., Yu, R., Chandran, K., (2008). Distinctive microbial ecology and biokinetics of autotrophic ammonia and nitrite oxidation in a partial nitrification bioreactor. *Biotechnol. Bioeng.* 100, 1078–1087.
- Chandran, K., Love, N.G. (2008) Physiological state, growth mode, and oxidative stress play a role in Cd(II) - Mediated inhibition of nitrosomonas Europara 19718. *Appl. Environ. Microbiol.*, 74, 2447-2453.
- Chandran, K., Smets, B.F. (2000a) Applicability of two-step models in estimating nitrification kinetics from batch respirograms under different relative dynamics of ammonia and nitrite oxidation. *Biotechnol. Bioeng.*, 70, 54-64.
- Chandran, K., Smets, B.F. (2000b) Single-step nitrification models erroneously describe batch ammonia oxidation profiles when nitrite oxidation becomes rate limiting. *Biotechnol. Bioeng.*, 68, 396-406.
- Chandran, K., Smets, B.F. (2005) Optimizing experimental design to estimate ammonia and nitrite oxidation biokinetics parameters from batch respirograms. *Water research*, 39, 4969-4978.
- Chen, Y., Cheng, J.J., Creamer, K.S. (2008). Inhibition of anaerobic digestion process: A review. *Biores. Tech.*, 99, 4044-4064.
- Chérif Ben-Youssef, Alejandro Zepeda, Anne-Claire Texier, Jorge Gomez. (2009) A two-step nitrification model of ammonia and nitrite oxidation

- under benzene inhibitory and toxic effects in nitrifying batch cultures. *Chemical Engineering Journal* 152, 264–270.
- Corominas, L., Rieger, L., Takács, I., Ekama, G., Hauduc, H., Vanrolleghem, P.A., Oehmen, A., Gernaey, K.V., van Loosdrecht, M.C.M. and Comeau, Y. (2010). New framework for standardized notation in wastewater treatment modelling. *Wat. Sci. Tech.*, 61(4), 841-857.
- Dias I.F. and Bhat J.V. (1965). *Microbial ecology of activated sludge. II. Bacteriophages, Bdellovibrio, coliforms and other organisms. Applied Microbiology*, 13, 257-261.
- Dunn, I. J., Uzman, S. & Studer, B. (1985). Kinetics and dynamics of nitrification in biofilm fluidized sandbed reactor *Conservation and Recycling* 8, 143-152.
- Edward VH (1970). The influence of high substrate concentrations on microbial kinetics. *Biotechnol. Bioeng.*, 12: 679-712.
- Ewert, D.L and Paynter, M.J.B. (1980). Enumeration of bacteriophages and host bacteria in sewage and the activated sludge treatment process. *Applied Environmental Microbiology*, 39, 576–83.
- Ford D. L., Churchwell R. L. and Kachtick J. W. (1980). Comprehensive analysis of nitrification of chemical processing wastewater. *J.W.P.C.F* 52 (11), 2726-2746.
- Fuhs G. W. (1974) Nutrients and aquatic vegetation effects. *J. envir. Engng Div. Am. Soc. cir. Engrs* 100, 269, 277-278.
- Fromm, P.O., Gillette, J.R., (1968). Effect of ammonia on blood ammonia and nitrogen excretion of rainbow trout (*Salmo gairdneri*). *Comp. Biochem.*

- Physiol. 26, 887–896.
- Gardy, C.P.L.J., Daigger, G.T., Lim, H.C. (1999) Biological wastewater treatment. Marcel Dekker: New York.
- Gastens D.J. and Rozich A.F. (1986). Analysis of batch nitrification using substrate inhibition kinetics. *Biotechnol. Bioengng* 28, 461-465.
- Gee, C.S., Pfeffer, J.T., Suidan, M.T. (1990) Nitrosomonas and Nitrobacter interactions in biological nitrification. *J. Environ. Eng., Am. Soc. Civ. Eng.*, 116, 4-17.
- Gee, C.S., Suidan, M.T., Pfeffer, J.T., Suidan, M.T. (1990) Modeling of nitrification under substrate-inhibition conditions. *J. Environ. Eng., Am. Soc. Civ. Eng.*, 116, 18-31.
- Gendig, C., Domogala. G., Agnoli. F., Pagga. U., Strotmann, U. (2003). Evaluation and further development of activated sludge respiration inhibition test. *Chemosphere*. 52, 2103-2115.
- Goar, W. R., Jose, L.A., Adelina, V., Ramon, G., Jose, A. B., Ignacio, B., and Jose, J.M. (2000). A rapid, direct method for assessing chloring effect on filamentous bacteria in activated sludge. *Water Res.* 34(15), 3894-3898.
- Guisasola, A., Jubany, I., Baeza, J.A., Carrera, J., Lafuente, J. (2005) Respirometric estimation of the oxygen affinity constants for biological ammonium and nitrite oxidation. *J. Chem. Technol. Biotechnol.*, 80(4), 388-396.
- Gujer, W., Jenkins, D. (1974) A nitrification model for contact stabilization activated sludge processes. *Water Research*, 9(5), 5.
- Hall. I.R. (1974). Some studies on nitrification in the activated sludge process.

- J. Wat. Poll. Con. 73:538.
- Han K, Levenspiel O (1988). Extended Monod kinetics for substrate, product, and cell inhibition, *Biotechnol. Bioeng.*, 32:430–437.
- Hantula, J., Kurki, A., Vuoriranta, P. and Bamford, D. (1991). Ecology of bacteriophages infecting activated sludge bacteria. *Applied Environmental Microbiology*, 57, 2147–2151.
- Hao, X., Wang, Q., Zhang, X., Cao, Y., van Loosdrecht, M.C.M. (2009). Experimental evaluation of decrease in bacterial activity due to cell death and activity decay in activated sludge. *Water Res.* 43, 3604-3612.
- Hassan M. M. (1981) Nitrification in a packed bed biological flow reactor with and without inhibition. M.S. thesis, Univ. of Petroleum & Minerals, Dhahran, Saudi Arabia.
- Haug, R. T., McCarty, P. L. (1972) nitrification with submerged filters. *J. Water Pollut. Control Fed.* 44(11), 2086-2102.
- Hellinga, C., Schellen, A.A.J.C., Mulder, J.W., van Loosdrecht, M.C.M. and Heijnen, J.J. (1998). The SHARON Process: An innovative method for nitrogen removal from ammonium-rich wastewater. *Water. Science & Technology*, 37(9), 135-142.
- Hellinga C., van Loosdrecht M.C.M., Heijnen J.J. (1999). Model based design of a novel process for nitrogen removal from concentrated flows. *Mathematical and Computer Modeling of Dynamical Systems* 5(4):351-371.
- Henze, M., Gujer, W., Mino, T. & van Loosdrecht, M.C.M. (2000). Activated sludge models ASM1, ASM2, ASM2d, and ASM3. IWA Scientific and

Technical Report No. 9.

- Hill, G.A., Robinson, C.W. (1975). Substrate inhibition kinetics: phenol degradation by *Pseudomonas putida*. *Biotechnol. Bioeng.* 17, 1599-1615.
- Hockenbury, M.R., Grady, L., C.P.L. 1977. Inhibition of nitrification-effects of selected organic compounds. *Jornal WPCF.* 49(5), 768-777.
- Hooper, A. B., Vannelli, T., Bergmann, D. J., Arciero, D. M. (1997) Enzymology of the oxidation of ammonia to nitrite by bacteria. *Antonie van Leeuwenhoek*, 71, 59-67.
- Iacopozzi, I., Innocenti, V., Marsili-Libelli, S. & Giusti, E. (2007). A modified activated sludge model no. 3 (ASM3) with two-step nitrification-denitrification. *Environmental Modelling & Software* 22(6), 847-861.
- IWAPRC Task Group on Mathematical Modeling for Design and Operation of Biological Wastewater Treatment. (1986). Final report: activated sludge model. IWAPRC science and technical reports No. 1.
- Joss, A., Derlon, N., Cyprien, C., Burger, S., Szivak, I., Traber, J., Siegrist, H., Morgenroth, E. (2011). Combined Nitritation–Anammox: Advances in Understanding Process Stability. *Environ. Sci. Technol.*, 45 (22), 9735–9742.
- Jubany, I., Baeza, J.A., Carrera, J., Lafuente, J. (2005). Respirometric calibration and validation of a biological nitrite oxidation model including biomass growth and substrate inhibition. *Water Res.* 39, 4574-4584.
- Jubany I.,(2007). Operation, modelling and automatic control of complete and partial nitrification of highly concentrated ammonium wastewater,

Ph.D.Thesis, Universitat Autònoma de Barcelona, Barcelona, Spain, ISBN:978-84-690-7378-0(<http://www.tesisenxarxa.net/TESISUAB/AVAILABLE/TDX-1005107-170622//ijg1de1.pdf>).

Jubany,I., Carrera,J., Lafuente, J., Baeza, J.A. (2008). Start-up of a nitrification system with automatic control to treat highly concentrated ammonium wastewater: experimental results and modeling. *Chem. Eng. J.* 144, 407-419.

Jubany, I., Lafuente, J., Baeza, J.A., Carrera, J. (2009). Total and stable washout of nitrite oxidizing organism from a nitrifying continuous activated sludge system using automatic control based on Oxygen Uptake Rate measurements. *Water Res.* 43, 2761 -2772.

Kaelin, D., Manser, R., Rieger, L., Eugster, J., Rottermann, K. & Siegrist, H. (2009). Extension of ASM3 for two-step nitrification and denitification and its calibration and validation with batch tests and pilot scale data. *Water Res.* 43, 1680-1692.

Kopp, J.B., Murphy, K.L. (1995). Estimation of the active nitrifying biomass in activated sludge. *Water Research* 29(8), 1855-1862.

Kappeler, J., Gujer, W. (1992). Estimation of kinetics parameters of heterotrophic biomass under aerobic conditions and characterization of wastewater for activated sludge modelling. *Water. Sci. Technol.*, 25 (6), 125-139.

Khan, M.A, Satoh, H, Katayama, H, Kurisu, F, and Mino, T. (2002). Bacteriophages isolated from activated sludge processes and their polyvalency. *Water. Research*, 36, 3364–3370.

- Kong, Z., Vanrolleghem, P.m Willems, P., Verstraete, V. (1996).
 Simultaneous determination of inhibition kinetic of carbon oxidation and nitrification with a respirometer. *Water Res.* 30(4), 825-836.
- Knowles, G., Downing, A.L., Barrett, M.J. (1965) Determination of kinetics constants for nitrifying bacteria in mixed culture, with the aid of an electronic computer. *J. Gen. Microbiol.*, 38, 263-278.
- Kovar KK, Egli T (1998). Growth kinetics of suspended microbial cells: from single substrate- controlled growth to mixed-substrate kinetics, *Microb. Mol. Biol. Rev.*, 62: 646–666.
- Kumar A, Kumar S, Kumar S (2005). Biodegradation kinetics of phenol and catechol using *Pseudomonas putida* MTCC 1194. *Biochem. Eng.J.*, 22, 151–159.
- Laudelout, H. et al. (1974). Effect of temperature on velocity of oxidation of ammonia to nitrate in mixed nitrifier culture. *Ann. Microbiol.* 125B:75.
- Laudelout, H., R. Lambert and M.L. Pham. (1976). The effect of pH and partial pressure of oxygen on nitrification. *Ann.Microbiol.* 127A:367.
- Lide, D.R. (2006). *CRC Handbook of Chemistry and Physics*. CRC Press. International standard book number-13: 978-1-4200-9084-0.
- Lina, B., Michele, P., Benoit, B., Josee, C., Raymond, D. (1999).
 LIVE/DEAD[®] BacLight[™]: application of a new rapid staining method for direct enumeration of viable and total bacteria in drink water. *Journal of Microbiological Methods*, 37,77-86
- Liu, B., Naka, D., Jarvis, I., Goel, R., Yasui, H. (2011). A kinetic expression for the growth and decay of nitrite oxidising bacteria. *Proc. of 4th*

IWA-ASPIRE, 14-17-2, 2-6/October/2011, Tokyo, Japan.

- Liu, B., Jarvis, I., Naka, D., Goel, R., Yasui, H. (2013). A benchmark simulation to verify an inhibition model on decay stage for nitrification. *Water Science and Technology*, 68(6), 1242-1250
- Liu, B, Goel, R., Terashima, M., Yasui, H. (2013). Models for Reversible and Unreversible Inhibitions of Biological Nitrite Oxidation. *Journal of Japan Society of Civil Engineers*, Ser.G, Vol.69, No.7, III_503-513.
- Luca, D., Luca, V., Cotor, F. & Raileanu, L. (1987). In vivo and in vitro cytogenetic damage induced by sodium nitrite. *Mutat. Res.* 189, 333-339.
- Loveless, J.E. and H.A. Painter. (1968). The influence of metal ion concentration and pH value on the growth of nitrosomonas strain isolated from activated sludge. *J.Gen. Microbiol.* 52:1.
- Luong JHT (1987). Generalization of Monod kinetics for analysis of growth data with substrate inhibition. *Biotechnol. Bioeng.*, 29: 242-248.
- Magri A., Corominas L., Lopez H., Campos E., Colprim J., Flotats X. (2007). A model for simulation of Sharon process: pH as a key factor. *Environmental Technology* 28(3):255-265.
- Makinia, J. (2010). *Mathematical Modelling and Computer Simulation of Activated Sludge Systems*. IWA publishing, London, UK.
- Mandoni, P., Donatella, D., Guglielmi, G. (1999). Response of SOUR and AUR to heavy metal contamination in activated sludge. *Water Res.*, 33(19), 2459-2464.
- Manser, R., Gujer, W. & Siegrist, H. (2005) Consequences of mass transfer effects on the kinetics of nitrifiers *Water Res.* 39, 4633-4642.

- María Eugenia Suárez-Ojeda, Albert Guisasola, Julián Carrera, (2010) Inhibitory impact of quinone-like compounds over partial nitrification. *Chemosphere* 80 (2010) 474–480.
- Mauret M., Paul E., Puech-Costes E., Maurette M. T. and Baptiste P. (1996) Application of experimental research methodology to the study of nitrification in mixed culture. *Wat. Sci. Tech.* 34 (1-2), 245-252.
- Metcalf and Eddy, inc. (2003) *Wastewater Engineering: treatment and reuse*, 4th ed.; Tchobanoglous, G.; Burton, F. L.; Stensel, H. D., Eds.; McGraw-Hill: New York.
- Monod J (1949). The growth of bacterial cultures. *Annu. Rev. Microb.* 3:371-394.
- Moussa, M. S., Hooijmans, C. M., Lubberding, H. J. & van Loosdrecht, M. C. M. (2005). Modelling nitrification, heterotrophic growth and predation in activated sludge *Water Res.* 39,5080-5098.
- Mulchandani A, Luong JHT (1989). Microbial inhibition kinetics revisited, *Enzyme Microb. Technol.*, 11: 66-73.
- Munz, G., Lubello, C., Oleszkiewicz, J.A., (2011). Factors affecting the growth rates of ammonium and nitrite oxidizing bacteria *Chemosphere* 83, 720-725
- Munz, G., Gori, R., Cammilli, L., Lubello, C., (2008). Characterization of tannery wastewater and biomass in a membrane bioreactor using respirometric analysis. *Bioresour. Technol.* 99, 8612–8618.
- Munz, G., Lubello, C., Oleszkiewicz, J.A., (2011). Modeling the decay of ammonium oxidizing bacteria. *Water Res.* 45, 557–564.

- Munz, G., Mori, G., Vannini, C., Lubello, C., (2010). Kinetic parameters and inhibition response of ammonia- and nitrite-oxidizing bacteria in membrane bioreactors and conventional activated sludge processes. *Environ. Technol.* 31, 1557–1564.
- Neufeld, R.D., Hill, A.J., Adekoya, D.O. (1980). Phenol and free ammonia inhibition to *Nitrosomonas* activity. *Water Res.* 14, 1695-1703.
- Ni, B. J., Fang, F., Xie, W. M. & Yu, H. Q. (2008). Growth, maintenance and product formation of autotrophs in activated sludge: Taking the nitrite-oxidizing bacteria as an example *Water Res.*42, 4261-4270.
- Nowak, O., Svardal, K. & Schweighofer, P. (1995). The dynamic behaviour of nitrifying activated sludge systems influenced by inhibiting wastewater compounds. *Water Science and Technology* 31 (2), 115-124.
- Nuhoglu N, Yalcin B (2005). Modeling of phenol removal in a batch reactor, *Process Biochem.*, 40: 1233-1239.
- Okpokwasili GC, Nweke CO (2005). Microbial growth and substrate utilization kinetics, *Afr. J. Biotechnol.*, 5 (4): 305-317.
- Ostace, G.S., Cristea, V.M. and Agachi, P.S. (2011). Cost reduction of the wastewater treatment plant operation by MPC based on modified ASM1 with two-step nitrification/denitrification model. *Computers and Chemical Engineering*, 35, 2469-2479.
- Painter, H.A. (1970) A review of literature on inorganic nitrogen metabolism in microorganisms. *Water Research*, 4, 393-450.
- Park, S. and Bae, W. (2009). Modeling Kinetics of ammonium oxidation and nitrite oxidation under simultaneous inhibition by free ammonia and free

- nitrous acid. *Process Biochemistry*, **44**, 631-640.
- Parsonage, D., Greenfield, A. J. & Ferguson, S. J. (1985) The high affinity of *Paracoccus denitrificans* cells for nitrate as an electron acceptor analyse of possible mechanisms of nitrate and nitrite movement across the plasma membrane and the basis for inhibition by added nitrite of oxidase activity in permeabilized cells. *Biochim Biophys Acta* 807, 81-95.
- Peeters, W.L., A.D. Van Goal and H. Laudelout. (1969). Kinetic study of oxygen limited respiration in nitrifying bacteria. *Bact. Proc.* 141.
- Pilar Monfort, Elena Kosenko, Slaven Erceg, Juan-José Canales, Vicente Felipo. (2002) Molecular mechanism of acute ammonia toxicity: role of NMDA receptors *Neurochemistry International*, Volume 41, Issues 2–3, Pages 95–102
- Pynaert, K., Smets, B.F., Wyffels, S., Beheydt, D., Siciliano, D.S., Verstraete, W. (2003) Characterization of an autotrophic nitrogen-removing biofilm from a highly loaded lab-scale rotating biological contactor. *Appl. Environ. Microbiol.*, 69, 3626-3635.
- Rebelo, M.F., Rodriguez, E.M., Santos, E.A., Ansaldo, M., (2000). Histopathological changes in gills of the estuarine crab *Chasmagnathus granulata* (Crustacea-Decapoda) following acute exposure to ammonia. *Comp. Biochem. Phys.* 125C. 157–164.
- Rozich, A.F., Gaudy A.F., Adamo, P.C. (1985). Selection of growth rate model for activated sludges treating phenol. *Water Res.* 19(4), 481-490.
- Ruiz, G., Jeison, D. & Chamy, R. (2003) Nitrification with high nitrite accumulation for the treatment of wastewater with high ammonia

- concentration *Water Res.* 37, 1371-1377.
- Russo, R.C., (1985). Ammonia, nitrite and nitrate. In: Rand, G.M., Petrocelli, S.R. (Eds.), *Fundamentals of Aquatic Toxicology*. Hemisphere, Washington, DC, pp. 455–471.
- Schramm, A., De Beer, D., Wagner, M., Amann, R. (1998) Identification and activities in situ of *Nitrosospira* and *Nitrospira* Spp. as dominant populations in a nitrifying fluidized bed reactor. *Appl. Environ. Microbiol.*, 64, 3480-3485.
- Seung, Y. W., Chan, W. L., Sang, I. L. & Ben, K. (2002) Nitrite inhibition of aerobic growth of *Acinetobacter* sp. *Water Res.* 36, 4471-4476.
- Shafkat A. Beg and Mirza M. Hassan. (1987). Effect of inhibitors on nitrification in a packed-bed biological flow reactor. *Water Research.* 21(2), 191-198.
- Sheintuch M., Tartakovsky B., Narkis N. and Rebhun M. (1995). Substrate inhibition and multiple states in a continuous nitrification process. *Water Research.* 29 (3), 953-963.
- Shindala A. (1972) Nitrogen and phosphorus removal from wastewater Part. I. *War. Sewage Wks* 119, 66-77.
- Sin, G., Kaelin, D., Kampschreur, M.J., Takacs, I., Wett, B., Gernaey, K.V., Rieger, L., Siegrist, H. and van Loosdrecht, M. (2008) Modelling nitrite in wastewater treatment systems: A discussion of different modelling concepts. *Water Sci. Technol.* 58(6), 1155-1171.
- Speece, R.E. (1996). *Anaerobic Biotechnology for Industrial Wastewaters*. Archae Press, Nashville, TN., USA.

- Speece R.E. and McCarty P.L. (1964). Nutrient requirements and biological solids accumulation in anaerobic digestion, *Proceedings of the First International Conference. on Water Pollution and Control*, Pergamon Press, Oxford, UK.
- Starr M.P. and Baigent N.L. (1966). Parasitic interaction of *Bdellovibrio bacteriovorus* with other bacteria. *Journal of Bacteriology*, **91**, 2006-2017.
- Stensel H. D. (1971) Biological kinetics of suspended growth denitrification process. Ph.D. dissertation, Cornell Univ.
- Stensel H. D., Loehr R. C. and Lawrence A. W. (1973) Biological kinetics of suspended growth denitrification. *J. Wat. Poll. C*
- Stensel, H.D. and J.L. Barnard. (1992). Principles of Biological Nutrient Removal, In Design and Retrofit of Wastewater Treatment Plants for Biological Nutrient Removal, *eds.*, Barnard, J.L., Randall, C.W. and Stensel, H.D., pp. 25-84, Technomic Publishing Co. Inc., Lancaster, USA.
- Stolp H. and Starr M.P. (1965). Bacteriolysis. *Research in Microbiology*, **19**, 79-104.
- Taylor, G.J., Stadt, K.J., Dale, M.R.T. (1992). Modelling the interactive effects of aluminium, cadmium, manganese, nickel and zing stress using the Weibull frequency distribution. *Environmental and Experimental Botany*. **32**. 281-293.
- Turk O. and Mavinic D. S. (1986). Preliminary assessment of a shortcut in nitrogen removal from wastewater. *Can. J. Civ. Eng.* **13**, 600-605.
- Turk O. and Mavinic D. S. (1987). Selective inhibition: a novel concept for removing nitrogen from highly nitrogenous wastes. *Environ. Technol.*

*Lett.*8, 419- 426.

Vadivelu, V.M., Yuan, Z., Fux, C., Keller, J. (2006). The inhibitory effects of free nitrous acid on the energy generation and growth processes of an enriched Nitrobacter culture. *Environ. Sci. Technol.*, 40, 4442-4448.

van Dongen, L.G.J.M., Jetten, M.S.M., van Loosdrecht, M.C.M. (2001). *The Combined Sharon/Anammox Process, A sustainable method for N-removal from sludge water*. Water and wastewater practitioner series: STOWA report. UK: IWA publishing.

Van Hulle SWH, Volcke EIP., Teruel JL., Donckels B., van Loosdrecht M.C.M., Vanrollegem PA. (2007). Influence of temperature and pH on kinetics of the Sharon nitrification process. *Journal of Chemical Technology and Biotechnology* 82(5) 471-480.

van Loosdrecht, M.C.M. & Henze, M. (1999). Maintenance, endogenous respiration, lysis, decay and predation. *Water Sci. Technol.*, 39, 107-117.

Volskay, V. and Grady, C.P.L. Jr. (1988). Toxicity of selected RCRA compounds to activated sludge microorganisms. *J. Water. Pollut. Control. Fed.*, 60 (10), 1850-1856.

Vorhees C. V., Butcher R. E., Brunner R. L. & Wootten V. (1984). Developmental toxicity and psychotoxicity of sodium nitrite in rats. *Food and chemical toxicology* 22-1. 1-6

Wang SJ, Loh KC (1999). Modeling the role of metabolic intermediates in kinetics of phenol biodegradation. *Enzyme Microb. Technol.* 25: 177-184.

WEF (Water Environment Federation). (2005). *Biological Nutrient Removal (BNR) Operation in Wastewater Treatment Plants*: WEF Manual of

- Practice No. 30, 1 edition.; New York: McGraw-Hill Professional.
- WEF (Water Environment Federation). (2010). *Nutrient removal*. WEF MOP 34, 1 edition.; New York: Alexandria, Va: McGraw-Hill Professional.
- Wett, B. & Rauch, W. (2003) The role of inorganic carbon limitation in biological nitrogen removal of extremely ammonia concentrated wastewater *Water Res.* 37, 1100-1110.
- Weibull, W. (1952). A statistical distribution function of wide application. *ASME Journal of Applied Mechanics.* 293-297.
- Wiesmann, U. (1994) Biological nitrogen removal from wastewater. In advances in biochemical engineering biotechnology. Fiechter, A., Ed., Springer-Verlag:Berlin, Germany.
- Wong-Chong G. M. and Loehr R. C. (1978) Kinetics of microbial nitrification: nitrite-nitrogen oxidation. *Wat. Res.* 12, 605-609.
- Yamamoto T., Takaki K., Koyama T. & Furukawa K. (2008). Long-term stability of partial nitrification of swine wastewater digester liquor and its subsequent treatment by Anammox. *Bioresource Technology* 99, 6419-6425.
- Yano S. Koga (1969). Dynamic behavior of the chemostat subject to substrate inhibition, *Biotechnol. Bioeng.*, 11:139–153.
- Yarbrough, J. M., Rake, J. B. & Eagon, R. G. (1980). Bacterial inhibition effects of nitrite: Inhibition of active transport, but not of group translocation, and of intracellular enzymes. *Applied and Environmental Microbiology.* 39, 831-834.
- Zhonghua Huang , Phillip B. Gedalanga , Pitiporn Asvapathanagul , , Betty

H. Olson (2010). Influence of physicochemical and operational parameters on Nitrobacter and Nitrospira communities in an aerobic activated sludge bioreactor. *Water Research* Volume 44(15), 4351–4358.

Ziglio, G., Andreottola, G., Barbesti, S., Boschetti, G., Bruni, L., Foladoria, P., Villa, R., (2002). Assessment of activated sludge viability with flow cytometry. *Water Res.* 36 (2), 460–468.

Zimmerman, R. A, Bradshaw, A. T & Richard, D. (2004). *Water Environment Research Foundation Acclimation of Nitrifiers for Activated Sludge Treatment: A Bench-Scale Evaluation* IWA Publishing London UK.

List of Figures

| | |
|---|----|
| Figure 1. 1 Simplified nitrogen cycle in nature (WEF, 2010)..... | 3 |
| Figure 1. 2 Biochemical pathway for ammonia oxidation (Hopper <i>et al.</i> , 1997; Arp & Stein, 2003) | 8 |
| Figure 1. 3 Biochemical pathway for nitrite oxidation in <i>Nitrobacter</i> . (Bock <i>et al.</i> , 1992)..... | 9 |
| Figure 2. 1 Microbial ecology and phylogenetic diversity of AOO and NOO relevant to activated sludge (WEF, 2010)..... | 18 |
| Figure 2. 2 Relationship between specific growth rate of AOO and ammonia-N concentration as predicted by Monod equation (dissolved oxygen is assumed to be no limiting) | 22 |
| Figure 2. 3 The relationship between μ_{max} and Temperature..... | 39 |
| Figure 2. 4 Some results of NOO maximum growth rate as a function of SRT from different researchers..... | 42 |
| Figure 2. 5 the different OUR responses of NOO under different training date..... | 44 |
| Figure 3. 1 Nitrite concentrations change during experimental operation.. | 50 |
| Figure 3. 2 Comparison of before and after treatment by ultrasonic wave.. | 51 |
| Figure 3. 3 Ratio of living bacteria to the total counted cells under different ultrasonication..... | 52 |
| Figure 3. 4 Living bacterial ratio calculation under different sample numbers | |

| | |
|--|----|
| and confidence intervals..... | 54 |
| Figure 3. 5 Change of NOO stained in green (living cells with intact cell membrane) along with time | 56 |
| Figure 3. 6 Decay versus nitrite concentration | 57 |
| Figure 3. 7 Change of NOO stained in red (dead cells with damaged cell membrane) along with time | 59 |
| Figure 3. 8 Change of total NOO stained along with time | 60 |
| Figure 3. 9 Counted OUR and VSS and simulation results. | 63 |
| | |
| Figure 4. 1 Shape of global switching function f and dependency on the coefficient n | 72 |
| Figure 4. 2 Measured and simulated maximum OUR of NOO at pH = 7.3 fifteen minutes after collection of fresh sludge from the reactor. | 79 |
| Figure 4. 3 Experimental OUR plots and the simulated curves for the 6 datasets of the long-term batch tests at pH = 7.3. | 81 |
| Figure 4. 4 NOO activity recovery phenomenon in long-term continuous batch tests..... | 83 |
| Figure 4. 5 Improper reproductivity of the inhibition model on growth process under long-term incubation (Initial nitrite = 500 mg-N/L, pH=7.3)..... | 85 |
| Figure 4. 6 Dependence of free ammonia (FA) and free nitrous acid (FNA) on pH in the solution described by Anthonisen <i>et al.</i> (1976). | 92 |
| Figure 4. 7 Marginal lines of FNA and FA inhibition concentrations with pH (top: marginal line by FNA, bottom: marginal line by FA; plots indicated | |

NOO's activity deterioration NOO served by Anthonisen *et al.* (1976)). 94

| | |
|--|-----|
| Figure 5. 1 Reactor configuration..... | 102 |
| Figure 5. 2 Operating condition for SRT 20 d (synthetic wastewater)..... | 106 |
| Figure 5. 3 Nitirifier reaction rate (top) and effluent nitrate (bottom) for SRT 20 d operation (synthetic wastewater)..... | 107 |
| Figure 5. 4 Operating condition for SRT 10 d (synthetic wastewater)..... | 108 |
| Figure 5. 5 Nitirifier reaction rate (top) and effluent nitrate (bottom) for SRT 10 d operation (synthetic wastewater)..... | 109 |
| Figure 5. 6 Operating condition for SRT 5 d (synthetic wastewater)..... | 110 |
| Figure 5. 7 Nitirifier reaction rate (top) and effluent nitrate (bottom) for SRT 5 d operation (synthetic wastewater)..... | 111 |
| Figure 5. 8 | 112 |
| Figure 5. 9 Nitirifier reaction rate (top) and effluent nitrate (bottom) for SRT 20 d operation (dewater solid wastewater)..... | 113 |
| Figure 5. 10 Benchmark simulation result at 20-day SRT (+: Ammonium, Δ : Nitrite, O: Nitrate)..... | 115 |
| Figure 5. 11 Benchmark simulation result at 10-day SRT (+: Ammonium, Δ : Nitrite, O: Nitrate)..... | 116 |
| Figure 5. 12 Benchmark simulation result at 5-day SRT (+: Ammonium, Δ : Nitrite, O: Nitrate)..... | 117 |
| Figure 6. 1 Bioaugmentation with nitrifiers developed from high-strength ammonia synthetic wastewater at 20-day SRT in seed bioreactor..... | 127 |

| | |
|--|-----|
| Figure 6. 2 Bioaugmentation with nitrifiers developed from high-strength ammonia synthetic wastewater at 20-day SRT under low-strength synthetic wastewater (test 1)..... | 128 |
| Figure 6. 3 Bioaugmentation with nitrifiers developed from high-strength ammonia synthetic waste at 20-day SRT under low-strength synthetic wastewater (test 2)..... | 128 |
| Figure 6. 4 Bioaugmentation with nitrifiers developed from high-strength ammonia synthetic waste at 20-day SRT using clarified activated sludge supernatant..... | 129 |
| Figure 6. 5 Bioaugmentation with nitrifiers developed from high-strength ammonia synthetic waste at 20-day SRT using activated sludge supernatant..... | 129 |
| Figure 6. 6 Bioaugmentation with nitrifiers developed from dewatered biosolids supernatant at 20-day SRT in seed bioreactor..... | 133 |
| Figure 6. 7 Bioaugmentation with nitrifiers developed from dewatered biosolids supernatant at 20-day SRT using diluted dewatered supernatant as substrate (test 1)..... | 133 |
| Figure 6. 8 Bioaugmentation with nitrifiers developed from dewatered biosolids supernatant at 20-day SRT using diluted dewatered supernatant as substrate (test 2)..... | 134 |
| Figure 6. 9 Bioaugmentation with nitrifiers developed from dewatered biosolids supernatant at 20-day SRT using clarified activated sludge supernatant as substrate (test 1)..... | 134 |
| Figure 6. 10 Bioaugmentation with nitrifiers developed from dewatered | |

| | |
|--|-----|
| biosolids supernatant at 20-day SRT using clarified activated sludge supernatant as substrate (test 2)..... | 135 |
| Figure 6. 11 Bioaugmentation with nitrifiers developed from dewatered biosolids supernatant at 20-day SRT using activated sludge supernatant as substrate..... | 135 |
| Figure 6. 12 Bioaugmentation with nitrifiers developed from nitrifying tricking filter biomass using low-strength synthetic waste as substrate (test 1). | 139 |
| Figure 6. 13 Bioaugmentation with nitrifiers developed from nitrifying tricking filter biomass using low-strength synthetic waste as substrate (test 2). | 139 |
| Figure 6. 14 Bioaugmentation with nitrifiers developed from nitrifying tricking filter biomass using clarified activated sludge supernatant as substrate (test 1)..... | 140 |
| Figure 6. 15 Bioaugmentation with nitrifiers developed from nitrifying tricking filter biomass using clarified activated sludge supernatant as substrate (test 2)..... | 140 |
| Figure 6. 16 Bioaugmentation with nitrifiers developed from nitrifying tricking filter biomass using clarified activated sludge supernatant as substrate (test 3)..... | 141 |
| Figure 6. 17 Bioaugmentation with nitrifiers developed from nitrifying tricking filter biomass using activated sludge supernatant as substrate (test 1). | 141 |
| Figure 6. 18 Bioaugmentation with nitrifiers developed from nitrifying | |

tricking filter biomass using activated sludge supernatant as substrate
(test 2). 142

List of Tables

| | |
|---|----|
| Table 1. 1 Process kinetics and stoichiometry for heterotrophic bacterial growth in an aerobic environment | 12 |
| Table 1. 2 Process kinetics and stoichiometry for nitrification..... | 13 |
| Table 2. 1 Estimated aerobic decay rates at 20°C in conventional activated sludge (CAS) and membrane bioreactor (MBR) system (adapted from Manser, 2006)..... | 23 |
| Table 2. 2 AOO and NOO yield values | 23 |
| Table 2. 3 Comparison of kinetics parameter for ammonia oxidizing organism (AOO) and nitrite oxidizing organism (NOO) | 24 |
| Table 2. 4 The kinetics values of non-competitive Monod-type function from literatures. | 31 |
| Table 2. 5 Equations used to describe decay process of NOO in recently published papers on two-step nitrification. Symbols are as reported in the cited papers..... | 34 |
| Table 2. 6 Some reported oxygen half-saturation values in nitrification process..... | 40 |
| Table 2. 7 Kinetics values from three times batch tests in different periods | 45 |
| Table 3. 1 The Gujer Matrix for growth, decay and poisoning of the NOO enriched sludge | 62 |
| Table 3. 2 Kinetic and stoichiometric parameters for biological nitrite | |

| | |
|---|-----|
| oxidation..... | 65 |
| Table 4. 1 The Gajer Matrix for biological nitrite oxidation | 90 |
| Table 4. 2 Kinetic and stoichiometric parameters for biological nitrite oxidation..... | 91 |
| Table 5. 1 NOO inhibition model including toxicity threshold | 99 |
| Table 5. 2 Coefficient list for the inhibition model | 118 |
| Table 6. 1 Synthetic wastewater characteristics | 123 |
| Table 6. 2 Typical dewatered biosolids supernatant characteristics | 124 |
| Table 6. 3 Bioaugmentation analyses with nitrifiers developed from high-strength ammonia synthetic waste at 20-day SRT | 126 |
| Table 6. 4 Parameters values from simulations | 130 |
| Table 6. 5 Bioaugmentation analyses with nitrifiers developed from dewatered biosolids supernatant at 20-day SRT | 132 |
| Table 6. 6 Parameters values from simulations | 136 |
| Table 6. 7 Bioaugmentation analyses with nitrifiers from nitrifying tricking filter biomass. | 138 |
| Table 6. 8 Parameters values from simulations | 143 |

Acknowledgement

The research would not have been possible without the support of many people. Many thanks to my adviser, Prof. Hidenari Yasui, who always take care of my study and life during my master and doctor course in Japan. Before I entered the University of Kitakyushu, I have no any professional knowledge of environmental protection, wastewater treatment, and activated sludge model at all, he grew me up from zero on environmental issue. More important things obtained from Prof. Hidenari Yasui are the academic attitude and thought in daily laboratory life.

Thanks to my doctoral committee members : professor Hidenari Yasui (Chair), professor Kiwao Kadokami, associate professor Hiroki Cho, assistant professor Mitsuharu Terashima Thanks to Prof. Mitsuharu Terashima, who offered guidance and support in daily experiments. Thanks to Dr. Rajeev Goel, Hydromantis Inc., for his help on GPS-X support and valuable advice on mathematics model. Thank Jer-Horng Wu, National Cheng Kung University, Taiwan for his help on identifying microbial species in the nitrifying sludge and a technic method of live/dead bacterial staining.

Thanks to my classmate Dr. Ian Javis, Dr. Magnus So and Mr. Daisuke Naka for experimental discussion and help in daily experimental life.

Thanks to the Japan Ministry of Education and Kitakyushu Industry and

Science Promotion Organization for awarding me a Dissertation Completion Fellowship, providing me with the financial means to complete this research. And finally, thanks to my wife, son, parents, and numerous relatives and friends who endured this long process with me, always offering support and love to me.

Publications List

Journal paper:

1. **Bing Liu**, Rajeev Goel, Mitsuharu Terashima, Hidenari Yasui (2013)
Models for Reversible and Unreversible Inhibitions of Biological Nitrite Oxidation. **Journal of Japan Society of Civil Engineers**, Ser.G, Vol.69, No.7, III_503-513. (in Japanese)
2. **Bing Liu**, Ian Jarvis, Daisuke Naka, Rajeev Goel, Hidenari Yasui (2013).
A Benchmark Simulation to Verify an Inhibition Model on Decay Stage for Nitrification. **Water Science and Technology**. Vol.68(6), 1242-1250.
3. **Bing Liu**, Daisuke Naka, Ian Jarvis, Rajeev Goel, Hidenari Yasui. (2012).
A Kinetic Expression for the Growth and Decay of Nitrite Oxidising Bacteria. Japanese **Journal of Water Treatment Biology** Vol.48, No.3, 89-97.

Published Book (Translated)

«Methane Fermentation», Translated by **Bing Liu** & Yonghai Xue, 263 pages, Chemical Industry Press, ISBN 978-7-122-19504-3.

International and domestic conference paper

1. **Bing Liu**, Rajeev Goel, Jer-Horng WU, Mitsuharu Terashima, Hidenari Yasui (2014) Exogenous decay of nitrifying bacteria under high nitrite concentration. *Journal of water environment and technology*. (International conference)
2. **Bing Liu**, Rajeev Goel, Mitsuharu Terashima, Hidenari Yasui (2013)

Models for Reversible and Unreversible Inhibitions of Biological Nitrite Oxidation. Journal of Japan Society of Civil Engineers, Ser.G, Vol.69, No.7, III_503-513. (Japanese domestic meeting)

3. **Bing Liu**, Ian Jarvis, Rajeev Goel, Hidenari Yasui (2013). Nitrification process simulation using IWA benchmark datasets. The 2nd International Anammox Symposium. Seoul, Korea. P30-31. (International conference)
4. Ian Jarvis, **Bing Liu** and Hidenari Yasui. (2013). The effect of influent ammonia concentration on partial nitrification in a randomly packed plastic tricking filter. The 2nd International Anammox Symposium. Seoul, Korea. P85. (International conference)
5. Ian Jarvis, **Bing Liu** and Hidenari Yasui. (2013). Evaluation a tricking filter for partial nitrification and the associated energy saving. The proceeding of Japan Society on Water Environment, Kyushu Branch 2012 Research Publication Meeting, P. 67. (Japanese domestic meeting)
6. **Bing Liu**, Ian Jarvis, Daisuke Naka, Rajeev Goel, Hidenari Yasui. (2012). A Benchmark Simulation to Verify an Inhibition Model on Decay Stage for Nitrification. IWA Nutrient Removal and Recovery 2012 Conference abstracts (95-97) . (International conference)
7. **Bing Liu**, Ian Jarvis, Daisuke Naka, Magnus, So and Yasui, H. (2012). A benchmark simulation to verify kinetics inhibition on growth and decay for nitrite oxidizing bacteria. The proceeding of Japan Society on Water Environment, Kyushu Branch 2012 Research Publication Meeting, P. 33. (Japanese domestic meeting)
8. Ian Jarvis, **Bing Liu** and Hidenari Yasui. (2012). Performance evaluation

- of a partial nitrification tricking filter. The proceeding of Japan Society on Water Environment, Kyushu Branch 2012 Research Publication Meeting, P. 31. (Japanese domestic meeting)
9. **Bing Liu**, Daisuke Naka, Ian Jarvis, Yonghai Xue, Hidenari Yasui. (2011). An Expression for the Recovery and Poisoning of Nitrite Oxidizing Bacteria in High Nitrite Substrate Concentrations. Proceedings of 1st International Anammox Symposium, 53-60. (International conference)
 10. **Bing Liu**, Daisuke Naka, Ian Jarvis, Hidenari Yasui. (2011). A Kinetic Expression for the Growth and Decay of Nitrite Oxidising Bacteria. Taiwan-Japan bilateral symposium 2011, 35-37. (International conference)
 11. **Bing Liu**, Naka, D., Jarvis, I., Goel, R. and Yasui, H. (2011) "A Kinetic Expression for the Growth and Decay of Nitrite Oxidising Bacteria". Proc. of 4th IWA-ASPIRE, in CD-ROM, 2-6/October/2011, Tokyo, Japan. (International conference)
 12. **Bing Liu**, Daisuke Naka, Ian Jarvis, Rajeev Goel, Hidenari Yasui. (2011). Nitrogen Removal for Post-treatment of Anaerobic Digestion Liquor. Proceeding of the 7th International Conference on Environmental Anaerobic technologies and Bioenergy, 1-10. (International conference)
 13. **Bing Liu**, Naka, D., Magnus, So., Jarvis, I. and Yasui, H. (2011). A Kinetic Expression for the Growth and Decay of Nitrite Oxidising Bacteria. The proceeding of 45th Japan Society on Water Environment Annual Meeting, 1-D-14-2. p.160. (Japanese domestic meeting)
 14. **Bing Liu**, Naka, D., Magnus, So. Jarvis, I. and Yasui, H. (2011). A model for

growth and decay of nitrite oxidizing bacteria. The proceeding of Japan Society on Water Environment, Kyushu Branch 2011 Research Publication Meeting, P. 8. (Japanese domestic meeting)